Effects of temperature, carbonate chemistry and light intensity on the coccolithophores *Emiliania huxleyi* and *Gephyrocapsa oceanica*

Dissertation

in fulfillment of the requirements for the degree "Dr. rer. nat."

of the Faculty of Mathematics and Natural Sciences

at Christian-Albrechts University Kiel

submitted by

Yong Zhang

Kiel

July 2015

C | A | U
Christian-Albrechts-Universität zu Kiel

GEOMAR
Helmholtz Centre for Ocean Research Kiel

First referee: Prof. Dr. Ulf Riebesell

Second referee: Prof. Dr. Ulrich Sommer

Date of the oral examination: 02. 10. 2015

Approved for publication:

Table of Contents

Summary

Partial pressures of atmospheric carbon dioxide (pCO_2) have been increasing since the industrial revolution and are projected to continue to increase in this century. About one third of the anthropogenic CO_2 emissions have been absorbed by the ocean, thereby decreasing the surface ocean seawater pH. In addition, rising pCO_2 increases global temperatures in the air and then in the surface ocean. Increasing surface seawater temperatures are thought to enhance vertical stratification, shoaling the surface mixed layer and increasing the average light intensity in the upper mixed layer. This thesis focuses on effects of temperature, pCO_2 and light intensity on coccolithophores (calcifying marine phytoplankton). The thesis comprises 5 chapters: Chapter 1 is a general introduction to climate change and how it affects the ocean, marine carbon cycling, and effects of changing ocean on marine phytoplankton; Chapters 2-4 are first-authored published or submitted manuscripts; Chapter 5 provides a synthesis of the results, discussing the potential for coccolithophores to cope with climate/ocean change and giving an outlook on future research perspectives.

Chapter 2 investigates effects of a range of temperatures on growth rates of 11 *Emiliania huxleyi* genotypes, originating from the North Atlantic waters off Bergen and the warmer central Atlantic waters at the Azores. The Bergen genotypes grew well at low temperatures and the Azores genotypes performed better at high temperatures (Figure 1A). Optimum temperature for growth rate of the Azores population was higher than that of the Bergen population. Within each population, genotype-by-environment (G x E) interactions and phenotypic plasticity were identified.

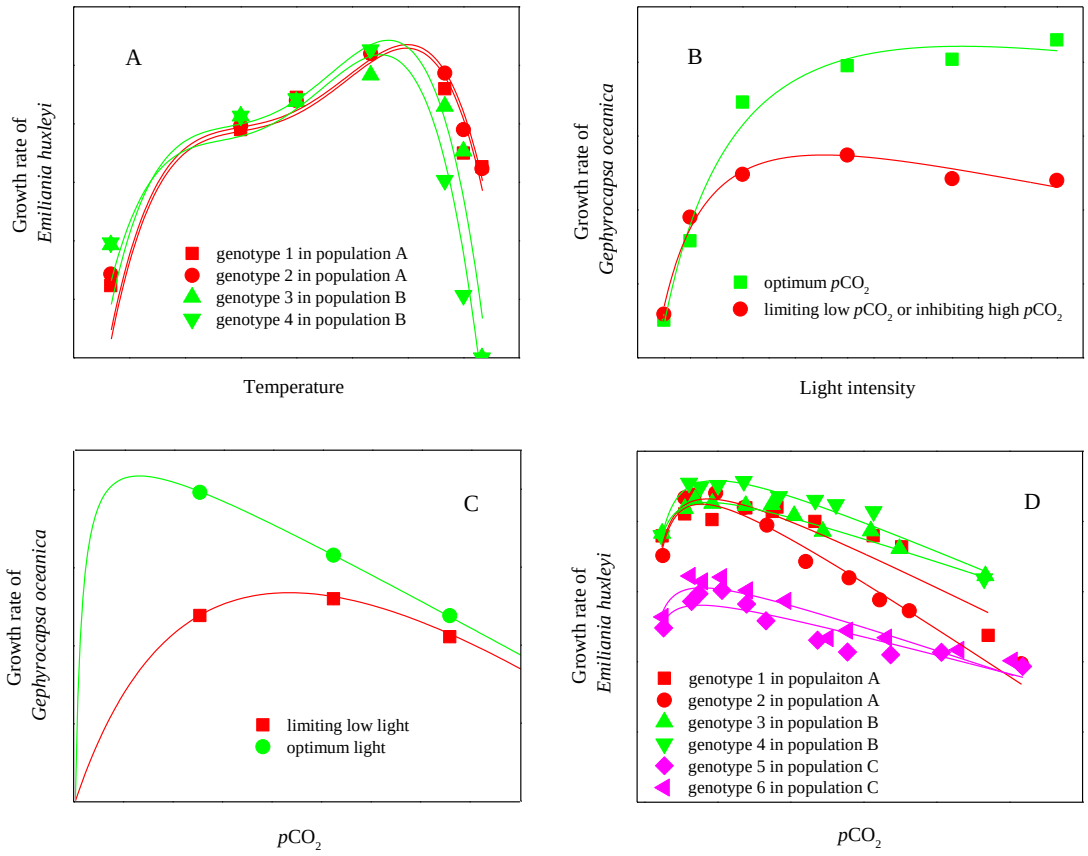

Figure 1. Conceptual figure on the effects of temperature, carbonate chemistry and light intensity on growth rates of *Emiliania huxleyi* and *Gephyrocapsa oceanica*. (A) Growth rate responses of different *E. huxleyi* genotypes isolated from warm or cool waters to a broad range of temperatures. (B) Light response of growth rate of *G. oceanica* at optimum pCO_2, limiting low pCO_2 or inhibiting high pCO_2 levels. (C) Optimum response of growth rate of *G. oceanica* to elevated pCO_2 at optimum light or limiting low light intensities. (D) Optimum responses of growth rates of different *E. huxleyi* genotypes to elevated pCO_2 in distinct populations. Curves in panel (A) were based on chapter 2, in panels (B) and (C) on chapter 3, in panel (D) on chapter 4.

Combined effects of three pCO_2 levels (511, 1048 and 1515 µatm) and six light intensities (50 to 800 μmol photons m^{-2} s^{-1}) on the coccolithophore *Gephyrocapsa oceanica* were investigated in Chapter 3. Rising pCO_2 reduced the maximum rates for growth, photosynthetic carbon fixation and calcification (Figure 1B). Increasing light intensity enhanced the sensitivity of the pCO_2 responses for growth, carbon fixation and calcification rates, and shifted the pCO_2 optima towards

lower levels (Figure 1C). Based on the results of this and previous studies, we proposed a conceptual framework, potentially explaining the modulating effects of light intensity and pCO_2 on physiological processes of coccolithophores.

Previous inconsistent results on physiological responses of *E. huxleyi* to rising pCO_2 required to analyse this issue in more detail. Chapter 4 investigates the population- and genotype-specific responses of *E. huxleyi* to a broad CO_2 range. Growth, photosynthetic carbon fixation and calcification rates of three populations and of 17 genotypes displayed optimum response patterns to a broad CO_2 gradient (Figure 1D). Distinct populations were identified by different growth, carbon fixation and calcification rates among the three populations, and significant differences in CO_2 or pH sensitivity in terms of physiological rates may be related to local pCO_2 variability. Within each population, G x E interactions, phenotypic plasticity and trade-offs may help to maintain the genotypic diversity of *E. huxleyi* populations, with the potential to acclimate to changing oceans.

The data presented in this thesis help us better understand the responses of coccolithophores to increasing temperature, pCO_2 and light intensity. It provides a significant step forward in our understanding of the mechanisms (such as local adaptation, G x E interactions, phenotypic plasticity and trade-offs), which allow natural phytoplankton species to adapt to different environmental conditions. Genotype-specific optimum temperature or CO_2 level for growth rate may alter population composition in the changing ocean. In addition, interacting effects of light and pCO_2 on coccolithophores may give directions for future research on combined effects of different environmental conditions on marine phytoplankton.

Zusammenfassung

Der Partialdruck von CO_2 in der Atmosphäre steigt seit Beginn der industriellen Revolution stetig an. Dieser Anstieg sich wird aller Wahrscheinlichkeit nach auch weiter fortführen. Die Ozeane haben ca. 1/3 des anthropogenen CO_2s absorbiert, was auch zu einer Abnhahme des Seewasser pHs führt. Zusätzlich führt die Zunahme des pCO_2 in der Atmosphäre zu einem Anstieg der Luft-und Meerwassertemperatur. Es wird angenommen, dass die ansteigende Oberflächenwassertemperatur zu verstärkter vertikaler Schichtung und dadurch zu einer Abflachung der durchmischten Oberflächenschicht und erhöhter Durchschnittslichtinensität führt. Diese Doktorarbeit behandelt die Effekte von Temperatur, pCO_2 und Lichtintensität auf Coccolithophoriden (kalzifizierendes marines Phytoplankton). Sie beinhaltet fünf Kapitel. Kapitel 1 ist eine umfassende Einleitung zum Klimawandel und wie dieser die Ozeane, den marinen Kohlenstoffkreislauf, marines phytoplankton beeinflusst. Kapitel 2-4 sind die Erstautorpublikationen, die entweder bereits veröffentlicht oder eingereicht wurden. Kapitel 5 ist die Synthese der Doktorarbeit. Sie beeinhaltet eine Diskussion wie Coccolithophoriden vom Klimawandel betroffen sind und beschreibt zukünftige Perspektiven in diesem Wissenschaftszweig.

Kapitel 2 untersucht Effekte eines Temperaturgradienten auf die Wachstumsraten von elf *Emiliania huxleyi* Genotypen, isoliert aus dem Nord Atlantik in der Nähe von Bergen und dem wärmeren Zentralatlantik nahe der Azoren. Die Bergen Genotypen wuchsen gut bei niedrigen Temperaturen während die Genotypen von den Azoren höhere Temperaturen vorzogen (Abbildung 1A). Die optimale Wachstumstemperatur für die Azoren- war höher als für die Bergenpopulation. Innerhalb beider Populationen konnten sogenannte Genotyp-Umwelt (G x E) Interaktionen und

phänotypische Plastizität identifiziert werden.

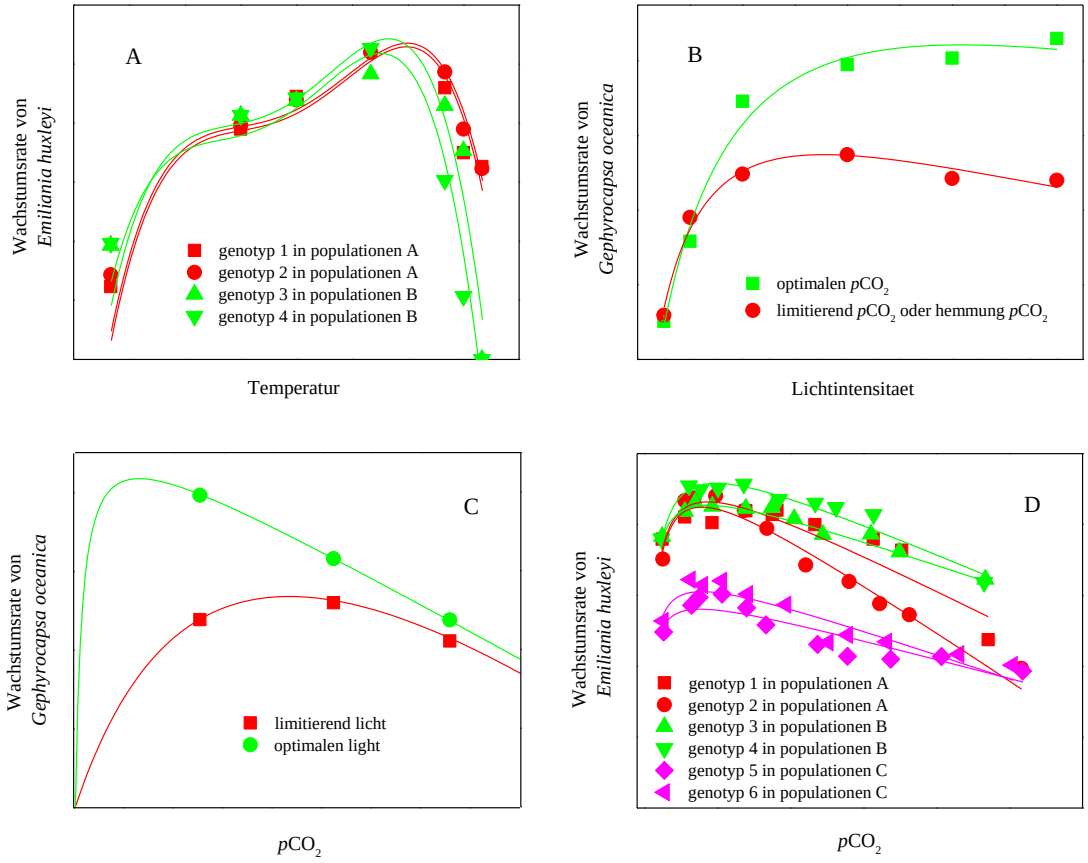

Abbildung 1. Konzeptionelle Darstellung des Einflusses von Temperatur, Karbonatchemie und Lichtintensität auf die Wachstumsraten von *Emiliania huxleyi* und *Gephyrocapsa oceanica*. (A) Wachstumsraten von verschiedenen *E. huxleyi* Genotypen als Funktion der Temperatur. Die Genotypen wurden an unterschiedlichen Warm- und Kaltwasserhabitaten isoliert. (B) Die Reaktion der Wachstumsrate von *G. oceanica* auf verschiedene Lichtintensitäten bei unterschiedlichen pCO_2 Werten. (C) Die Optimumreaktion der Wachstumsraten von *G. oceanica* also Funktion des pCO_2. Die zwei Kurven stellen die Reaktion bei optimalen (grün) bzw. limitierenden (rot) Lichtverhältnissen dar. (D) Die Optimumreaktion der Wachstumsraten von verschiedenen *E. huxleyi* Populationen als Funktion des pCO_2. Die gezeigten Daten in (A), (B), (C), und (D) werden jeweils in Kapitel 2, 3, 3 und 4 besprochen.

In Kapitel 3 wurden kombinierte Effekte dreier pCO_2 Level (511, 1048 und 151 µatm) und sechs Lichtintensitäten (50 bis 800 µmol Photonen m^{-2} s^{-1}) auf die Kalkalge *Gephyrocapsa oceanica* untersucht. Steigender pCO_2 reduzierte maximale Raten für Wachstum,

photosynthetische Kohlenstoffixierung und Kalzifizierung (Abbildung 1B). Die Erhöhung der Lichtintensität verstärkte die pCO_2 Sensitivitäten der Wachstums-, Kohlenstofffixierungs-, und Kalzifizierungsrate, indem sie deren pCO_2 Optima zu geringeren Werten verschob (Abbildung 1C). Auf diese Ergebnisse und die früherer Studien aufbauend wurde ein konzeptionelles Verständnis entwickelt wie Lichtintensität und pCO_2 physiologische Prozesse in Kalkalgen modulieren könnten.

Uneindeutige Forschungsergebnisse zur physiologischen Reaktion der Kalkalge *E. huxleyi* unter erhöhtem pCO_2 vorangegangener Studien verlangen nach einer genaueren Betrachtung dieser Problematik. Kapitel 4 beschäftigt sich mit der populations- und genotypenspezifischen Reaktion von *E. huxleyi* über einen breiten CO_2 Bereich. In Abbildung 1D sind Optimumskurven der jeweiligen Wachstums-, Kohlenstofffixierungs- und Kalzifizierungsraten der drei *Emiliania huxleyi* Populationen mit insgesamt 17 Genotypen dargestellt. Alle drei Populationen unterscheiden sich signifikant in Wachstums-, Kohlenstofffixierungs- und Kalzifizierungsraten und es ist anzunehmen, dass G x E Interaktionen, phänotypische Plastizität und Kosten-Nutzen-Abwägungen wichtig für die genetische Vielfalt innerhalb einer *E. huxleyi* Population sind.

Die in dieser Arbeit vorgestellten Ergebnisse liefern einen wichtigen Beitrag zum besseren Verständnis der Reaktionen von Coccolithophoriden auf erhöhte Temperatur-, CO_2- und Lichtbedingungen, sowie der Bedeutung von lokaler Anpassung, GxE Interaktionen, phänotypischer Plastizität und Kosten-Nutzen-Abwägungen bei der Anpassung natürlicher Phytoplanktonpopulationen an veränderte Umweltbedingungen. So ist zum Beispiel anzunehmen, dass optimale genotypspezifische Temperatur oder CO_2 Wachstumsbedingungen zu Änderungen

in der Populationszusammensetzung in einem sich wandelnden Ozean führen können. Des weiteren können wechselwirkende Effekte von Licht und pCO_2 auf Coccolithophoriden Anregungen für zukünftige Forschungsvorhaben, die sich mit den Auswirkungen verschiedener kombinierter Umweltfaktoren auf marines Phytoplankton beschäftigen, liefern.

Chapter 1. General Introduction

1.1 Changes in surface seawater temperature, CO_2, and light intensity

The Earth's surface temperature has successively increased faster than any preceding period since 1850 (Hansen et al., 2006). On a global scale, ocean temperature at the surface increases quickest, and temperature in the upper 75 m of the oceans has increased by about 0.44 ^{o}C since 1971 (IPCC, 2013). Global surface temperature increases by the end of this century are projected to be 2 to 4 ^{o}C, and the global ocean will also continue to warm (IPCC, 2013).

The largest contribution to global warming since the mid-20th century was caused by both the anthropogenic increase in greenhouse gases such as carbon dioxide (CO_2), methane (CH_4) and nitrous oxide (N_2O), and other anthropogenic forcings such as land surface properties changes (IPCC, 2013). The combustion of fossil fuels, net land use change and deforestation have increased the partial pressure of atmospheric carbon dioxide (pCO_2) from about 280 µatm in pre-industrial periods to about 400 µatm at present day (Monastersky, 2013). Importantly, atmospheric pCO_2 is projected to reach beyond 750 µatm by the end of this century (IPCC, 2013). The ocean has absorbed about 30% of the emitted anthropogenic CO_2 (Sabine et al., 2004). Increasing seawater CO_2 concentrations form carbonic acid leading to a reduction in seawater pH. The pH of ocean surface water has decreased by about 0.12 units from the beginning of the industrial era, corresponding to a 26% increase in hydrogen ion concentration (Houghton et al., 2001). Within the next 100 years, the pH of ocean surface waters is projected to further decrease by 0.3 to 0.4 units, representing a 100 to 150% increase in the proton [H^+] concentration (Houghton et al., 2001). Such reductions in surface seawater pH are commonly referred to as

ocean acidification (Doney et al., 2009).

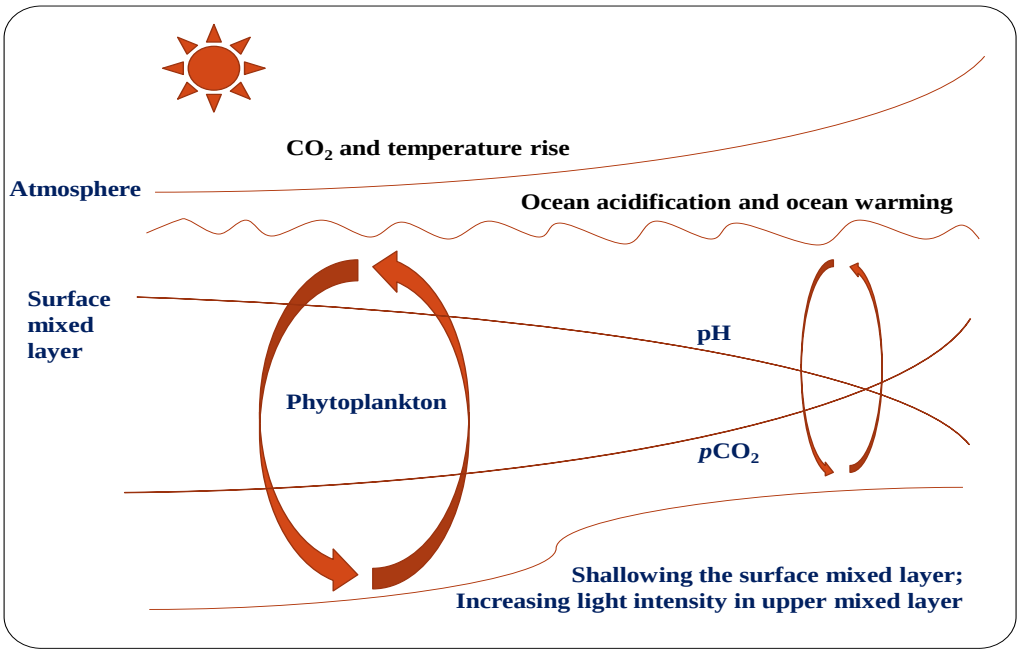

Figure 2. Conceptual figure of ocean changes associated with climate change. Increase in global surface temperature leads to ocean warming, which enhances water column stratification. This would increase exposure of phytoplankton to solar photosynthetically active radiation (PAR). Increase in atmospheric CO_2 leads to higher CO_2 dissolution in surface oceans and decreases surface ocean pH.

During the 21st century as global mean surface temperature rises, it is likely that the Arctic sea ice cover, Northern Hemisphere spring snow cover and global glacier volume will continue to decrease (IPCC, 2013). These are expected to drive decreasing ice-albedo and then the proportion of solar radiation reflected by Earth's surface. As a consequence, a higher amount of solar radiation is absorbed by Earth's surface (Sarmiento et al., 2004). At the same time, rising mean global temperature enhances water column stratification which would lead to decreased mixing between the surface ocean and deep layers (Bopp et al., 2001). This expected shoaling of the upper mixed layer would increase the mean light intensity experienced by phytoplankton suspended in this layer (Sarmiento et al., 2004) (Figure 2).

1.2 Seawater carbonate system

When gaseous carbon dioxide ($CO_2(g)$) dissolves in water, part of it reacts with water to form carbonic acid (H_2CO_3) (Soli and Byrne, 2002). Being relatively instable, H_2CO_3 dissociates into bicarbonate (HCO_3^-) and protons (H^+). H^+ combines with carbonate ions (CO_3^{2-}), which further increases HCO_3^- concentrations. At equilibrium, the concentration of H_2CO_3 is only about 1/1000 of the concentration of $CO_2(aq)$, and H_2CO_3 is difficult to separate from $CO_2(aq)$ analytically (Butler, 1998). Thus, $CO_2^*(aq)$ in water is conveniently defined as the sum of H_2CO_3 and $CO_2(aq)$.

$$CO_2(g) \rightleftharpoons CO_2^*(aq) \quad (1)$$

$$CO_2^*(aq) + H_2O \overset{K_1}{\rightleftharpoons} HCO_3^- + H^+ \overset{K_2}{\rightleftharpoons} CO_3^{2-} + H^+ \quad (2)$$

the notations (g) and (aq) refer to the state of the species, i.e. a gas or in aqueous solution respectively, and K_1 and K_2 are the first and second equilibrium constants, respectively (Dickson et al., 1981). Another important constant is the solubility coefficient K_0, which depends on temperature, salinity and pressure of seawater. Gaseous CO_2 ($CO_2(g)$) dissolves in seawater following Henry's law:

$$[CO_2^*(aq)] = K_0 \times fCO_2 \quad (3)$$

where $[CO_2^*(aq)]$ denoting the concentration of $CO_2^*(aq)$. fCO_2 is the fugacity of CO_2 determined in the gas phase in equilibrium with the water at known temperature and salinity (Dickson et al., 2007). Please note that fugacity should be used instead of partial pressure as CO_2 is not an ideal gas. However, the difference between fCO_2 and pCO_2 is typically on the order of less than 1%.

The sum of all carbon species in seawater is referred to as total dissolved inorganic carbon (DIC).

$$DIC = [CO_2^*(aq)] + [HCO_3^-] + [CO_3^{2-}] \quad (4)$$

The concentrations of the three different species, $CO_2^*(aq)$, HCO_3^- and CO_3^{2-} are a function of pH according to Figure 3 (Hansson, 1973). At a typical present day surface ocean pH of 8.1, about 90% of DIC is present as HCO_3^-, about 9% as CO_3^{2-}, and less than 1% as $CO_2^*(aq)$.

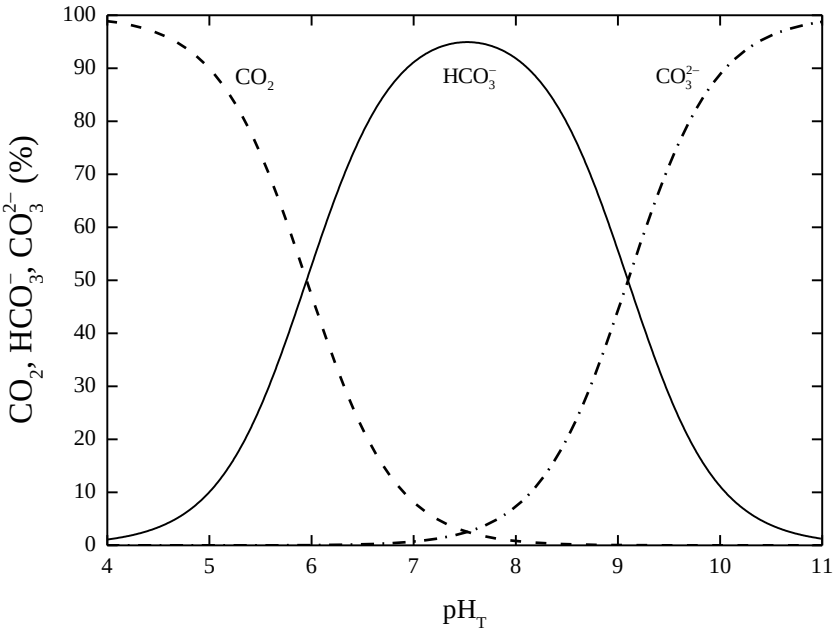

Figure 3. Relative proportion of the three carbonate species CO_2, HCO_3^- and CO_3^{2-} in seawater with a salinity of 35 at 15 ^oC to the total inorganic carbon pool as a function of pH (on the total scale).

Another important parameter of the carbonate system is total alkalinity (TA). The currently most precise definition of TA is given by Dickson (DOE, 1994) as "The total alkalinity of a natural water is thus defined as the number of moles of hydrogen ion equivalent to the excess of proton acceptor (bases formed from weak acids with a dissociation constant $K \leq 10^{-4.5}$, at 25 ^oC and zero ionic strength) over proton donors (acids with $K > 10^{-4.5}$) in one kilogram of sample." Hence, for typical open ocean seawater the expression of total alkalinity (TA) reads:

$$TA = [HCO_3^-] + 2[CO_3^{2-}] + [B(OH)_4^-] + [OH^-] + [HPO_4^{2-}] + 2[PO_4^{3-}]$$

$$+ [H_3SiO_4^-] + [NH_3] + [HS^-] - [H^+]_F - [HSO_4^-] - [HF] - [H_3PO_4] \quad (5)$$

where $[H^+]_F$ is the free concentration of hydrogen ion. The six different parameters (DIC, TA, pH, $fCO_2, HCO_3^-, CO_3^{2-}$) of the seawater carbonate system are interdependent and change in one parameter will affect others. Determination of any two of them is suitable to calculate the concentrations of the remaining four with the stoichiometric equilibrium constants.

The ocean CO_2 uptake capacity is attributed to the reaction of CO_3^{2-} with $CO_2^*(aq)$.

$$CO_3^{2-} + CO_2^*(aq) + H_2O \rightarrow 2\,HCO_3^- \quad (6)$$

As a consequence of uptake of atmospheric CO_2, surface ocean DIC is increasing with increasing atmospheric pCO_2. This process is known as "ocean carbonation" (Riebesell et al., 2009). According to equation (6), in the future ocean the concentration of HCO_3^- will increase and CO_3^{2-} will decrease, which will attenuate the ocean CO_2 uptake capacity. One molecule of CO_3^{2-}, CO_2 and H_2O are converted to two molecules of HCO_3^-, which is neutral for total alkalinity (TA) (Wolf-Gladrow et al., 2007).

1.3 Phytoplankton and marine carbon cycle

The global carbon cycle is the biogeochemical cycle by which carbon is exchanged among the terrestrial realm, the atmosphere and the oceans (Sundquist, 1985). The carbon exchanges between three reservoirs occur as the result of various chemical, physical, geological, and biological processes (Sundquist, 1985). Although the terrestrial standing stock biomass is much higher than that in the ocean, approximately 40% of the global annual net primary production occurs in the ocean (Field et al., 1998; Falkowski and Raven, 2007). Owing to relative high turnover rates of

biogenic material, the ocean represents the second largest reservoir of carbon near the surface of the Earth (Falkowski and Raven, 2007). At under-saturated CO_2 conditions, the surface oceans take up CO_2 from atmosphere. The oceanic carbon flux from the surface to the deep ocean is determined by two processes, the solubility pump and the biological pump, which establish a vertical gradient of dissolved inorganic carbon (DIC) (Volk and Hoffert, 1985). The abiotic solubility pump is driven by the increasing solubility of CO_2 with decreasing temperature. As warm surface waters move from low to high latitudes, subsequent cooling results in an increasing CO_2 solubility (Holligan, 1992; Joos et al., 1999). During deep-water formation at high latitudes, this cold CO_2-rich water is then transported to the deep ocean. This explains about 30-40% of the surface-to-depth DIC gradient (Riebesell et al., 2009). The other 60-70% of the vertical carbon gradient is caused by the biological carbon pump: the sinking of biogenic material from the sunlit surface layer to the deep ocean (Rost and Riebesell, 2004).

Based on the biological processes responsible for carbon fixation, two biological carbon pumps can be distinguished: the organic carbon pump and the carbonate counter pump (Figure 4). The organic carbon pump is driven by the photosynthetic carbon fixation of phytoplankton in the ocean's surface, causing a net flux of CO_2 from the atmosphere to the surface ocean. Particulate organic carbon (POC) sinks out of the photic zone and then transports carbon to deeper layers. Only about 0.1% of POC reaches the deep-sea floor and is stored in sediments while the remainder is remineralized in the water-column on its way down (Westbroek et al., 1993). The carbonate counter pump is driven by the formation of calcium carbonate ($CaCO_3$) shell material by calcifying plankton such as coccolithophores, foraminifera and pteropods (Rost and Riebesell, 2004). $CaCO_3$ precipitation consumes DIC and total alkalinity (TA) in the surface ocean and

releases CO_2 to the environment (one CO_3^{2-} ion equals one unit of DIC or two units of TA), causing an increase in CO_2 partial pressure in the surface ocean. Decreased calcification with rising pCO_2 will lead to decline in the strength of the carbonate counter pump. Normally, under over-saturated waters, $CaCO_3$ sinking from the surface to the deep ocean is mainly preserved above the saturation horizon, and starts to dissolve below the saturation horizon in under-saturated waters (Zeebe and Wolf-Gladrow, 2001).

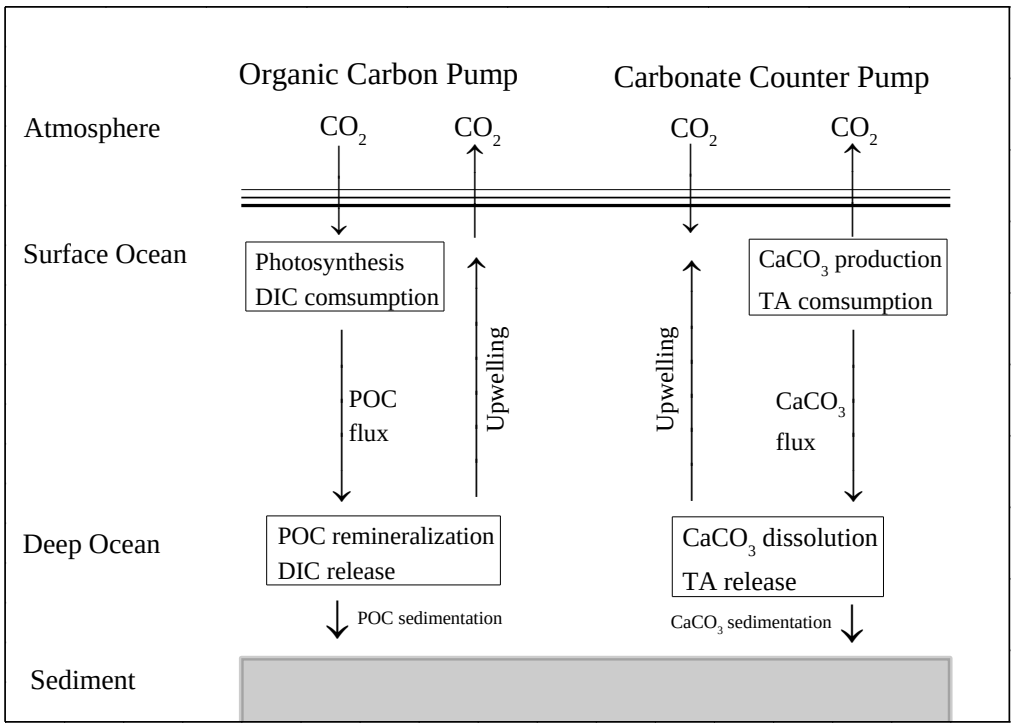

Figure 4. Schematic diagram of the two types of the biological carbon pump: the organic carbon pump and the carbonate counter pump. Photosynthetic POC production in the surface ocean and its subsequent transport to depth constitute a CO_2 sink in the ocean. In contrast, biogenic production of $CaCO_3$ and its transport to depth release CO_2 to the surface layer. DIC and TA are transported from deeper layer to the surface by upwelling and mixing.

Both organic carbon pump and carbonate counter pump cause the DIC to be lowered in the surface sea water and to be increased in the deep ocean. Thus, the organic carbon and carbonate counter pumps reinforce each other in terms of maintaining a vertical DIC gradient. Whereas, the

formation of particulate inorganic carbon (PIC) in surface waters represents a potential source of CO_2, the production of POC represents a sink of CO_2 (Riebesell et al., 2009). The relative importance of the two biological carbon pumps is represented by the ratio of PIC to POC (or *rain ratio*). When PIC/POC decreases, the ocean's capacity to sequester CO_2 increases and vice-versa. The PIC/POC depends on both PIC production by coccolithophores, foraminifera and pteropodes and POC production by phytoplankton, mostly diatoms (Rost and Riebesell, 2004).

Rising atmospheric CO_2 leads to higher sea-surface temperature (SST), therefore reducing the CO_2 solubility (Joos et al., 1999). It is estimated that increasing SST by the end of the 21st century will reduce the oceanic uptake of anthropogenic carbon by 9-15% (about 45-70 gigatons carbon (10^{15} g C) (Matear and Hirst, 1999). Rising SST is thought to increase the thermal stratification which would decrease nutrient supply and increase mixed-layer light intensities (Bopp et al., 2001; Sarmiento et al., 2004). In the low- and mid-latitudes, phytoplankton growth is limited by low surface nutrient concentrations. Increasing SST could further diminish the upward nutrient supply and lower primary productivity, leading to a decline in the strength of the biological carbon pump. At high latitudes, intense vertical mixing circulates phytoplankton over deep mixed layers, resulting in light-limitation in phytoplankton growth (Riebesell et al., 2009). Rising SST could reduce vertical mixing and increase mean light intensity in the upper mixed layer, which may increase primary productivity. Thus, more organic materials could be transported to the deep ocean at high latitudes (Sarmiento et al., 2004). Subsequent lowering of the consumption of alkalinity by calcification in the surface ocean increases the CO_2 uptake capacity from the atmosphere. Being denser than particulate organic carbon, $CaCO_3$ in the bathypelagic zones of the ocean has been proposed to act as ballast, accelerating the downward flux of the

particulate organic material. Reduced $CaCO_3$ could reduce the export of biogenic matter to depth, which may reduce the uptake capacity for atmospheric CO_2 by the surface ocean (Armstrong et al., 2002; Heinze, 2004).

1.4 Photosynthesis and inorganic carbon acquisition of phytoplankton

Photosynthesis is a process used by photoautotrophic plants and other organisms to convert light energy into chemically fixed energy, which can be later released to fuel the organism's activities. The main accessory pigment chlorophyll in marine phytoplankton can absorb sunlight, fuelling the electron transport chain, ultimately leading to the reduction of NADP to NADPH. In addition, a proton gradient across the chloroplast membrane drives the ATP synthase to synthesize ATP (Falkowski and Raven, 2007; White, 2007).

$$2NADP^+ + 3ADP + 3Pi + 2H_2O \xrightarrow{light} 2NADPH + 2H^+ + 3ATP + O_2 \quad (7)$$

Using the newly formed ATP and NADPH, the enzyme ribulose-1,5-bisphosphate carboxylase/oxygenase (RuBisCO) captures CO_2 from the intracellular environments, and drives the combination of CO_2 with the ribulose-1,5-bisphosphate (RuBP). Photosynthesis can be described as a process in which CO_2 and H_2O are used to synthesize carbohydrates while oxygen is produced using energy from light (Falkowski and Raven, 2007; White, 2007).

$$CO_2 + 2H_2O \xrightarrow{light} (CH_2O) + H_2O + O_2 \quad (8)$$

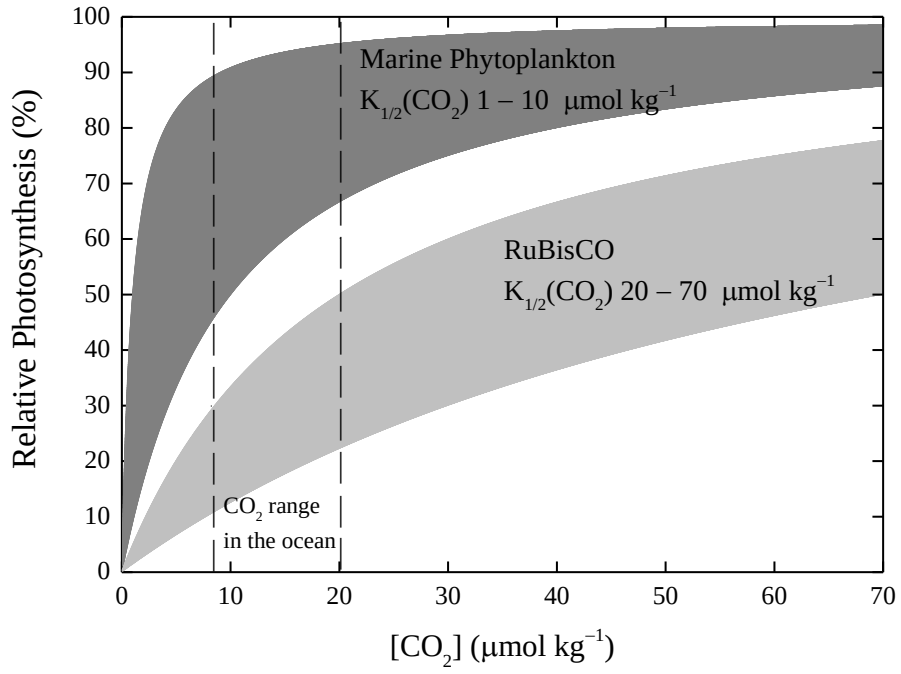

Figure 5. Comparison of CO_2 fixation between marine phytoplankton cells and isolated RuBisCO. Half saturation constants ($K_{1/2}$) for photosynthetic CO_2 fixation of marine phytoplankton are generally lower than that of RuBisCO, which indicates the operation of CCM in marine phytoplankton (Badger et al., 1998).

On the geological history at the relatively low atmospheric CO_2 and high O_2 levels, RuBisCO has only a low affinity for CO_2, functioning at only about 25% of its catalytic capacity (Moroney and Ynalvea, 2007). In order to increase CO_2 concentration at the site of carboxylation of RuBisCO, most marine phytoplankton developed so-called carbon concentration mechanisms (CCMs) (Giordano et al., 2005). CCMs involve the active uptake of CO_2 and/or HCO_3^- into the algal cell and/or the chloroplast, and utilisation of the enzyme carbonic anhydrase (CA) which accelerates the otherwise slow rate of conversion between CO_2 and HCO_3^- (Giordano et al., 2005; Moroney and Ynalvea, 2007). The CO_2 half saturation constants ($K_{1/2}(CO_2)$) for RuBisCO range between 20 – 70 μmol L^{-1} (Raven and Johnston, 1991), while $K_{1/2}(CO_2)$ for photosynthetic carbon fixation of marine phytoplankton are between 1 – 10 μmol L^{-1} (Badger et al., 1998) (Figure 5).

This indicates the active uptake of inorganic carbon by marine phytoplankton. CCM activity is energy-dependent and is influenced by environmental conditions such as CO_2 concentration, temperature and light intensity. Regulation of CCM activity allows phytoplankton to use the inorganic carbon effectively and then optimize the energy and other resource allocation efficiencies (Raven, 1991; Hopkinson et al., 2011).

1.5 Biogeographic distribution and adaptation of marine phytoplankton

Phytoplankton populations are distributed over large geographic ranges, and are characterized by large sizes, and high growth rates, while most of them are passive drifters (Collins et al., 2014). The environment that marine phytoplankton encounter is very heterogeneous on short time scales (Hutchinson, 1961). Different seawater bodies, created by frontal boundaries, are characterized by special temperature, dissolved nutrient concentrations and light penetration (Reusch and Boyd, 2013). Owing to extrinsic barriers such as ocean boundaries, a large population could be broken up into smaller units, then gene flow (or gene exchange) between these separated populations may be limited, and genetic differentiation can take place between them (Lewis et al., 1997). In order to adapt to respective local environments, eventually morphological and physiological differentiation between separated populations occurs. Several studies indicate that genetic differentiation and biogeographic structuring may be common to both marine and freshwater phytoplankton populations (Rynearson and Armbrust, 2004; Casteleyn et al., 2010; Cook et al., 2013).

Phytoplankton adapt to novel environments either through selection of new, beneficial mutations or through selection on pre-existing genetic variation where the latter is likely to be

faster (Collins et al., 2014; Reusch, 2014). Standing genetic variation is the presence of more than one allele at a locus in a population (Barrett and Schluter, 2008). Gene flow between populations which experience different environmental conditions, or hybridization with other species could preserve high amounts of standing genetic variation (Godhe et al., 2013). Phenotypic plasticity may also play an important role for phytoplankton to adapt to changing environments, and different phenotypes may potentially form the basis for selection (Kremp et al., 2012). Phenotypic plasticity is defined as the ability of a genotype to change the phenotype in different environments (Bradshaw, 1965). A genotype-by-environment (G x E) interaction occurs when the phenotypic response of a genotype varies across environments or when distinct genotypes within populations perform differently across environments (De Jong, 1990). G x E interactions are commonly found in phytoplankton population and may help to maintain the population diversity (Gsell et al., 2012). Phenotypic plasticity and G x E interaction can be illustrated by reaction norm experiments. A reaction norm describes the pattern of phenotypic expression of a genotype across a range of environments such as temperature or pCO_2 (Gsell et al., 2012). Studies on the effect of ocean change on marine phytoplankton should take genetic and physiological variability into consideration. In addition, more work is needed to investigate the evolutionary response of phytoplankton to changing ocean conditions (Lohbeck et al., 2012; Schlüter et al., 2014).

1.6 Effects of temperature, carbonate chemistry and light intensity on marine phytoplankton

1.6.1 Effect of temperature on growth of marine phytoplankton

Temperature determines metabolic rates and acts directly on physiological processes (Beardall and

Raven, 2004). In order to understand how increasing surface seawater temperature (SST) will affect marine phytoplankton, a number of studies have investigated the temperature responses in terms of growth rates of different phytoplankton species or strains (Brand, 1982; Buitenhuis et al., 2008; Feng et al., 2008; Boyd et al., 2013; Hyun et al., 2014). At five or seven temperatures (-1.8 to 20 ^{o}C or 2 to 35 ^{o}C), Suzuki and Takahashi (1995) determined growth responses of eight diatom species, which were isolated from various temperature environments ranging from temperate ones to the Arctic. Kaeriyama et al. (2011) examined effects of six temperatures (10 to 35 ^{o}C) on growth rates of seven *Skeletonema* species isolated from Dokai Bay in Southern Japan. Using 25 phytoplankton strains including diatoms, dinoflagellates and cyanobacteria, Boyd et al. (2013) provided functional responses of phytoplankton growth rates to elevated temperature (1 to 8 ^{o}C or 4 to 35 ^{o}C). For coccolithophores, Buitenhuis et al. (2008) determined growth rates of six coccolithophorid strains as a function of temperature (5 to 25 ^{o}C). All above studies showed that the growth rate response of each phytoplankton species or strain to the incubation temperature is characterized by thermal performance curves (TPC). The common shape of a TPC is an increase in growth rate with increasing temperature until reaching a maximum, followed by a steep decrease towards the upper limit of the growth range (Huey and Kingsolver, 1979).

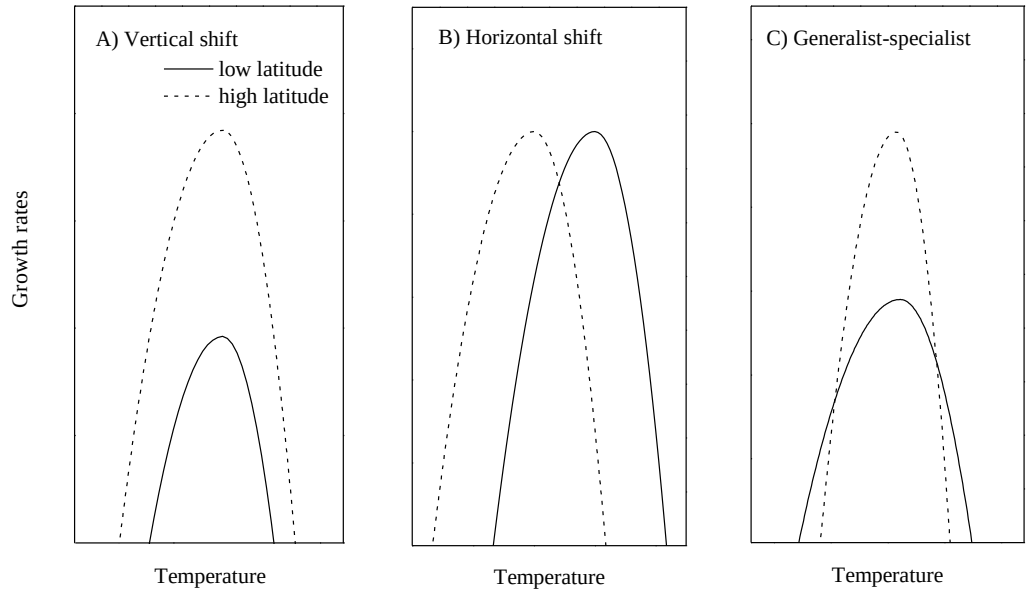

Figure 6. Three theoretical models for variation in thermal reaction norms. (A) Vertical shift model, which represents variation in overall growth rates across all temperatures. (B) Horizontal shift model, which represents variation in the location of the maximum growth rates. (C) Generalist-specialist model, which represents variation in the width of the growth rates curves and trade-off between width and maximal growth rates (Izem and Kingsolver, 2005).

Several models were developed to describe the TPC. And these models normally explained three modes of biological interest: maximal growth rate at optimal temperature or overall growth rate across all temperatures (vertical shift model; Figure 6A), optimal temperature as horizontal shift of maximal growth rate (horizontal shift model; Figure 6B), generalist-specialist trade-off as width (generalist-specialist model; Figure 6C) (Izem and Kingsolver, 2005; Boyd et al., 2013). Vertical shift model represents difference in maximal growth rate or in overall growth rate across all temperatures; horizontal shift model represents difference in optimum temperature of growth rate and generalist-specialist model represents difference in temperature niche width of growth rate (Izem and Kingsolver, 2005). Temperature dependent growth rates of phytoplankton are in agreement with their geographical distributions (Kaeriyama et al., 2011; Boyd et al., 2013). Normally, phytoplankton isolated from tropical waters has higher optimal temperatures and

narrower temperature niches than those isolated from polar and temperate waters (Boyd et al., 2013). And phytoplankton from cool waters has optimum temperatures that are much higher than their mean annual temperatures, while those from warm waters have optima closer to the mean temperatures (Thomas et al., 2012). These findings are inline with the results in Chapter 2 in this thesis.

1.6.2 Effect of carbonate chemistry on growth, photosynthetic carbon fixation and calcification rates of coccolithophores and diatoms.

Physiological responses of marine phytoplankton to increasing pCO_2 are probably dependent on the mechanisms of inorganic carbon uptake, intracellular assimilation and the leakage of CO_2 from the cytoplasm (Rost et al., 2006; Riebesell and Tortell, 2011). The cell membranes of marine phytoplankton are permeable to CO_2, and leakage of CO_2 decreases if the CO_2 gradient between cytoplasm and external medium decreases (Rost et al., 2006; Hopkinson et al., 2011). Elevated pCO_2 in the seawater reduces the CO_2 gradient between cytoplasm and external seawater and therefore the leakage of CO_2. This may facilitate carbon fixation and growth rates (Riebesell and Tortell, 2011).

Phytoplankton differ widely in their photosynthetic apparatus and activities of CCMs (Giordano et al., 2005). With low-efficiency CCMs, coccolithophores are considered to be more sensitive to changing carbonate chemistry than other marine phytoplankton groups such as diatoms (Rost and Riebesell, 2004). Until now, a large number of studies have investigated the effects of carbonate chemistry on coccolithophores (Riebesell et al., 2000; Langer et al., 2006; 2009; Bach et al., 2011; Hoppe et al., 2011; Bach et al., 2015). When pCO_2 increased from about

150 to 890 µatm, Riebesell et al. (2000) reported increased carbon fixation rates and reduced calcification rates in *Emiliania huxleyi* and *Gephyrocapsa oceanica*. With increasing pCO_2 from about 100 to 920 µatm, Langer et al. (2006) found that carbon fixation rates of *Calcidiscus leptoporus* remained constant and its calcification rates displayed an optimum response. And carbon fixation and calcification rates of *Coccolithus pelagicus* did not change significantly over a pCO_2 range tested at about 150 to 915 µatm (Langer et al., 2006). Based on a broad pCO_2 gradient (400 to 1800 µatm or 500 to 3631 µatm), Krug et al. (2011) proposed that calcification and photosynthetic carbon fixation rates in all coccolithophores are likely to display an optimum response. It may be that limiting carbon concentrations at low pCO_2 levels can directly limit the carbon fixation, calcification and growth rates of coccolithophores. With rising pCO_2 levels, increasing DIC is thought to stimulate carbon fixation and calcification rates by supplying increasing amounts of substrate. However, low pH at high pCO_2 levels is suggested to reduce these rates (Bach et al., 2011; 2015). This might be linked to the fact that activities of enzymes involved in carbon fixation are inhibited by low pH (Portis et al., 1986). Thus, over a broad pCO_2 range, there should be thresholds for pCO_2 levels (optimum pCO_2). Below optimum pCO_2 photosynthetic carbon fixation, calcification and growth rates of coccolithophores could be enhanced by the increasing CO_2 and HCO_3^- concentrations, while above optimum pCO_2 these process rates may be reduced by the low pH. The carbon availability was identified as the factor responsible for the observed rates on the left side of the optimum, the low pH was most likely the driving factor on the right side of the optimum (Bach et al., 2011; Sett et al., 2014; Bach et al., 2015). However, we cannot rule out the effect of pH on the left side of the optimum.

With high efficiency CCMs in diatoms, a number of studies showed that rising pCO_2

increases their growth and photosynthetic carbon fixation rates. For example, enhanced growth and carbon fixation rates were found in *Asterionella glacialis*, *Thalassiosira punctigera* and *Scrippsiella trochoidea* at 280 to 1000 µatm (Burkhardt et al., 1999), in *Phaeodactylum tricornutum* at 380 to 1000 µatm (Wu et al., 2011), in *T. pseudonana* at 390 to 750 µatm (McCarthy et al., 2012). Recently, one study showed that carbon fixation and growth rates of *A. glacialis* have an optimum response with pCO_2 increasing from 320 to 3400 µatm (Barcelos e Ramos et al., 2014). It is unclear whether growth and carbon fixation rates of other diatom species or strains will also show an optimum response to a broad pCO_2 range. If this is right, as mentioned above, we expected that low pH would be responsible for the decline in growth and carbon fixation rates of diatoms on the right side of the optimum over a broad pCO_2 gradient. However, several studies found that changes in pH have little effects on growth rates of diatoms. For example, no significant differences were found in growth rates of *Skeletonema costatum* at 6.5 to 8.5 (Taraldsvik and Myklestad, 2000), of *Chaetoceros muelleri* at 7.4 to 8.2 (Thornton, 2009). Whereas, it has to be noted that in comparison to other studies, both studies of Taraldsvik and Myklestad (2000) and Thornton (2009) differed markedly in experimental setup and design with for instance relatively high cell densities, acid instead of DIC adjustments and no defined carbonate chemistry speciation. Based on these results, I summarize that carbon fixation rates of some diatom species will increase with increasing pCO_2 from 280 to 1000 µatm. These elevated pCO_2 will display neutral or positive effect on growth rates of diatoms. When pCO_2 increases from 1000 µatm to higher levels, one does not know the response patterns of growth and carbon fixation rates of diatoms.

1.6.3 Combined effects of carbonate chemistry and temperature on marine phytoplankton.

Most studies on combined effects of pCO_2 and temperature on marine phytoplankton focus on two pCO_2 levels and two temperatures (Feng et al., 2008; Fiorini et al., 2011; Hyun et al., 2014). In comparison to rising pCO_2, increasing surface seawater temperatures normally have a larger effect on photosynthetic carbon fixation and growth rates of marine phytoplankton (Hare et al., 2007; Kremp et al., 2012; Coello-Camba et al., 2014). And influence of temperature on carbon fixation and growth rates may occur irrespective of rising pCO_2 (Hyun et al., 2014).

When measuring at a wide range of temperatures, growth rates of marine phytoplankton display a thermal performance curve (TPC) pattern at present-day pCO_2 level. Until now, few studies investigated the influence of ocean acidification on the TPC pattern of growth rates of phytoplankton. In detail, we do not know how ocean acidification shifts the optimum temperature (*m*), changes the temperature niche width (*w*), and affects the maximal growth rate (V_{max}) or the overall growth rate across all temperatures (*h*) of marine phytoplankton.

When measuring at a broad pCO_2 range, one study showed that when temperatures increase from 15 ^{o}C to 20 ^{o}C or 25 ^{o}C, the maximum growth rates of *E. huxleyi* and *G. oceanica* are stimulated and the optimum pCO_2 levels for growth rates are shifted towards high values (Sett et al., 2014). These may occur in other coccolithophores as well. The reason may be that high temperature could strongly accelerate metabolisms in coccolithophores, and then increase the inorganic carbon requirements for their growth. In comparison to the negative effect of $[H^+]$ when pCO_2 optimum shift towards high levels at high temperatures, the positive effect of increasing carbon substrate on growth possibly dominate. While, at limiting low or inhibiting high

temperatures, we donot know whether photosynthetic carbon fixation, calcification and growth rates of coccolithophores could also display optimum responses to a broad pCO_2 gradient. This is because that at limiting low or inhibiting high temperatures, temperature is the dominant factor determining the metabolisms and then difference in pCO_2 may have less effect on metabolisms.

1.6.4 Combined effects of carbonate chemistry and light intensity on marine phytoplankton.

Dissolved inorganic carbon is the substrate for photosynthesis and calcification of marine phytoplankton. Light is captured and transferred into the energy-conserving compounds NADPH and ATP, which are used to fix CO_2. Thus, CO_2 and light are two essential factors for physiological processes of marine phytoplankton. Under a matrix of low and high levels of pCO_2 and irradiance, combined effects of CO_2 and light on photosynthesis, calcification and growth rates of cyanobacteria, diatoms and coccolithophores have been investigated by several studies (e. g. Xia and Gao, 2003; MacKenzie et al., 2004; Kranz et al., 2010; Rokitta and Rost, 2012). For example, Kranz et al. (2010) showed synergistic stimulating effects of high light (200 compared to 50 μmol photons m^{-2} s^{-1}) and high pCO_2 (900 μatm compared to 150 μatm) on growth and POC production rates of cyanobacterium *Trichodesmium* IMS101. For coccolithophores, a group of calcifying phytoplankton considered particularly sensitive to ocean acidification, Rokitta and Rost (2012) determined that physiological processes are governed primarily by light intensity, and changes in pCO_2 level can exacerbate or weaken the effect of light intensity on these processes. These studies showed that light and pCO_2 act interactively on growth, photosynthetic carbon fixation and calcification rates of phytoplankton. In detail, it means that changing light intensities can decrease or increase the sensitivity of phytoplankton response to pCO_2 in terms of their growth,

carbon fixation and calcification rates. Or changes in pCO_2 levels can inhibit or enhance the light responses of physiological rates of phytoplankton.

When measuring at a range of light intensities at present-day pCO_2, photosynthetic carbon fixation and growth rates of phytoplankton normally increase with increasing light intensity, level off at saturation light intensity and then decline again at inhibiting light intensity (Gao et al., 2012; Li and Campbell, 2013). Recently, ocean acidification was found to modulate the light response curves in terms of carbon fixation and growth rates of diatoms. For the diatoms *P. tricornutum*, *T. pseudonana* and *S. costatum*, Gao et al. (2012) and Li and Campbell (2013) found that at low light intensities (50 to 150 μmol photons m^{-2} s^{-1}) ocean acidification enhanced their carbon fixation and growth rates, however, at high light intensities (above 200 μmol photons m^{-2} s^{-1}) ocean acidification reduced their carbon fixation and growth rates significantly. Gao et al. (2012) suggested that at low light intensity, saved energy from down-regulation of CCMs activity at elevated pCO_2 may lead to higher carbon fixation and growth rates. While, at high light intensity, energy saved at elevated pCO_2 may enhance the photo inhibition and then lead to reduced carbon fixation and growth rates.

As mentioned above, CCM efficiencies differ in different phytoplankton groups (Rost and Riebesell, 2004). For coccolithophores, which possess less efficient CCMs, it is unclear whether growth and carbon fixation rates are also enhanced by ocean acidification at low light intensity while they are synergistically reduced by ocean acidification and high light intensity. In addition, few study focused on how light intensity modulates the optimum response patterns of physiological rates of coccolithophores at a broad pCO_2 range.

1.7 Thesis outline

This thesis reports the effects of the three environmental parameters temperature, pCO_2 and light intensity on the physiological performance of the coccolithophores *Emiliania huxleyi* and *Gephyrocapsa oceanica*. In addition, population- and genotype-specific responses of *E. huxleyi* to a broad range of temperatures and pCO_2 were investigated.

In Chapter 2, we compared the growth rate responses of two *Emiliania huxleyi* populations, and of 5 or 6 *E. huxleyi* genotypes within each population to seven temperatures (8 to 28 ^{o}C). We found that growth rates of the Bergen population were higher at low temperatures, and lower at high temperatures in comparison to the Azores population. Optimum temperature of growth rate of the Bergen population was lower than the Azores population. Within populations, genotype-by-environment (G x E) interactions and phenotypic plasticity were identified. These results were used to discuss a possible role of variation between and within natural *E. huxleyi* population to cope with changing ocean conditions.

In Chapter 3, we investigated the responses of physiological rates of the coccolithophore *G. oceanica* to rising pCO_2 under a variety of light intensities. Rising pCO_2 was found to reduce the maximum values for growth, photosynthetic carbon fixation and calcification rates. In addition, our results imply that optimum pCO_2 for maximum carbon fixation, calcification, and growth rates are shifted towards lower levels by increasing light intensities. Based on this and previous studies, we developed a conceptual frameworks which shows interactive modulating effects of light intensity and pCO_2 level on growth, carbon fixation and calcification rates of coccolithophores.

In Chapter 4, we investigated population- and genotype-specific responses of *E. huxleyi* to a broad pCO_2 range. Growth, photosynthetic carbon fixation and calcification rates of three *E.*

huxleyi populations containing 17 genotypes in total showed optimum responses to a broad pCO_2 gradient (120 to 3070 μatm). Distinct populations were physiologically identified, and differences in CO_2 or pH sensitivity in terms of physiological rates may be related to local pCO_2 variability. G x E interactions, phenotypic plasticity and trade-offs within each population were identified. These results showed that *E. huxleyi* species contains a large number of distinct populations, and each population contains a lot of different genotypes, which allows *E. huxleyi* species to distribute in and acclimate to highly dynamic environments.

References

Armstrong R.A., Lee C., Hedges J.I., Honjo S., Wakeham S.G. (2002) A new, mechanistic model for organic carbon fluxes in the ocean based on the quantitative association of POC with ballast minerals. *Deep-Sea Research* 49: 219–236.

Badger M.R., Andrews T., Whitney S.M., Ludgwig M., Yellowlees D.C., Leggat W., Price G.D. (1998) The diversity and coevolution of Rubisco, plastids, pyrenoids, and chloroplast-based CO_2 -concentrating mechanisms in algae. *Canadian Journal of Botany* 76: 1052–1071.

Bach L.T., Riebesell U., Gutowska M.A., Federwisch L., Schulz K.G. (2015) A unifying concept of coccolithophore sensitivity to changing carbonate chemistry embedded in an ecological framework. *Progress in Oceanography* 135: 125–138.

Bach L.T., Riebesell U., Schulz K.G. (2011) Distinguishing between the effects of ocean acidification and ocean carbonation in the coccolithophore *Emiliania huxleyi*. *Limnology and Oceanography* 56: 2040–2050.

Barcelos e Ramos J., Schulz K.G., Brownlee C., Sett S., Azevedo E.B. (2014) Effects of increasing seawater carbon dioxide concentrations on chain formation of the diatom *Asterionellopsis glacialis*. *PLoS ONE* 9: e90749. doi: 10.1371/journal.pone.0090749

Barrett R.D., Schluter D. (2008) Adaptation from standing genetic variation. *Trends in Ecology & Evolution* 23: 38–44.

Beardall J., Raven J.A. (2004) Potential effects of global change on microalgal photosynthesis, growth and ecology. *Phycologia* 43: 26–40.

Bopp L., Monfray P., Aumont O., Dufresne J.L., Le Treut H., Madec G., Terray L., Orr J.C. (2001) Potential impact of climate change on marine export production. *Global Biogeochemical Cycles* 15: 81–99.

Boyd P.W., Rynearson T.A., Armstrong E.A., Fu F.X., Hayashi K., Hu Z.X., Hutchins D.A., Kudela R.M., Litchman E., Mulholland M.R., Passow U., Strzepek R.F., Whittaker K.A., Yu E., Thomas M.K. (2013) Marine phytoplankton temperature versus growth responses from polar to tropical waters – outcome of a scientific community-wide study. *PLoS ONE* 8: e63091.doi: 10.1371/journal.pone.0063091

Bradshaw A.D. (1965) Evolutionary significance of phenotypic plasticity in plants. *Advances in Genetics* 13: 115–155.

Brand L. E. (1982) Genetic variability and spatial patterns of genetic differentiation in the reproductive rates of the marine coccolithophores *Emiliania huxleyi* and *Gephyrocapsa oceanica*. *Limnology and Oceanography* 27: 236–245.

Buitenhuis E.T., Pangerc T., Franklin D.J., Quéré C.L., Malin G. (2008) Growth rates of six coccolithophorid strains as a function of temperature. *Limnology and Oceanography* 53: 1181–1185.

Burkhardt S., Riebesell U., Zondervan I. (1999) Effects of growth rate, CO_2 concentration, and cell size on the stable carbon isotope fractionation in marine phytoplankton. *Geochimica et Cosmochimica Acta* 63: 3729–3741.

Butler J.N. (1998) Ionic equilibrium: solubility and pH calculations. p. 559. Wiley Interscience, New York, United States of America.

Casteleyn G., Leliaert F., Backeljau T., Debeer A., Kotaki Y., Rhodes L., Lundholm N., Sabbe K., Vyverman W. (2010) Limits to gene flow in a cosmopolitan marine planktonic diatom.

Proceedings of the National Academy of Sciences of the United States of America 107: 12952–12957.

Coello-Camba A., Agustí S., Holding J., Arrieta J.M., Duarte C.M. (2014) Interactive effect of temperature and CO_2 increase in Arctic phytoplankton. *Frontiers in Marine Science* 1: 1–10.

Collins S., Rost B., Rynearson T.A. (2014) Evolutionary potential of marine phytoplankton under ocean acidification. *Evolutionary Applications* 7: 140–155.

Cook S.S., Jones R.C., Vaillancourt R.E., Hallegraeff G.M. (2013) Genetic differentiation among Australian and Southern Ocean populations of the ubiquitous coccolithophore *Emiliania huxleyi* (Haptophyta). *Phycologia* 52: 368–374.

De Jong G. (1990) Quantitative genetics of reaction norms. *Journal of Evolutionary Biology* 3: 447–468.

Dickson A.G. (1981) An exact definition of total alkalinity and a procedure for the estimation of alkalinity and total inorganic carbon from titration data. *Deep-Sea Research* 28: 609–623.

Dickson A.G., Sabine C.L., Christian J.R. (2007) Guide to best practices for ocean CO_2 measurements. *PICES Special Publication* 3: 1–191.

DOE (1994) Handbook of methods for the analysis of the various parameters of the carbon dioxide system in seawater, version 2. In: Dickson A.G. and Goyet C. [Eds.], Carbon dioxide information analysis center. Oak Ridge National Laboratory.

Doney S.C., Fabry V.J., Feely R.A., Kleypas J.A. (2009) Ocean acidification: the other CO_2 problem. *Annual Review of Marine Science* 1: 169–192.

Falkowski P.G., Raven J. (2007) Aquatic photosynthesis (Second Edition). Princeton University Press, Princeton, United States of America.

Feng Y.Y., Warner M.E., Zhang Y.H., Sun J., Fu F.X., Rose J.M., Hutchins D.A. (2008) Interactive effects of increased pCO_2, temperature and irradiance on the marine coccolithophore *Emiliania huxleyi* (Prymnesiophyceae). *European Journal of Phycology* 43: 87–98.

Field C.B., Behrenfeld M.J., Randerson J.T., Falkowski P. (1998) Primary production of the biosphere: integrating terrestrial and oceanic components. *Science* 281: 237–240.

Fiorini S., Middelburg J.J., Gattuso J.P. (2011) Effects of elevated CO_2 partial pressure and temperature on the coccolithophore *Syracosphaera pulchra*. *Aquatic Microbial Ecology* 64: 221–232.

Gao K., Xu J., Gao G., Li Y., Hutchins D.A., Huang B.Q., Wang L., Zheng Y., Jin P., Cai X., Häder D.P., Li W., Xu K., Liu N., Riebesell U. (2012) Rising CO_2 and increased light exposure synergistically reduce marine primary productivity. *Nature Climate Change* 2: 519–523.

Giordano M., Beardall J., Raven J.A. (2005) CO_2 concentrating mechanisms in algae: mechanisms, environmental modulation and evolution. *Annual Review of Plant Biology* 56: 99–131.

Godhe A., Egardt J., Kleinhans D., Sundqvist L., Hordoir R., Jonsson P.R. (2013) Seascape analysis reveals regional gene flow patterns among populations of a marine planktonic diatom. *Proceedings of the Boyal Society B* 280: 20131599.doi: 10.1098/rspb.2013.1599

Gsell A.S., De Senerpont-Domis L.N., Przytulska-Bartosiewicz A., Mooij W.M., Van Donk E., Ibelings B.W. (2012) Genotype-by-temperature interactions may help to maintain clonal diversity in *Asterionella Formosa* (Bacillariophyceae). *Journal of Phycology* 48: 1197–1208.

Hansen J., Sato M., Ruedy R., Lo K., Lea D.W., Medina-Elizade M. (2006) Global temperature change. *Proceedings of the National Academy of Sciences of the United States of America*

103: 1428–14293.

Hansson I. (1973) A new set of pH-scales and standard buffers for sea water. *Deep-Sea Research* 20: 479–491.

Hare C.E., Leblanc K., DiTullio G.R., Kudela R.M., Zhang Y.H., Lee P.A., Riseman S., Hutchins D.A. (2007) Consequences of increased temperature and CO_2 for phytoplankton community structure in the Bering Sea. *Marine Ecology Progress Series* 352: 9–16.

Heinze C. (2004) Simulating oceanic $CaCO_3$ export production in the greenhouse. *Geophysical Research Letters* 31: L16308. doi: 10.1029/2004GL020613.

Holligan P.M. (1992) Do marine phytoplankton influence global climate? In: Falkowski P.G. and Woodhead A.D. [Eds.], Primary productivity and biogeochemical cycles in the sea. pp. 487–501. Plenum Press, New York, United States of America.

Hopkinson B.M., Dupont C.L., Allen A.E., Morel F.M.M. (2011) Efficiency of the CO_2-concentrating mechanism of diatoms. *Proceedings of the National Academy of Sciences of the United States of America* 8: 3830– 3837.

Hoppe C.J.M., Langer G., Rost B. (2011) *Emiliania huxleyi* shows identical responses to elevated pCO_2 in TA and DIC manipulations. *Journal of Experimental Marine Biology and Ecology* 406: 54–62

Houghton J.T., Ding Y., Griggs D.J., Noguer M., van der Linden P.J., Xiao S.D., Maskell K., Johnson C.A. (2001) Climate change 2001: the scientific basis. pp. 36–40. Cambridge University Press, Cambridge, United Kingdom.

Huey R.B., Kingsolver J.G. (1979) Integrating thermal physiology and ecology of ectotherms: A discussion of approaches. *American Zoologist* 19: 357–366.

Hutchinson G.E. (1961) The paradox of the plankton. *The American Naturalist* 95: 137–145.

Hyun B., Choi K.H., Jang P.G., Jang M.C., Lee W.J., Moon C.H., Shin K. (2014) Effects of increased CO_2 and temperature on the growth of four diatom species (*Chaetoceros debilis*, *Chaetoceros didymus*, *Skeletonema costatum* and *Thalassiosira nordenskioeldii*) in laboratory experiments. *Journal of Environmental Science International* 23: 1003–1012.

Intergovernmental Panel on Climate Change (2013) Climate Change 2013: The Physical Science Basis. Contribution of Working Group I to the Fifth assessment report of the Intergovernmental Panel on Climate Change. pp. 5–12. Cambridge University Press, Cambridge, United Kingdom.

Izem R., Kingsolver J.G. (2005) Variation in continuous reaction norms: Quantifying directions of biological interest. *The American Naturalist* 166: 277–289.

Joos F., Plattner G.K., Stocker T.F., Marchal O., Schmittner A. (1999) Global warming and marine carbon cycle feedbacks on future atmospheric CO_2. *Science* 284: 464–464.

Kaeriyama H., Katsuki E., Otsubo M., Yamada M., Ichimi K., Tada K., Harrison P.J. (2011) Effects of temperature and irradiance on growth of strains belonging to seven *Skeletonema* species isolated from Dokai Bay, southern Japan. *European Journal of Phycology* 46: 113–124.

Kranz S.A., Levitan O., Richter K.U., Prášil O., Berman-Frank I., Rost B. (2010) Combined effects of CO_2 and light on the N_2-fixing cyanobacterium *Trichodesmium* IMS101: physiological responses. *Plant Physiology* 154: 334–345.

Kremp A., Godhe A., Egardt J., Dupont S., Suikkanen S., Casabianca S., Penna A. (2012) Intraspecific variability in the response of bloom-forming marine microalgae to changed

climate conditions. *Ecology and Evolution* 2: 1195–1207.

Krug S.A., Schulz K.G., Riebesell U. (2011) Effects of changes in carbonate chemistry speciation on *Coccolithus braarudii*: a discussion of coccolithophorid sensitivities. *Biogeosciences* 8: 771–777.

Langer G., Geisen M., Baumann K.H., Kläs J., Riebesell U., Thoms S., Young J.R. (2006) Species-specific responses of calcifying algae to changing seawater carbonate chemistry. *Geochemistry Geophysics Geosystems* 7: 1–12.

Lewis R.J., Jensen S.I., DeNicola D.M., Miller V.I., Hoagland K.D., Ernst S.G. (1997) Genetic variation in the diatom *Fragilaria capucina* (*Fragilariaceae*) along a latitudinal gradient across North America. *Plant Systematics and Evolution* 204: 99–108.

Li G., Campbell D.A. (2013) Rising CO_2 interacts with growth light and growth rate to alter photosystem II photoinactivation of the coastal diatom *Thalassiosira pseudonana*. *PLoS ONE* 8: e55562. doi:10.1371/journal.pone.0055562.

Lohbeck K.T., Riebesell U., Reusch T.B.H. (2012) Adaptive evolution of a key phytoplankton species to ocean acidification. *Nature Geoscience* 5: 346–351.

MacKenzie T.D.B., Burns R.A., and Campbell D.A. (2004) Carbon status constrains light acclimation in the cyanobacterium *Synechococcus elongates*. *Plant Physiology* 136: 3301–3312.

Matear R.J., Hirst A.C. (1999) Climate change feedback on the future oceanic CO_2 uptake. *Tellus* 51B: 722–733.

McCarthy A., Rogers S.P., Duffy S.J., Campbell D.A. (2012) Elevated carbon dioxide differentiation alters the photophysiology of *Thalassiosira pseudonana* (Bacillariophyceae) and *Emiliania huxleyi* (Haptophyta). *Journal of Phycology* 48: 635–646.

Monastersky R. (2013) Global carbon dioxide levels near worrisome milestone. *Nature* 497: 13–14.

Moroney J.V., Ynalvez R.A. (2007) Proposed carbon dioxide concentrating mechanism in *Chlamydomonas reinhardtii*. *Eukaryotic Cell* 6: 1251–1259.

Portis A.R., Salvucci M.E., Ogren W.L. (1986) Activation of Ribulosebisphosphate Carboxylase/Oxygenase at physiological CO_2 and Ribulosebisphosphate concentrations by Rubisco activase. *Plant Physiology* 82: 967–971.

Raven J. A. (1991) Physiology of inorganic C acquisition and implications for resource use efficiency by marine phytoplankton: relation to increased CO_2 and temperature. *Plant Cell and Environment* 14: 779–794.

Raven J.A., Johnston A.M. (1991) Mechanisms of inorganic-carbon acquisition in marine phyoplankton and their implications for the use of other resources. *Limnology and Oceanography* 36: 1701–1714.

Reusch T.B., Boyd P.W. (2013) Experimental evolution meets marine phytoplankton. *Evolution* 67: 1849–1859.

Reusch T.B.H. (2014) Climate change in the oceans: evolutionary versus phenotypically plastic responses of marine animals and plants. *Evolutionary Applications* 7: 104–122.

Riebesell U., Körtzinger A., Oschlies A. (2009) Sensitivities of marine carbon fluxes to ocean change. *Proceedings of the National Academy of Sciences of the United States of America* 106: 20602–20609.

Riebesell U., Tortell P.D. (2011) Effects of ocean acidification on pelagic organisms and

ecosystems. In: Gattuso J.P. and Hansson L. [Eds.], Ocean acidification. pp. 99–121. Oxford University Press, Oxford, United Kingdom.

Riebesell U., Zondervan I., Rost B., Tortell P.D., Zeebe R.E., Morel F.M.M. (2000) Reduced calcification of marine plankton in response to increased atmospheric CO_2. *Nature* 407: 364–367.

Rokitta S.D., Rost B. (2012) Effects of CO_2 and their modulation by light in the life-cycle stages of the coccolithophore *Emiliania huxleyi*. *Limnology and Oceanography* 57: 607–618.

Rost B., Riebesell U. (2004) Coccolithophores and the biological pump: responses to environmental changes. In: Thierstein H.R. and Young J.R. [Eds.], Coccolithophores: from molecular biology to global impact. pp. 99–125. Springer, Berlin, Germany.

Rost B., Riebesell U., Sültemeyer D. (2006) Carbon acquisition of marine phytoplankton: Effect of photoperiod length. *Limnology and Oceanography* 51: 12–20.

Rynearson T.A., Armbrust E.V. (2004) Genetic differentiation among populations of the planktonic marine diatom *Ditylum Brightwellii* (*Bacillariophyceae*). *Journal of Phycology* 40: 34–43.

Sabine C.L, Feely R.A., Gruber N., Key R.M., Lee K., Bullister J.L., Wanninkhof R., Wong C.S., Wallace D.W.R., Tilbrook B., Millero F.J., Peng T.H., Kozyr A., Ono T., Rios A.F. (2004) The oceanic sink for anthropogenic CO_2. *Science* 305: 367–371.

Sarmiento J.L., Slater R., Barber R., Bopp L., Doney S.C., Hirst A.C., Kleypas J., Matear R., Mikolajewicz U., Monfray P., Soldatov V., Spall S.A., Stouffer R. (2004) Response of ocean ecosystems to climate warming. *Global Biogeochemical Cycles* 18: GB3003. doi: 10.1029/2003GB002134

Schlüter L., Lohbeck K.T., Gutowska M.A., Gröger J.P., Riebesell U., Reusch T.B.H. (2014) Adaptation of a globally important coccolithophore to ocean warming and acidification. *Nature Climate Change* 4: 1024–1030.

Sett S., Bach L.T., Schulz K.G., Koch-Klavsen S., Lebrato M., Riebesell U. (2014) Temperature modulates coccolithophorid sensitivity of growth, photosynthesis and calcification to increasing seawater pCO_2. *PLoS ONE* 9: E88308. doi:10.1371/journal.pone.0088308

SoliA.L., Byrne R.H. (2002) CO_2 system hydration and dehydration kinetics and the equilibrium CO_2/H_2CO_3 ratio in aqueous NaCl solution. *Marine Chemistry* 78: 68–73.

Sundquist E.T.G. (1985) Geological perspectives on carbon dioxide and the carbon cycle. In: Sundquist E.T. and Broecker W.S. [Eds.], The carbon cycle and atmospheric CO_2: natural variations Archean to present. pp 5–59. Geophysical Monograph 32, American Geophysical Union Washington, D.C., United States of America.

Suzuki Y., Takahashi M. (1995) Growth responses of several diatom species isolated from various environments to temperature. *Journal of Phycology* 31: 880—888.

Taraldsvik M., Myklestad S. (2000) The effect of pH on growth rate, biochemical composition and extracellular carbohydrate production of the marine diatom *Skeletonema costatum*. *European Journal of Phycology* 35: 189–194.

Thomas M.K., Kremer C.T., Klausmeier C.A., Litchman E. (2012) A global pattern of thermal adaptation in marine phytoplankton. *Science* 338: 6110, 1085–1088.

Thornton D.C. (2009) Effect of low pH on carbohydrate production by a marine planktonic diatom(*Chaetoceros muelleri*). *Research Letters in Ecology* 2009: 105901. doi: 10.1155/2009/105901

Volk T., Hoffert M.I. (1985) Ocean carbon pumps: analysis of relative strengths and efficiencies in ocean-driven atmospheric CO_2 changes. In: Sundquist E.T. and Broecker W.S. [Eds.],The carbon cycle and atmospheric CO_2: natural variations Archean to present. pp 99–110. Geophysical Monograph 32, American Geophysical Union Washington, D.C., United States of America.

Westbroek P., Brown C.W., van Bleijswijk J., Brownlee C., Brummer G.J., Conte M., Egge J., Fernández E., Jordan R., Knappertsbusch M., Stefels J., Veldhuis M., van der Wal P., Young J. (1993) A model system approach to biological climate forcing. The example of *Emiliania huxleyi*. *Global and Planetary Change* 8: 27–46.

White D. (2007) The physiology and biochemistry of prokaryotes (Third Edition). Oxford University Press, Oxford, United Kingdom.

Wolf-Gladrow D.A., Zeebe R.E., Klaas C., Körtzinger A., Dickson A.G. (2007) Total alkalinity: The explicit conservative expression and its application to biogeochemical processes. *MarineChemistry* 106: 287–300.

Wu Y., Gao K., Riebesell U. (2010) CO_2-induced seawater acidification affects physiological performance of the marine diatom *Phaeodactylum tricornutum*. *Biogeosciences* 7: 2915–2923.

Xia J., Gao K. (2003) Effects of doubled atmospheric CO_2 concentration on the photosynthesis and growth of *Chlorella pyrenoidosa* cultured at varied levels of light. *Fisheries Science* 69: 767–771.

Zeebe R.E., Wolf-Gladrow D.A. (2001) CO_2 in seawater: equilibrium, kinetics, isotopes. p 24. Elsevier, Amsterdam, the Netherlands.

Chapter 2: Between- and within-population variations in thermal reaction norms of the coccolithophore *Emiliania huxleyi*

Limnol. Oceanogr., 59(5), 2014, 1570–1580

doi:10.4319/lo.2014.59.5.1570

Between- and within-population variations in thermal reaction norms of the coccolithophore *Emiliania huxleyi*

Yong Zhang,[1] Regina Klapper,[2,a] Kai T. Lohbeck,[1,2] Lennart T. Bach,[1] Kai G. Schulz,[1,b] Thorsten B. H. Reusch,[2] and Ulf Riebesell[1,*]

[1] Biological Oceanography, GEOMAR Helmholtz-Centre for Ocean Research Kiel, Kiel, Germany
[2] Evolutionary Ecology of Marine Fishes, GEOMAR Helmholtz-Centre for Ocean Research Kiel, Kiel, Germany

Abstract

Thermal reaction norms for growth rates of six *Emiliania huxleyi* isolates originating from the central Atlantic (Azores, Portugal) and five isolates from the coastal North Atlantic (Bergen, Norway) were assessed. We used the template mode of variation model to decompose variations in growth rates into modes of biological interest: vertical shift, horizontal shift, and generalist–specialist variation. In line with the actual habitat conditions, isolates from Bergen (Bergen population) grew well at lower temperatures, and isolates from the Azores (Azores population) performed better at higher temperatures. The optimum growth temperature of the Azores population was significantly higher than that of the Bergen population. Neutral genetic differentiation was found between populations by microsatellite analysis. These findings indicate that *E. huxleyi* populations are adapted to local temperature regimes. Next to between-population variation, we also found variation within populations. Genotype-by-environment interactions resulted in the most pronounced phenotypic differences when isolates were exposed to temperatures outside the range they naturally encounter. Variation in thermal reaction norms between and within populations emphasizes the importance of using more than one isolate when studying the consequences of global change on marine phytoplankton. Phenotypic plasticity and standing genetic variation will be important in determining the potential of natural *E. huxleyi* populations to cope with global climate change.

The increase of atmospheric carbon dioxide concentrations is projected to result in a global mean temperature increase by up to 4°C until the end of this century (Intergovernmental Panel on Climate Change 2013), resulting in a concomitant warming of the surface ocean. Ocean warming will affect marine organisms and likely result in migration, adaptation, or extinction (Thomas et al. 2012; Reusch 2014; Winter et al. 2013). The coccolithophore *Emiliania huxleyi* is the most abundant calcifying phytoplankton species in contemporary oceans. It is distributed from the tropics to high-latitude regions and from midocean to inshore waters with temperature ranges from 2°C to 28°C (McIntyre and Bé 1967). A recent genome study revealed large genomic differences in isolates from several ocean regions and suggests that *E. huxleyi* is a species complex that may partly explain its wide distribution range (Read et al. 2013). A wealth of studies has focused on the effects of ocean change on growth, calcification, and photosynthesis in *E. huxleyi* (Riebesell and Tortell 2011). However, most rely on a single isolate that is considered to be representative for the *E. huxleyi* species complex. It has been argued that besides the phenotypic variability of a single isolate, the genotypic variability that is commonly found between different isolates will also be important to understand responses of natural phytoplankton populations to ocean change (Kremp et al. 2012; Schaum et al. 2012; Tatters et al. 2013).

Various factors, such as nutrient concentrations (Fernández et al. 1996) or frontal boundaries formed by ocean currents (Palumbi 1994), may drive the distribution of phytoplankton in the oceans. As a consequence of ocean boundaries, populations may get separated and allow local adaptation to the respective environment (Leducq et al. 2014). Populations can adapt to their local environment either through selection of new, beneficial mutations or through selection on existing genetic variation (Collins et al. 2013; Reusch 2014). High-standing genetic variation is commonly found in phytoplankton populations (Medlin et al. 2000; Rynearson and Armbrust 2004; Iglesias-Rodríguez et al. 2006) and likely translates into phenotypic variability (Kremp et al. 2012; Schaum et al. 2012; Boyd et al. 2013). Phenotypic plasticity is the ability of a genotype to change its phenotype across environments (Bradshaw 1965) and can be assessed by the reaction norm of a particular trait (Boyd et al. 2013; Reusch 2014). When comparing reaction norms, a genotype-by-environment (G × E) interaction is evident when the phenotypic response of a genotype varies across environments or when distinct genotypes perform differently across these environmental conditions (De Jong 1990). In fact, such variation among genotypes within a population is the raw material for rapid adaptive evolution in the face of global change (Sgrò and Hoffmann 2004). Within a single trait, associated fitness cannot be maximized at all environmental conditions, which results in a trade-off (Agrawal et al. 2010). For

* Corresponding author: uriebesell@geomar.de

Present addresses:
[a] Department of Safety and Quality of Milk and Fish Products, Federal Research Institute for Nutrition and Food, Max Rubner-Institute, Hamburg, Germany
[b] Centre for Coastal Biogeochemistry, School of Environmental Science and Management, Southern Cross University, Lismore, NSW, Australia

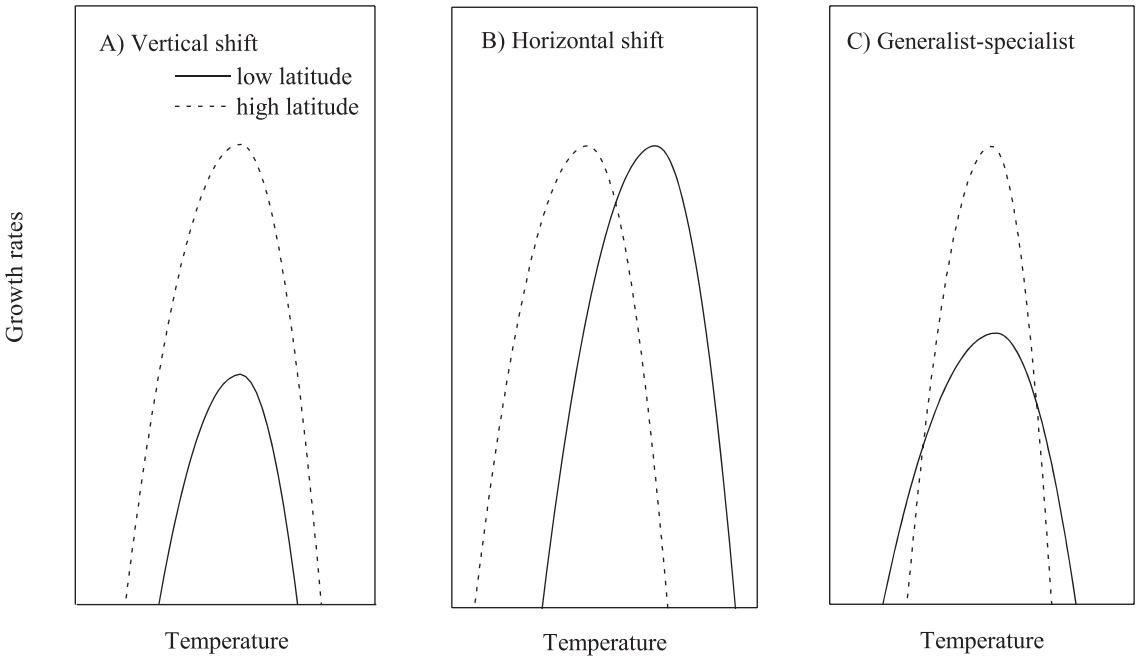

Fig. 1. Three theoretical models for variation in thermal reaction norms. (A) Vertical shift model, which represents variation in overall growth rates across all temperatures and vertical shift variation, is linear and totally explained by one principal component. (B) Horizontal shift model, which represents variation in the location of the maximum growth rates and horizontal shift variation, is nonlinear and not simply explained by one principal component. (C) Generalist–specialist model, which represents variation in the width of the growth rates curves and trade-off between width and maximal growth rates. Generalist–specialist variation is also nonlinear and totally explained by three principal components.

example, primary productivity often cannot be maximized at high and low temperatures at the same time, resulting in trade-offs in thermal tolerance (Gsell et al. 2012).

Thermal reaction norms in phytoplankton have been well studied, although often only a limited temperature range was covered (Thomas et al. 2012). Measuring the growth rates of 73 *E. huxleyi* isolates at 16°C and 26°C, Brand (1982) concluded that low-latitude *E. huxleyi* populations are adapted to higher temperature and grow better at 26°C than those inhabiting the high-latitude regions. Optimum growth temperatures were found to be significantly lower for high-latitude than low-latitude *E. huxleyi* isolates (Conte et al. 1998). Buitenhuis et al. (2008) observed that *E. huxleyi* has a wider temperature range than three other coccolithophores, which may be related to its cosmopolitan distribution. However, different ocean regions may harbor locally adapted populations with genotypes that have very different temperature sensitivities. In order to address this question, we investigated whether variation in the physiological tolerance range between genotypes from different temperature regimes is larger than between distinct genotypes from the same location.

We assessed reaction norms over the entire temperature tolerance range using thermal performance curves (TPC), which describe the continuous phenotypic variation produced by a given isolate as a function of an environmental factor (Huey and Stevenson 1979). The common shape of a TPC is an increase in performance with increasing temperature until reaching a maximum, followed by a steep drop in performance (Huey and Stevenson 1979). Huey and Kingsolver (1989) developed a model that decomposes the variation in thermal reaction norms into three modes of biological interest: performance as vertical shift (*h*; Fig. 1A), optimal temperature as horizontal shift of maximal performance (*m*; Fig. 1B), and generalist–specialist trade-off as width (*w*; Fig. 1C). The template mode of variation (TMV) model not only decomposes the variation into predetermined modes of variation for a particular set of thermal performance curves but also quantifies the contributions of predicted modes of variation (Izem and Kingsolver 2005).

In this study, we compared *E. huxleyi* isolates from Bergen, Norway, and from the Azores, Portugal, at seven temperatures ranging from 8°C to 28°C. Single-cell isolates were raised to monoclonal populations and verified by microsatellite markers and therefore in the following are referred to as genotypes. We applied the TMV model to estimate the relative importance of the three biological modes in differentiation between populations. Further, variations within populations were compared across measured temperatures. Neutral genetic markers were used to investigate gene flow between populations and population structure. Based on our results, a possible role of variation between and within natural *E. huxleyi* populations to cope with changing ocean conditions is discussed.

Methods

Cell isolation sites and culture conditions—E. huxleyi (Lohm.) Hay and Mohler (morphotype A) genotypes 96,

Table 1. Sea surface temperatures (SST) for the Azores and Bergen.

	Location	Mean monthly SST range (°C)	Minimum monthly SST (°C)	Maximum monthly SST (°C)	References
Azores	38°34′N, 28°42′W	15.6–22.3	12.6	32.9	Wisshak et al. (2010)
Bergen	60°18′N, 05°15′E	6.0–16.0	−2	16.6	Samuelsen (1970); Locarnini et al. (2006)

85, 75, 73, 63, 62, 51, 42, 41, and 17 were isolated by K. T. Lohbeck from the Raunefjord, southwest of Bergen (60°18′N, 05°15′E), in May 2009, and *E. huxleyi* genotypes M23, M22, M21, M19, M17, M16, M13, M10, M8, and M7 were isolated by S. L. Eggers near Faial, at the Azores (38°34′N, 28°42′W), in May or June 2010. Sea surface temperatures (SST) range from 6.0°C to 16.0°C off Bergen (Locarnini et al. 2006; Samuelsen 1970) and from 15.6°C to 22.3°C at the Azores (Wisshak et al. 2010; Table 1). Stock cultures were kept at 15°C in 50 mL tissue culture flasks (Sarstedt) with ventilation caps. The cultures were grown in monoclonal, nonaxenic populations. Regularly performed automated cell counts and microscopic inspections verified that no significant bacterial fraction was present.

Artificial seawater (ASW) was prepared according to Kester et al. (1967), but with the addition of 2380 μmol kg^{-1} bicarbonate (Merck), resulting in initial concentrations of 2380 μmol kg^{-1} total alkalinity (TA) and dissolved inorganic carbon (DIC) at a salinity of 35. ASW was enriched with 64 μmol kg^{-1} nitrate (NO_3^-), 4 μmol kg^{-1} phosphate (PO_4^{3-}), f/8 concentrations for trace metals and vitamins (Guillard and Ryther 1962), 10 nmol kg^{-1} SeO_2 (Danbara and Shiraiwa 1999), and 2 mL kg^{-1} of sterile filtered (0.2 μm pore size, Sartobran P 300, Sartorius) North Sea water to prevent possible trace metal limitation during culturing. Enriched ASW was aerated with sterile ambient air (0.2 μm pore size, Midisart 2000 PTFE, Sartorius) with about 40 Pa ($\approx$ 400 μatm) partial pressure of CO_2 (P_{CO_2}) for 48 h at each temperature in a temperature-controlled incubation chamber (Rumed Rubarth Apparate GmbH). The dry air was humidified with Mill-Q water before aeration of the ASW to minimize evaporation. A 10 liter polycarbonate bottle was covered with insulation foil to minimize temperature exchange during filling of the culture flasks at room temperature. After aeration, the ASW medium was sterilized by gentle pressure filtration (0.2 μm pore size, Sartobran P 300) and carefully pumped into autoclaved 310 mL Duran square flasks (Schott). The flasks were filled with ASW medium leaving a minimum headspace of $\sim$ 1% to minimize gas exchange. The culture flasks were stored at treatment temperature until inoculation. Experimental cultures were kept in a RUMED Light Thermostat (Rubarth Apparate GmbH) at a photon flux density of 160 $\pm$ 5 μmol m^{-2} s^{-1} and a 16 : 8 light : dark cycle. Culture flasks were manually rotated twice a day at 5 and 12 h after the onset of the light phase to reduce sedimentation of the cells.

Experimental setup and procedures—For the temperature experiment, *E. huxleyi* genotypes 85, 75, 63, 62, 41, and 17 from Bergen and M23, M22, M21, M19, M13, and M10 from the Azores were grown at 8°C, 15°C, 18°C, 22°C, 26°C, 27°C, and 28°C. Bergen genotype 75 was contaminated with a significant bacteria fraction and therefore excluded from the analysis. Genotypes sharing the same isolation site are referred to as a "population." Each genotype was grown in five replicates. Prior to the start of the experiment, genotypes were acclimated to the experimental conditions for six to eight generations at 15°C and thereafter for another six to eight generations at the target temperature, followed by the temperature assay.

Cell densities were assessed using a Z2 Coulter Particle Count and Size Analyzer (Beckman). Exponential growth rates (μ) were calculated for each replicate according to

$$\mu = (\ln N_1 - \ln N_0)/d \quad (1)$$

where N_0 and N_1 are cell densities at the beginning and the end of a growth interval and d is the duration of the growth period in days. A dilute batch cycle started with an initial inoculum of about 100,000 cells ($\sim$ 320 cells mL^{-1}). To minimize changes in carbonate chemistry due to algal growth, cultures were transferred into the next dilute batch cycle before cell concentrations reached 100,000 cells mL^{-1}. A maximum DIC drawdown of 9% was calculated based on final cell numbers and cellular carbon quotas of *E. huxleyi* (Bach et al. 2011). The duration of a batch cycle were 10 (Bergen) and 12 (Azores) d in the 8°C treatment; 5 d in the 15°C, 27°C, and 28°C treatments; 3 d in the 22°C treatment; and 4 d in the 18°C and 26°C treatments. *E. huxleyi* genotype 17 was cultured 11 d at 27°C due to slow growth rates.

Carbonate chemistry sampling and measurements—Before inoculation, DIC samples were taken from culture media of each dilute batch cycle and were measured by an infrared CO_2 analyzer system (Automated Infra Red Inorganic Carbon Analyzer, Marianda). TA was measured from all treatments by open-cell potentiometric titration using a Metrohm Basic Titrino 794 according to Dickson et al. (2003). DIC and TA measurements were used to calculate CO_2 partial pressure in the ASW using the CO_2 System Calculations in MS Excel software (Lewis and Wallace 1998). Calculated P_{CO_2} and pH (on the total scale) were on average 45.3 $\pm$ 6.1 Pa and 8.007 $\pm$ 0.051, respectively.

TMV—Growth rates of each *E. huxleyi* genotype were predicted to show a thermal performance curve (TPC) shape along the temperature gradient. We used the TMV approach from Izem and Kingsolver (2005) to decompose the variation of growth rates into modes of biological

interest. The TMV model fits a common shape $z(t)$ for the growth rates over all data points (Fig. 1). We evaluated the fit of the predetermined common shape to the growth rates by rescaling the growth rates with respect to parameter estimates (h, m, w) for each genotype.

The first criterion was continuity, which can be described as

$$z_{i,j} = z_i(t_j) + \varepsilon_{i,j}; j \in \{1, \ldots, J\}, i \in \{1, \ldots, I\} \quad (2)$$

where t_j is the jth temperature t, i is the number of genotypes, and $\varepsilon_{i,j}$ represents technical or experimental errors. In the function (2), J is the number of the investigated temperatures, and I is the number of the investigated genotypes. In this study, $J = 7$ and $I = 11$. Then the common shape $z(t)$ for the TPC was generated using the following model with three parameters:

$$z_i = h_i + \frac{1}{w_i} z\left[\frac{1}{w_i}(t - m_i)\right] \quad (3)$$

where z_i is the common template shape of the curves for all genotypes. For each genotype i, the parameter h_i is the average growth rate, m_i is the optimum temperature, and w_i is the width and describes the generalist–specialist mode of variation. The common template shape $z(t)$ can be fitted using a polynomial of any degree. Since a polynomial of higher degree generally fits the data better, we chose to use the fourth-order polynomial, which also minimized the sum of squared errors. For further details, *see* Izem and Kingsolver (2005). Note that height h_i as defined here indicates the overall or ''average'' growth rates across all temperatures, not just the maximum growth rates at the optimal temperature. The maximum growth rate at the optimal temperature for each curve was obtained by the equation

$$z_{\max} = h_i + z(0)\frac{1}{w_i} \quad (4)$$

Data analyses—Parameters h, m, and w were calculated using Matrix Laboratory (MATLAB 7. 14, The MathWorks), and the scripts were provided by Izem and Kingsolver (2005). Statistical analyses were performed using R (version 2.15.2). The mean growth rate of five replicates and temperature were used to fit the growth rate curve and calculate h, m, and w for each genotype. A two-way ANOVA was conducted to examine the effect of population, temperature, and their interactions on growth rates. A one-way ANOVA was performed to test the statistical significance in h, m, and w between the Bergen and the Azores populations with ''population'' as predictor, and h, m, or w as response variable. A Tukey post hoc test was used to test for the genotype differentiation within a population when the ANOVA was significant. An F-test was used to test for variance differences between and within the populations. Further, a Levene test was conducted to test for homogeneity of variances in case of significant data, and a generalized least squares model was used to stabilize heterogeneity if variances were inhomogeneous. Normality was tested with a Shapiro–Wilk test.

Microsatellite genotyping—To test for neutral genetic variation between genotypes of the same and different origin, we used microsatellite genotyping with *E. huxleyi* specific primers (Iglesias-Rodríguez et al. 2006). Ten primers were tested, of which five primers—EHMS15, EHMS37, P02B12, P02F11, and P02E09—could be applied with reproducible results and variable alleles between populations and genotypes. Note that all 10 genotypes from each population were used for the microsatellite analysis. However, only six genotypes per population were chosen for the temperature experiment due to limited space in the climate chambers. For deoxyribonucleic acid (DNA) extraction, cells were filtered onto Cyclopore track-etched polycarbonate filters (0.8 μm pore size, Whatman). The filters were washed with 500 μL freshly sterile filtered ASW, and the cell suspension was transferred into Eppendorf tubes, which were centrifuged (5424 Centrifuge) for 10 min at 2348 relative centrifugal force. The supernatant was discarded, and the cell pellet was stored at -20°C. DNA was extracted using an Invisorb Spin Tissue Minikit (Invitek) according to the manufacturer's protocol. DNA concentration was measured with a Nanodrop spectrophotometer (Thermo Scientific). Microsatellite loci were amplified with the Dream Taq polymerase (Thermo Scientific) using 1 μL forward and reverse 6-carboxyfluorescein (Fam)- and hexachlorofluoresceine (Hex)-labeled primers per 10 μL reaction. The polymerase chain reaction (PCR) conditions were 3 min denaturation at 94°C, followed by 27 cycles of denaturation at 94°C, a primer-specific annealing temperature (*see* Table 2), and an elongation at 72°C for 1 min each step and a final elongation of 10 min at 72°C. One microliter of the PCR product was used for fragment length analysis on an Applied Biosystems 3130xL automated sequencer. Allele sizes were called automatically and afterward manually checked using GeneMarker version 1.85 (SoftGenetics LLC) against the size standard Rox350 (Applied Biosystems).

Genetic differentiation analysis—Allele frequencies, observed (H_o) and expected (H_e) heterozygosity, and deviation from the Hardy–Weinberg equilibrium (HWE) for each locus were calculated using the software Arlequin version 3.5 (Excoffier et al. 2005). Further, Wright's Fixation Index (F_{ST}) was used to assess population structure with the software Arlequin version 3.5 (Wright 1978). F_{ST}-values can range from 0, meaning a lack of differentiation, to 1, meaning that compared groups are distinct. Values of 0.05 show little genetic differentiation, 0.05–0.15 moderate genetic differentiation, 0.15–0.25 large genetic differentiation, and finally > 0.25 very large genetic differentiation (Wright 1978). The microsatellite data were analyzed for null alleles using the software Microchecker version 2.2.3 (van Oosterhout et al. 2004), with null allele frequencies tested by the method of Brookfield (1996). To detect the structure of the ''populations'' without any a priori assumptions, the Bayesian clustering algorithm implemented in Structure version 2.3.3 was applied to detect potential structuring among genotypes (Pritchard et al. 2000). A genetic admixture model was used with a burn-in period of 10,000

Table 2. Applied microsatellite primers for *E. huxleyi* (Iglesias-Rodríguez et al. 2006). Last column gives the optimized annealing temperatures used for PCR amplification. EMBL, European Molecular Biology Laboratory.

Locus	Primer sequence	EMBL accession number	Sequenced repeat motif	Annealing temperature PCR (°C)
EHMS15	F: TCGAGGCGCGTCACACAC	AJ487304	(GT)27GC	54
	R: GCGAGCGGTGGGCAATGT	AJ487305	(GT)9	
EHMS37	F: TGTGAGAGTGAGCACGCA	AJ494737	(GT)23	60
	R: TTGAGGAGGATTACGAGGTC	AJ494738		
P02B12	F: GGTTAATCGCAGCAAAGAGC	AJ487309	(GT)10	58
	R: CAGTCTTGATCGGGAACGA	AJ487311		
P02F11	F: CTCGTGTGGCTATGCCTATG	AJ487316	(GT)11	58
	R: TCCAAGAGCAAAGTGCAAAA	AJ487317		
P02E09	F: ACTCGGACTGGACGCACA	AJ494741	(GT)9	60
	R: GGCTGCTCTTCCCCTCTCTA	AJ494742		

reiterations and 100,000 Markov chain Monte Carlo iterations under default settings with number of clusters (K) varying from one to five. In order to detect the most likely number of genetic clusters, the post hoc function ΔK after Evanno et al. (2005) was used.

Results

Genetic structure—For the 10 analyzed isolates per population, the number of alleles varied between two and nine. A higher number of alleles among all loci were found in the Azores population compared to the Bergen population (Table 3). Heterozygote deficiencies were found in two of five tested loci in the Azores population (Markov chain method, $p < 0.05$). Table 3 gives H_o and H_e heterozygosities for both populations at each locus. H_e ranged from 0.19 to 0.92 and H_o varied between 0 and 1. In the Azores population, H_o varied between 0.22 and 0.89 and revealed heterozygote deficiencies at two of five loci tested. Evidence for null alleles was found in loci P02B12 and EHMS37. In the Bergen group, H_o varied between 0 and 1, and no deviation from the HWE was detected. Pairwise comparison revealed a significant population differentiation with an F_{ST} of 0.148 ($p < 0.01$). This complies with a moderate to strong genetic differentiation according to Wright (1978). Note that for the temperature experiment, only six genotypes per population were used, whereas the microsatellite analysis included four additional genotypes per population from stock cultures maintained at the GEOMAR Helmholtz-Centre for Ocean Research, Kiel, Germany. The structure analysis revealed a most likely number of genetic clusters of K = 2; thus, two distinct groups could be detected.

Between-population variation in growth rates—There was a temperature- and temperature versus population interaction-effect on growth rates (two-way ANOVA, $F_6 = 511.34$ for temperature treatments, $F_6 = 33.10$ for interaction, both $p < 0.001$). Growth rates of *E. huxleyi* genotypes in both populations initially increased with increasing temperature, reached a maximum, and then declined with further temperature increase (Fig. 2). The Bergen population grew faster at 8°C (ANOVA, $F_1 = 25.89$, $p < 0.001$) and failed to grow at 28°C. The Azores population grew slightly faster at 26°C and 27°C (ANOVA, $F_1 = 1.379$ for 26°C treatment, $F_1 = 0.481$ for 27°C treatment, both $p > 0.05$) and can still grow at 28°C.

Values of h (overall performance across all temperatures) were estimated to be −0.038 to 0.031 d^{-1} for the Azores population and −0.083 to 0.084 d^{-1} for the Bergen population. There was no difference in h between the populations (ANOVA, $F_1 = 0.028$, $p = 0.872$; Fig. 3A; Table 4). Estimated optimum temperatures m were higher in the Azores population with 23.4°C to 24.7°C, in comparison to the Bergen population with 22.5°C to 23.0°C (ANOVA, $F_1 = 22.69$, $p < 0.005$; Figs. 2C, 3B). Optimum growth rates z_{max} were 1.539 to 1.614 d^{-1} for the Azores population and 1.554 to 1.763 d^{-1} for the Bergen population. Statistical comparison of optimum growth rates between the Bergen and the Azores populations failed significance. This may be attributed to a lack of sufficient statistical power to detect differences with the

Table 3. Observed (H_o) and expected (H_e) heterozygosities for the Azores and the Bergen population, test for Hardy–Weinberg equilibrium, and number of alleles at each locus. Number of permutations: 10,000; number of steps in Markov chain: 1,000,000; number of dememorization steps: 100,000. Asterisks indicate significances when $p \leq 0.05$.

	Azores				Bergen			
Locus	H_o	H_e	p	Number of alleles	H_o	H_e	p	Number of alleles
E9	0.88889	0.83660	0.12110	7	1.00000	0.85263	0.27180	9
B12	0.44444	0.62092	0.01388*	5	0.00000	0.18947	0.05237	2
F11	0.66667	0.84314	0.06832	7	0.50000	0.39474	1.00000	2
S37	0.77778	0.92157	0.02004*	9	0.70000	0.76316	0.26366	6
S15	0.22222	0.20915	1.00000	2	0.77778	0.50327	0.17651	2

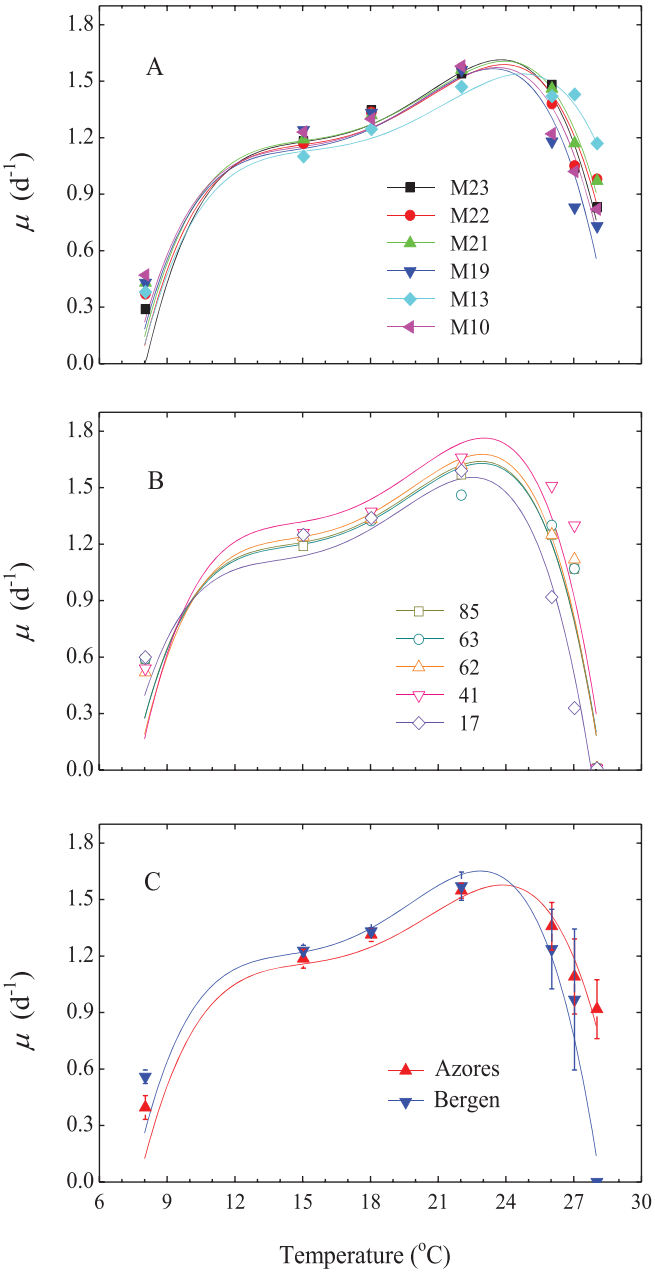

Fig. 2. Thermal reaction norms for growth rates of *E. huxleyi* genotypes. (A) Fitted growth rate curves of individual genotypes from the Azores. (B) Fitted growth rate curves of individual genotypes from Bergen. (C) Fitted growth rate curves for the Azores and the Bergen populations. The curves in panels A and B are fitted using function (3) based on mean growth rates of five replicates. The curves in panel C are fitted using function (3) based on average growth rates of six genotypes from the Azores and five genotypes from Bergen.

small sample size we used (ANOVA, $F_1 = 4.618$, $p = 0.060$; Fig. 3D). Values of w were remarkably larger for the Azores population with 1.034 to 1.109 than those for the Bergen population with 0.997 to 1.023 (ANOVA, $F_1 = 15.41$, $p < 0.005$; Figs. 2C, 3C). Larger m was correlated with larger w and h but with lower z_{max} for all genotypes. The TMV model explains more than 67% of the total variation in the data. A major biological result is that the horizontal shift mode accounts for the largest component of variation (45%). Generalist–specialist (18%) and vertical shift (4%) explain smaller fractions of the total variation in the data.

Within-population variation in growth rates—The continuous reaction norms of each genotype of the Azores and Bergen populations are shown in Fig. 2A,B. All genotypes grew at similar rates in the Bergen population between 8°C and 18°C and in the Azores population between 8°C and 22°C. Based on the local temperatures at the Azores and Bergen, we chose three temperatures (8°C, 22°C, and 27°C) and computed the correlations among growth rates between 8°C and 22°C, 22°C and 27°C, and 8°C and 27°C (Fig. 4). We found a positive trend in the correlation among growth rates between 8°C and 22°C and a negative trend between 22°C and 27°C for the Azores population. For the Bergen population, we found a negative trend in the correlation among growth rates between 8°C and 22°C and a positive trend between 22°C and 27°C. Negative trends in correlations among growth rates between 8°C and 27°C were found in both populations. However, all correlations failed statistical significance. Thermal reaction norms for growth rates showed that *E. huxleyi* genotypes, which at higher temperatures had higher growth rates compared to other genotypes of the same population, performed worse at lower temperatures and vice versa. There was no genotype that performed best across all temperatures (Fig. 2A,B; Table 4).

In the TMV model, m was positively correlated with w and h but negatively correlated with z_{max} in the Azores population. These correlations among m, h, w, and z_{max} are similar for all genotypes. Larger m was correlated with lower w and h but with larger z_{max} in the Bergen population. In most cases, correlations among m, h, w, and z_{max} in the Bergen population showed opposite trends for all genotypes. These results may be due to a greater contribution of the Azores genotypes to whole genotypes in correlations among m, h, w, and z_{max} or more genotypes used in the Azores population.

The within-population variations remained low over a range of temperatures from 15°C to 22°C and then rapidly increased at higher temperatures (Fig. 5). Variations at 26°C, 27°C, or 28°C were significantly higher than those at 22°C (F-test, $p < 0.05$). Normalized standard deviations in growth rates were higher in the Azores population at 8°C, 15°C, and 18°C compared to the Bergen population, while we observed the opposite trend at 22°C, 26°C, and 27°C (Fig. 5). Normalized standard deviations for growth rates of all 11 *E. huxleyi* genotypes were only higher at 8°C and 28°C, while at 15°C, 18°C, 22°C, 26°C, and 27°C, they were more or less the same as the normalized standard deviations for growth rates of five (Bergen) or six (Azores) genotypes. In summary, within-population variation in growth rates increased with increasing temperatures above 22°C, while between-population variation in growth rates was higher than within-population variation at both ends of the temperature range tested.

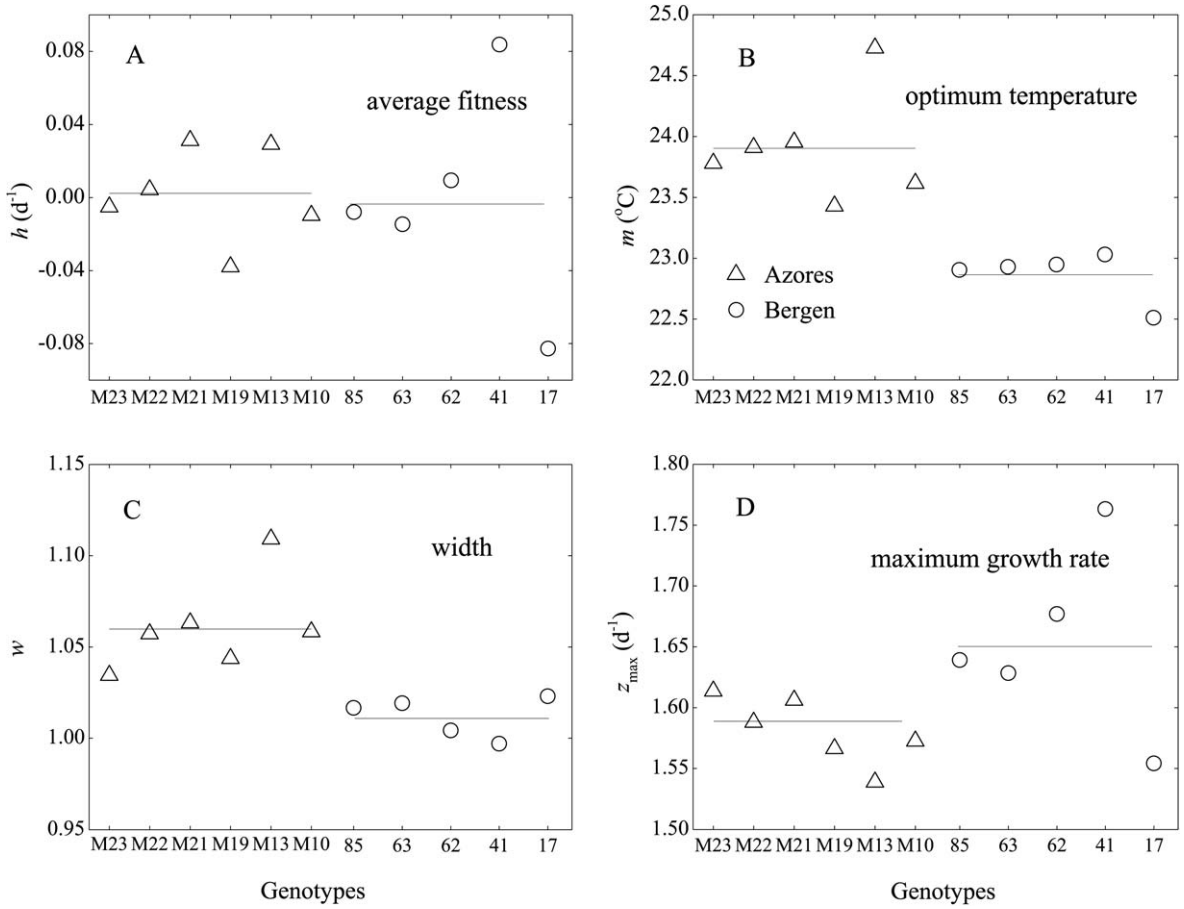

Fig. 3. Fitted parameters for growth rates of *E. huxleyi* genotypes from the Azores and Bergen. (A) Height parameter (h), (B) location parameter (m), (C) width parameter (w), and (D) maximum growth rate (z_{max}). Lines in each panel represent the average values of h, m, w, and z_{max} for the Azores and the Bergen populations. Data were calculated using functions (3) and (4) based on mean growth rates of five replicates.

Discussion

Population structure—Microsatellite markers were used to assess the differentiation between the Bergen and the Azores populations. We found genetic differentiation between these populations, which suggests limited gene flow and potential for local adaptation (Leducq et al. 2014). Based on our microsatellite analysis, two clearly separated genetic clusters were detected, corresponding to the geographical origin of the genotypes. This supports the interpretation from Iglesias-Rodríguez et al. (2006), who suggested that the genetic differentiation, based on the F_{ST}

Table 4. Growth rate (μ), height parameter (h), location parameter (m), width parameter (w), and maximum growth rate (z_{max}) of individual *E. huxleyi* genotype; μ is calculated using function (1); h, m, and w function (3); and z_{max} function (4). *See* text for details about calculations of all parameters.

	Temp.	Azores						Bergen				
Parameter	(°C)	M23	M22	M21	M19	M13	M10	85	63	62	41	17
μ (d^{-1})	8	0.289	0.374	0.427	0.431	0.382	0.471	0.584	0.584	0.514	0.530	0.595
	15	1.181	1.174	1.191	1.239	1.105	1.232	1.181	1.242	1.234	1.253	1.240
	18	1.344	1.336	1.319	1.332	1.245	1.299	1.323	1.314	1.323	1.363	1.329
	22	1.536	1.565	1.561	1.558	1.468	1.580	1.558	1.446	1.613	1.649	1.580
	26	1.478	1.394	1.459	1.180	1.430	1.215	1.241	1.295	1.237	1.503	0.911
	27	1.038	1.051	1.165	0.830	1.433	1.024	1.056	1.056	1.112	1.291	0.322
	28	0.829	0.979	0.968	0.729	1.174	0.822	0	0	0	0	0
h (d^{-1})		−0.005	0.004	0.031	−0.038	0.029	−0.010	−0.008	−0.015	0.009	0.084	−0.083
m (°C)		23.78	23.91	23.95	23.43	24.73	23.62	22.90	22.93	22.95	23.03	22.51
w		1.034	1.057	1.063	1.044	1.109	1.058	1.017	1.019	1.004	0.997	1.023
z_{max} (d^{-1})		1.614	1.588	1.606	1.566	1.539	1.573	1.639	1.628	1.677	1.763	1.554

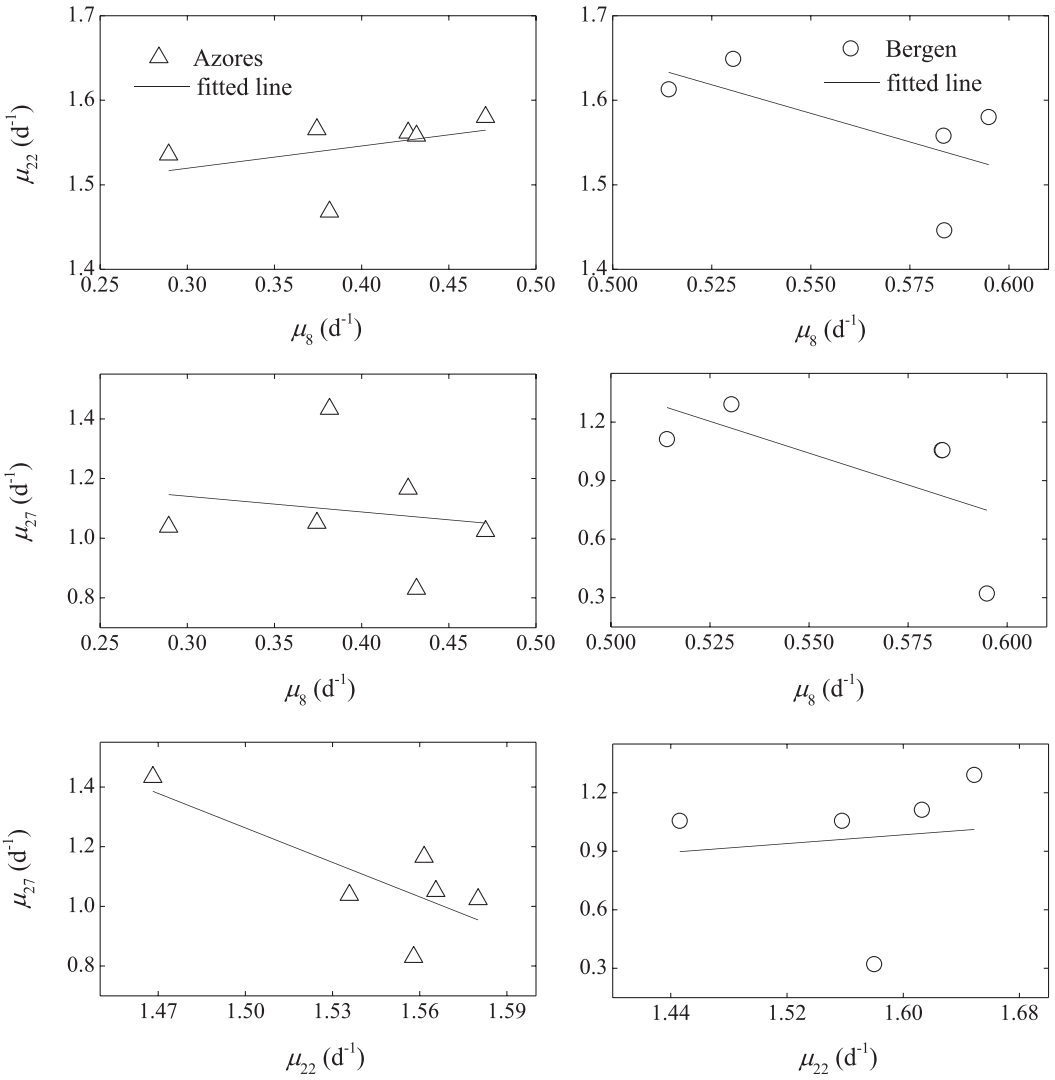

Fig. 4. Correlations among growth rates between 8°C and 22°C, 22°C and 27°C, and 8°C and 27°C. Solid lines were fitted linearly based on growth rates of six genotypes from the Azores and five genotypes from Bergen; μ_8, μ_{22}, and μ_{27} are the growth rates of each genotype at 8°C, 22°C, and 27°C, respectively.

they found, may indicate selection of different genotypes due to different environmental conditions and restricted gene flow across biogeographic provinces through barriers caused by current systems. Cook et al. (2013) also found significant genetic differentiation among *E. huxleyi* populations from seven sites south off Australia. These findings fit well to the results from a recent *E. huxleyi* genome study that reported large genomic differences between genotypes from different ocean regions (Read et al. 2013) and support the presence of biogeographic structuring in marine phytoplankton.

Between-population variation—Thermal reaction norms are a useful tool to describe the thermal adaptation of organisms (Conte et al. 1998). Here we applied the TMV model to investigate thermal reaction norms in *E. huxleyi* over the entire naturally encountered temperature range. Note that the TMV approach enables us to compare difference in the parameters *h*, *m*, and *w* between populations. However, these parameters do not necessarily represent the real growth rates, optimum temperatures for growth, or temperature niche widths of the genotypes. In this study, we chose to use the TMV model with the fourth-order polynomial degree (Fig. 2). This function has two vertex points that do not reflect any biological response. Rather, it is considered a statistical tool to investigate the continuous thermal reaction norms.

The TMV analysis revealed a significantly higher optimum growth temperature for the Azores than for the Bergen populations (Fig. 2), which is in agreement with the respective temperature regime at the geographical origin of each population. These results are in line with findings from this and other phytoplankton species that thrive in habitats characterized by distinct thermal regimes (Conte et al. 1998; Kremp et al. 2012; Flombaum et al. 2013).

Interestingly, the TMV analysis suggested a broader temperature niche for the Azores population (Fig. 3C) despite their occurrence in a narrower mean monthly SST

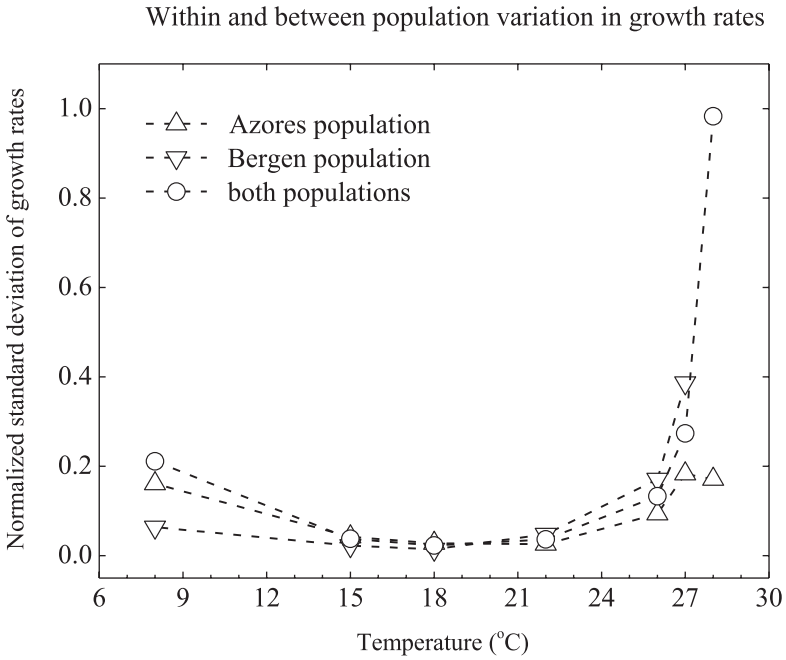

Fig. 5. Within-population variation in growth rates compared with between-population variation in growth rates. Data are calculated based on growth rates of six genotypes in the Azores population and five genotypes in the Bergen population and 11 genotypes in both populations. Normalized standard deviation is calculated as the ratio of the standard deviation to absolute growth rates.

range in lower-latitude waters (Table 1). This result may indicate that temperature niche width cannot be easily predicted based on the geographic origin of a phytoplankton population. The Bergen genotypes failed to grow at 28°C, while we were not able to investigate the lower extreme temperatures. Growth rate differences at 8°C suggest that the Bergen population will probably have a lower minimum growth temperature than the Azores population. Consequently, we may have underestimated the niche width of the Bergen population.

Optimum temperatures for growth are commonly reported to be considerably higher than annual mean temperatures at their origin for isolates from polar and temperate waters. By contrast, isolates from tropical water are usually closer to the annual mean temperatures found at the sites where they were isolated (Thomas et al. 2012). This pattern also applies to the Bergen genotypes, which displayed considerably higher optimum growth temperatures than the maximum SST at their sampling location. The temperature for maximal growth rates of *E. huxleyi* cultures commonly found under laboratory conditions is considerably higher than the temperatures at which those populations usually predominate in the field (Conte et al. 1998; Buitenhuis et al. 2008). This discrepancy may be explained by the artificial laboratory environment, which differs from the much more complex and variable natural environment. Growth rates were measured during the exponential growth period of individual genotypes, which were cultured under nutrient-replete conditions in our study. Optimal growth of *E. huxleyi* populations in Norwegian fjords typically occurs during May–July (Fernández et al. 1996). At this time, surface water temperatures range from about 8°C to 14°C (Locarnini et al. 2006), and growth is most likely controlled primarily by optimal nutrient and light availability (Fernández et al. 1996).

Within-population variation—In the present study, we applied continuous thermal reaction norms (Fig. 2A,B) to investigate plasticity and G × E interactions among clonal isolates from each population (Gsell et al. 2012). G × E interactions were identified by different slopes in the thermal reaction norms of individual genotypes within both populations (Fig. 2A,B). Variation in growth rates was most pronounced in the physiologically more demanding temperature ranges. The presence of ample phenotypic variability among isolates from natural populations has also been reported for other phytoplankton species (Kremp et al. 2012; Schaum et al. 2012) and fits well to the high-standing genetic variation commonly found in marine phytoplankton populations (Medlin et al. 2000; Rynearson and Armbrust 2004; Iglesias-Rodríguez et al. 2006). High genetic variation within populations suggests that rapid evolutionary adaptation by genotypic selection may have the potential to mitigate detrimental effects of global change (Lohbeck et al. 2012; Reusch 2014).

Reaction norms can be used to identify trade-offs in particular traits. For example, genotypes that show high growth rates in one treatment may grow worse in the other treatment (Agrawal et al. 2010). Trade-offs in fitness relevant traits are potentially important in maintaining genetic diversity within populations. For example, Gsell et al. (2012) compared reaction norms of different genotypes of the diatom *Asterionella formosa* from two different habitats and did not find a genotype that performed best at all temperatures. In order to test for trade-offs, we performed a correlation analysis using growth rates at

8°C, 22°C, and 27°C (Fig. 4). However, we were not able to detect any statistical significant correlations, probably because the sample size we used was too small to gain sufficient statistical test power.

Brand (1982) observed differences in growth rates when he exposed *E. huxleyi* isolates from different parts of the ocean to different temperatures already more than 30 yr ago. However, the importance of standing genetic variation in natural phytoplankton populations to cope with rapid environmental changes is only slowly being recognized (Kremp et al. 2012; Schaum et al. 2012; Reusch and Boyd 2013).

In this study, we have demonstrated neutral genetic and phenotypic variability within and between two *E. huxleyi* populations from the cool North Atlantic waters off Bergen and the warm central Atlantic waters at the Azores. Our findings provide supporting evidence that biogeographic structuring and local adaptation are common in populations of the widely distributed coccolithophore *E. huxleyi*. Variations in thermal reaction norms of different genotypes emphasize the difficulty in predicting ecological dynamics in future ocean scenarios from studying a single contemporary genotype (Kremp et al. 2012; Schaum et al. 2012; Boyd et al. 2013). Future research should therefore use multiple genotypes from various locations and also strengthen the focus on community-level experiments. High-standing genetic variation in natural *E. huxleyi* populations will likely be important for these populations to adapt to a rapidly changing ocean (Lohbeck et al. 2012; Reusch and Boyd 2013).

Acknowledgments

Y. Zhang and R. Klapper contributed equally to this article and share the first authorship. We thank Andrea Ludwig for dissolved inorganic carbon measurements, Jana Meyer for total alkalinity measurements, and Scarlett Sett, Allanah Paul, and Silke Lischka for fruitful discussions about the data set. We gratefully acknowledge the reviewers for their useful comments. This work was supported by the German Federal Ministry of Education and Research (Bundesministerium für Bildung und Forschung) in the framework of the collaborative project Biological Impacts of Ocean Acidification (BIOACID). We also thank Sarah L. Eggers for providing *E. huxleyi* isolates from the Azores and the China Scholarship Council (CSC) for its support of Yong Zhang.

References

Agrawal, A. A., J. K. Conner, and S. Rasmann. 2010. Tradeoffs and negative correlations in evolutionary ecology, p. 243–268. *In* M. A. Bell, W. F. Eanes, D. J. Futuyma and J. S. Levinton [eds.], Evolution after Darwin: The first 150 years. Sinauer Associates.

Bach, L. T., U. Riebesell, and K. G. Schulz. 2011. Distinguishing between the effects of ocean acidification and ocean carbonation in the coccolithophore *Emiliania huxleyi*. Limnol. Oceanogr. **56:** 2040–2050, doi:10.4319/lo.2011.56.6.2040

Boyd, P. W., and others. 2013. Marine phytoplankton temperature versus growth responses from polar to tropical waters—outcome of a scientific community-wide study. PLoS One **8:** e63091, doi:10.1371/journal.pone.0063091

Bradshaw, A. D. 1965. Evolutionary significance of phenotypic plasticity in plants. Adv. Genet. **13:** 115–155, doi:10.1016/S0065-2660(08)60048-6

Brand, L. E. 1982. Genetic variability and spatial patterns of genetic differentiation in the reproductive rates of the marine coccolithophores *Emiliania huxleyi* and *Gephyrocapsa oceanica*. Limnol. Oceanogr. **27:** 236–245, doi:10.4319/lo.1982.27.2.0236

Brookfield, J. F. Y. 1996. A simple new method for estimating null allele frequency from heterozygote deficiency. Mol. Ecol. **5:** 453–455, doi:10.1046/j.1365-294X.1996.00098.x

Buitenhuis, E. T., T. Pangerc, D. J. Franklin, C. L. Quéré, and G. Malin. 2008. Growth rates of six coccolithophorid strains as a function of temperature. Limnol. Oceanogr. **53:** 1181–1185, doi:10.4319/lo.2008.53.3.1181

Collins, S., B. Rost, and T. A. Rynearson. 2013. Evolutionary potential of marine phytoplankton under ocean acidification. Evol. Appl. **7:** 140–155, doi:10.1111/eva.12120

Conte, M. H., A. Thompson, D. Lesley, and R. Harris. 1998. Genetic and physiological influences on the alkenone/alkenoate versus growth temperatures relationship in *Emiliania huxleyi* and *Gephyrocapsa oceanica*. Geochim. Cosmochim. Acta **62:** 51–68, doi:10.1016/S0016-7037(97)00327-X

Cook, S. S., R. C. Jones, R. E. Vaillancourt, and G. M. Hallegraeff. 2013. Genetic differentiation among Australian and Southern Ocean populations of the ubiquitous coccolithophore *Emiliania huxleyi* (Haptophyta). Phycologia **52:** 368–374, doi:10.2216/12-111.1

Danbara, A., and Y. Shiraiwa. 1999. The requirement for selenium for the growth of marine coccolithophorids, *Emiliana huxleyi*, *Gephyrocapsa oceanica* and *Helladosphaera* sp. (Prymnewsiophyceae). Plant Cell Physiol. **40:** 762–766, doi:10.1093/oxfordjournals.pcp.a029603

De Jong, G. 1990. Quantitative genetics of reaction norms. J. Evol. Biol. **3:** 447–468, doi:10.1046/j.1420-9101.1990.3050447.x

Dickson, A. G., J. D. Afghan, and G. C. Anderson. 2003. Reference materials for oceanic CO_2 analysis: A method for the certification of total alkalinity. Mar. Chem. **80:** 185–197, doi:10.1016/S0304-4203(02)00133-0

Evanno, G., S. Regnaut, and J. Goudet. 2005. Detecting the number of clusters of individuals using the software Structure: A simulation study. Mol. Ecol. **14:** 2611–2620, doi:10.1111/j.1365-294X.2005.02553.x

Excoffier, L., G. Laval, and S. Schneider. 2005. Arlequin (version 3.0): An integrated software package for population genetics data analysis. Evol. Bioinf. **1:** 47–50. http://cmpg.unibe.ch/software/arlequin3

Fernández, E., E. Marañón, D. S. Harbour, S. Kristiansen, and B. R. Heimdal. 1996. Patterns of carbon and nitrogen uptake during blooms of *Emiliania huxleyi* in two Norwegian fjords. J. Plankton Res. **18:** 2349–2366, doi:10.1093/plankt/18.12.2349

Flombaum, P., and others. 2013. Present and future global distributions of the marine Cyanobacteria *Prochlorococcus* and *Synechococcus*. Proc. Natl. Acad. Sci. USA **110:** 9824–9829, doi:10.1073/pnas.1307701110

Gsell, A. S., L. N. De Senerpont-Domis, A. Przytulska-Bartosiewicz, W. M. Mooij, E. Van Donk, and B. W. Ibelings. 2012. Genotype-by-temperature interactions may help to maintain clonal diversity in *Asterionella Formosa* (Bacillariophyceae). J. Phycol. **48:** 1197–1208, doi:10.1111/j.1529-8817.2012.01205.x

Guillard, R. R., and J. H. Ryther. 1962. Studies of marine planktonic diatoms. I. Cyclotella nana Hustedt, and Detonulaconfervacea (cleve) Gran. Can. J. Microbiol. **8:** 229–239, doi:10.1139/m62-029

Huey, R. B., and J. G. Kingsolver. 1989. Evolution of thermal sensitivity of ectotherm performance. Trends Ecol. Evol. **4:** 131–135, doi:10.1016/0169-5347(89)90211-5

———, AND R. D. STEVENSON. 1979. Integrating thermal physiology and ecology of ectotherms: A discussion of approaches. Am. Zool. **19:** 357–366, doi:10.1093/icb/19.1.357

IGLESIAS-RODRÍGUEZ, M. D., O. M. SCHOFIELD, J. BATLEY, L. K. MEDLIN, AND P. K. HAYES. 2006. Intraspecific genetic diversity in the marine coccolithophore *Emiliania huxleyi* (Prymnesiophyceae): The use of microsatellite analysis in marine phytoplankton population studies. J. Phycol. **42:** 526–536, doi:10.1111/j.1529-8817.2006.00231.x

INTERGOVERNMENTAL PANEL ON CLIMATE CHANGE. 2013. Climate change 2013: The physical science basis. Contribution of Working Group I to the Fifth Assessment Report of the Intergovernmental Panel on Climate Change. Cambridge Univ. Press.

IZEM, R., AND J. G. KINGSOLVER. 2005. Variation in continuous reaction norms: Quantifying directions of biological interest. Am. Nat. **166:** 277–289, doi:10.1086/431314

KESTER, D., I. W. DUEDALL, D. N. CONNORS, AND R. M. PYTKOWICZ. 1967. Preparation of artificial seawater. Limnol. Oceanogr. **1:** 176–179, doi:10.4319/lo.1967.12.1.0176

KREMP, A., A. GODHE, J. EGARDT, S. DUPONT, S. SUIKKANEN, S. CASABIANCA, AND A. PENNA. 2012. Intraspecific variability in the response of bloom-forming marine microalgae to changed climate conditions. Ecol. Evol. **2:** 1195–1207, doi:10.1002/ece3.245

LEDUCQ, J. B., AND OTHERS. 2014. Local climatic adaptation in a widespread microorganism. Proc. R. Soc. B **281:** 1471–2954, doi:10.1098/rspb.2013.2472

LEWIS, E., AND D. W. R. WALLACE. 1998. Program developed for CO_2 system calculations [Internet]. ORNL/CDIAC-105. Carbon Dioxide Information Analysis Centre, Oak Ridge National Laboratory, U.S. Department of Energy. Available from http://cdiac.ornl.gov/oceans/co2rprt.html. (accessed 12 June 2007).

LOCARNINI, R. A., A. V. MISHONOV, J. I. ANTONOV, T. P. BOYER, AND H. E. GARCIA. 2006. World ocean atlas 2005. V. 1: Temperature. p. 123–134. *In* S. Levitus [ed.], NOAA Atlas NESDIS 61. U.S. Government Printing Office.

LOHBECK, K. T., U. RIEBESELL, AND T. B. H. REUSCH. 2012. Adaptive evolution of a key phytoplankton species to ocean acidification. Nat. Geosci. **5:** 346–351, doi:10.1038/ngeo1441

MCINTYRE, A, AND A. W. H. BÉ. 1967. Modern coccolithophoridae of the Atlantic Ocean—I. Placoliths and Cyrtoliths. Deep-Sea Res. **14:** 561–597, doi:10.1016/0011-7471(67)90065-4

MEDLIN, L. K., M. LANGE, AND E. M. NÖTHIG. 2000. Genetic diversity in the marine phytoplankton: A review and a consideration of Antarctic phytoplankton. Antarct. Sci. **12:** 325–333, doi:10.1017/ S0954102000000389

PALUMBI, S. R. 1994. Genetic divergence, reproductive isolation, and marine speciation. Ann. Rev. Ecol. Syst. **25:** 547–572, doi:10.1146/annurev.es.25.110194.002555

PRITCHARD, J. K., M. STEPHENS, AND P. DONNELLY. 2000. Inference of population structure using multilocus genotype data. Genetics **155:** 945–959.

READ, B. A., AND OTHERS. 2013. Pan genome of the phytoplankton *Emiliania* underpins its global distribution. Nature **499:** 209–213, doi:10.1038/nature12221

REUSCH, T. B. H. 2014. Climate change in the oceans: Evolutionary versus phenotypically plastic responses of marine animals and plants. Evol. Appl. **7:** 104–122, doi:10.1111/eva.12109

———, AND P. W. BOYD. 2013. Experimental evolution meets marine phytoplankton. Evolution **67:** 1849–1859, doi:10.1111/evo.12035

RIEBESELL, U., AND P. D. TORTELL. 2011. Effects of ocean acidification on pelagic organisms and ecosystems. p. 99–121. *In* J. P. Gattuso and L. Hansson [eds.], Ocean acidification. Oxford Univ. Press.

RYNEARSON, T. A., AND E. V. ARMBRUST. 2004. Genetic differentiation among populations of the planktonic marine diatom *Ditylum brightwelli* (Bacillariophyceae). J. Phycol. **40:** 34–43, doi:10.1046/j.1529-8817.2004.03089.x

SAMUELSEN, T. J. 1970. The biology of six species of Anomura (Crustacea, Decapoda) from Raunefjorden, western Norway. Sarsia **45:** 25–52.

SCHAUM, E., B. ROST, A. J. MILLAR, AND S. COLLINS. 2012. Variation in plastic responses of a globally distributed picoplankton species to ocean acidification. Nat. Clim. Change **3:** 298–302, doi:10.1038/nclimate1774

SGRÒ, C. M., AND A. A. HOFFMANN. 2004. Genetic correlations, tradeoffs and environmental variation. Heredity **93:** 241–248, doi:10.1038/sj.hdy.6800532

TATTERS, A. O., AND OTHERS. 2013. Short- and long-term conditioning of a temperate marine diatom community to acidification and warming. Phil. Trans. R. Soc. B **368:** 20120437, doi:10.1098/rstb.2012.0437

THOMAS, M. K., C. T. KREMER, C. A. KLAUSMEIER, AND E. LITCHMAN. 2012. A global pattern of thermal adaptation in marine phytoplankton. Science **338:** 6110, 1085–1088, doi:10.1126/science.1224836

VAN OOSTERHOUT, C., W. F. HUTCHINSON, D. P. M. WILLS, AND P. SHIPLEY. 2004. MICRO-CHECKER: Software for identifying and correcting genotyping errors in microsatellite data. Mol. Ecol. Notes **4:** 535–538, doi:10.1111/j.1471-8286.2004.00684.x

WINTER, A., J. HENDERIKS, L. BEAUFORT, R. E. M. RICKABY, AND C. W. BROWN. 2013. Poleward expansion of the coccolithophore *Emiliania huxleyi*. J. Plankton Res. **0:** 1–10, doi:10.1093/plankt/fbt110

WISSHAK, M., A. FORM, J. JAKOBSEN, AND A. FREIWALD. 2010. Temperate carbonate cycling and water mass properties from intertidal to bathyal depths (Azores). Biogeosciences **7:** 2379–2396, doi:10.5194/bg-7-2379-2010

WRIGHT, S. 1978. Evolution and the genetics of populations. V. 4: Variability within and among natural populations. Univ. of Chicago Press.

Associate editor: John Albert Raven

Received: 19 December 2013
Accepted: 11 May 2014
Amended: 24 May 2014

Chapter 3: The modulating effect of light intensity on the response of the coccolithophore *Gephyrocapsa oceanica* to ocean acidification

LIMNOLOGY
and
OCEANOGRAPHY

ASLO

Limnol. Oceanogr. 00, 2015, 00–00

doi: 10.1002/lno.10161

The modulating effect of light intensity on the response of the coccolithophore *Gephyrocapsa oceanica* to ocean acidification

Yong Zhang,*[1] Lennart T. Bach,[1] Kai G. Schulz,[2] Ulf Riebesell[1]

[1]Biological Oceanography, GEOMAR Helmholtz-Centre for Ocean Research Kiel, Kiel, Germany

[2]Centre for Coastal Biogeochemistry, School of Environmental Science and Management, Southern Cross University, Lismore, New South Wales, Australia

Abstract

Global change leads to a multitude of simultaneous modifications in the marine realm among which shoaling of the upper mixed layer, leading to enhanced surface layer light intensities, as well as increased carbon dioxide (CO_2) concentration are some of the most critical environmental alterations for phytoplankton. In this study, we investigated the responses of growth, photosynthetic carbon fixation and calcification of the coccolithophore *Gephyrocapsa oceanica* to elevated P_{CO_2} (51 Pa, 105 Pa, and 152 Pa) (1 Pa $\approx$ 10 μatm) at a variety of light intensities (50–800 μmol photons m^{-2} s^{-1}). By fitting the light response curve, our results showed that rising P_{CO_2} reduced the maximum rates for growth, photosynthetic carbon fixation and calcification. Increasing light intensity enhanced the sensitivity of these rate responses to P_{CO_2}, and shifted the P_{CO_2} optima toward lower levels. Combining the results of this and a previous study (Sett et al. 2014) on the same strain indicates that both limiting low P_{CO_2} and inhibiting high P_{CO_2} levels (this study) induce similar responses, reducing growth, carbon fixation and calcification rates of *G. oceanica*. At limiting low light intensities the P_{CO_2} optima for maximum growth, carbon fixation and calcification are shifted toward higher levels. Interacting effects of simultaneously occurring environmental changes, such as increasing light intensity and ocean acidification, need to be considered when trying to assess metabolic rates of marine phytoplankton under future ocean scenarios.

Atmospheric carbon dioxide (CO_2) concentrations are projected to increase from about 40 Pa (1 Pa $\approx$ 10 μatm) in 2013 beyond 75 Pa by the end of this century (IPCC 2013). Until today about one third of all anthropogenic CO_2 emissions have been absorbed by the ocean (Sabine et al. 2004). Increasing seawater CO_2 forms carbonic acid leading to a reduction in seawater pH. The pH of oceanic surface seawater is projected to decrease by 0.3–0.4 units within the next 100 yr (Houghton et al. 2001), representing a 100–150% increase in the proton concentration ($[H^+]$). These changes in CO_2 and $[H^+]$ can have positive effects for some phytoplankton functional groups while effects can be negative for others (Riebesell 2004).

Global warming, associated with increasing atmospheric CO_2 levels, enhances vertical stratification of the water column and decreases mixing between the surface ocean and deeper layers (Bopp et al. 2001). This expected shoaling of the upper mixed layer increases the average light intensity experienced by phytoplankton suspended in this layer (Sarmiento et al. 2004). Elevated light intensity may accelerate growth rates of some phytoplankton groups, while it might be stressful to others (Merico et al. 2004). When solar irradiance exceeds the capacity of common protective mechanisms, growth and electron transport rates of phytoplankton can be reduced (Gao et al. 2012). Depending on their photosynthetic apparatus, phytoplankton differ in their ability to cope with excess light intensities (Kaeriyama et al. 2011).

Most microalgae have developed energetically costly CO_2-concentrating mechanisms (CCMs) to avoid inorganic carbon limitation at the site of fixation (Giordano et al. 2005). CCMs involve the active uptake of CO_2 and/or HCO_3^- into the algal cell and/or the chloroplast. Given that the operation of CCMs is energetically costly, light availability may affect the activity of CCMs and the activity of CCMs may affect the energy reallocation in phytoplankton (Giordano et al. 2005). Energy saved from the down-regulation of CCMs in response to elevated CO_2 permits utilization in other processes such as growth or enzyme synthesis (Schippers et al. 2004; McCarthy et al. 2012).

Coccolithophores play an important role in the marine carbon cycle through the fixation of inorganic carbon via photosynthesis, as well as the precipitation of calcium

*Correspondence: yzhang@geomar.de

carbonate (Rost and Riebesell 2004). Coccolith formation has been suggested to reduce the risk of photo-damage of coccolithophores under high light conditions either by shading the cells like a sunshade (Braarud et al. 1952) or by contributing to excess energy dissipation (Barcelos e Ramos et al. 2012; Xu and Gao 2012). Declining pH generally reduces calcification rates (Bach et al. 2011; Riebesell and Tortell 2011), which may then put the cells at higher risk to suffer from photo-inhibition.

In this study, we investigated the combined effects of three P_{CO_2} levels and six light intensities on the cosmopolitan coccolithophore *Gephyrocapsa oceanica*. We measured the relative electron transport rate (rETR), growth rate, as well as carbon fixation and calcification rates to assess how light intensity modulates the effect of increasing P_{CO_2} on these parameters in *G. oceanica*.

Methods

Experimental setup

Gephyrocapsa oceanica (strain RCC 1303, isolated from Arcachon Bay, France in 1999) was grown in artificial seawater (ASW) under dilute batch culture conditions at 20°C. Light intensities were set to 50 μmol photons m^{-2} s^{-1}, 100 μmol photons m^{-2} s^{-1}, 200 μmol photons m^{-2} s^{-1}, 400 μmol photons m^{-2} s^{-1}, 600 μmol photons m^{-2} s^{-1}, and 800 μmol photons m^{-2} s^{-1} of photosynthetically active radiation (PAR) in a RUMED Light Thermostat (Rubarth Apparate GmbH) at a 16 : 8 h light : dark cycle. Light intensities were measured at every position in the light chamber where the bottles were put, using a Li-250A data logger (Li-Cor, Heinz Walz GmbH, Effeltrich).

ASW with a salinity of 35 was prepared according to Kester et al. (1967), but with the addition of 2350 μmol kg^{-1} bicarbonate (as opposed to 2330 μmol kg^{-1} in the original recipe). ASW was enriched with 64 μmol kg^{-1} nitrate (NO_3^-), 4 μmol kg^{-1} phosphate (PO_4^{3-}), f/8 concentrations for trace metals and vitamins (Guillard and Ryther 1962), 10 nmol kg^{-1} SeO_2 (Danbara and Shiraiwa 1999), and 2 mL kg^{-1} of sterile filtered (0.2 μm pore size, Sartobran® P 300, Sartorius) North Sea water to prevent possible trace metal limitation during culturing. Enriched ASW was aerated for 48 h at 20°C (0.2 μm pore size, Midisart® 2000 PTFE, Sartorius) with air containing 40, 84 or 112 Pa P_{CO_2} (ALPHAGAZ™). The dry air/CO_2 mixture was humidified with Milli-Q water before aeration into the ASW to minimize evaporation. After aeration, the ASW medium was sterile-filtered (0.2 μm pore size, Sartobran® P 300, Sartorius) with gentle pressure and carefully pumped into autoclaved 0.5 L or 2 L polycarbonate bottles (Nalgene® Bottles). Samples to assess carbonate chemistry conditions at the beginning of the experiment (total alkalinity (TA) and dissolved inorganic carbon (DIC) analysis) were taken from the sterile-filtered medium. 0.5 L bottles were used to acclimate cells to experimental conditions for 7–9 generations (one replicate, maximum final cell number in these acclimation cultures were 23,000 cells mL^{-1}). Depending on growth rate, acclimation time was between 9 (slowest growth) and 4 (fastest growth) days. The main experiment culture was conducted in 2 L bottles (four replicates). The initial cell concentrations in the main experiment culture and in the pre-culture were about 220 cells mL^{-1}. Bottles for both the acclimation culture and the main experiment were filled with ASW medium leaving a minimum headspace of less than 1% to keep gas exchange at a minimum. Cells were transferred from 0.5 L to 2 L bottles at the same time. The volume of the inoculum was calculated (*see* below) and the same volume of ASW was taken out from 2 L bottles before inoculation. All culture bottles were stored at the experimental temperature of 20°C for 3 or 4 d prior to inoculation. Culture bottles were manually rotated twice a day at 5 h and 12 h after the onset of the light phase to reduce sedimentation of the cells.

Carbonate chemistry measurements

Samplings started 3 h after the onset of the light period and lasted no longer than 2 h. Dissolved inorganic carbon (DIC) samples were sterile filtered (0.2 μm pore size, Filtropur S 0.2, Sarstedt) by gentle pressure into 50 mL Duran Winkler flasks (Schott). The bottles were filled with samples from bottom to top and with overflow, tightly closed without headspace, and stored at 4°C. DIC concentrations were measured by an infrared CO_2 analyzer system (Automated Infra Red Inorganic Carbon Analyzer, Marianda). Samples for total alkalinity (TA) measurements were filtered with GF/F filters (0.7 μm nominal pore size, Whatman), poisoned with a saturated $HgCl_2$ solution (0.5‰ final concentration), and stored at 4°C. TA was measured in duplicate by open-cell potentiometric titration using a 862 Compact Titrosample (Metrohm) according to Dickson et al. (2003). DIC and TA samples were collected and measured before and at the end of incubations. Measurements of DIC and TA were corrected with certified reference material (Batch 115, Prof. A. Dickson, La Jolla, California). The carbonate system was calculated from TA, DIC, phosphate, temperature, and salinity using the CO2 System Calculations in MS Excel software (Pierrot et al. 2006) with temperature and salinity dependent stoichiometric equilibrium constants K_1 and K_2 for carbonic acid taken from Roy et al. (1993).

Photosynthetic measurements

The effective quantum yield of photosystem II (PSII) of algae samples was assessed using a Phytoplankton Analyzer PHYTO-PAM (Heinz Walz GmbH) 5 h after the onset of the light phase. Samples were kept in the dark for 15 min at room temperature (about 20°C). Gain setting was adjusted with algae sample via the Auto-Gain function and the effect of background signal was suppressed with the help of the Zero Offset function with filtered culture water. PAR levels between 1 μmol photons m^{-2} s^{-1} and 1659 μmol photons

m^{-2} s^{-1} were applied in 14 steps of 30 s each in light response curve measurements.

The relative electron transport rate (rETR) was calculated according to Schreiber et al. (1995), where:

$$\text{rETR}=\text{Yield} \times \text{PAR} \times 0.5 \times 0.84 \ \left(\mu\text{mol electrons } \text{m}^{-2}\text{s}^{-1}\right) \quad (1)$$

where yield (F_v/F_m) is defined as the ratio of photons emitted to photons absorbed by PSII (Schreiber et al. 1995). Implicit in this equation is the assumption that half of the quanta of the incident PAR are distributed to PSII and 84% of incident PAR is absorbed by photosynthetic pigments in a standard leaf (Björkman and Demmig 1987).

Photosynthesis vs. irradiance curves (P-I curves) were obtained by plotting calculated rETR vs. corresponding PAR values. P-I curve fitting was performed using a theoretical light response function according to a modified version of the photosynthesis model of Eilers and Peeters (1988).

$$y=\frac{\text{PAR}}{a\times\text{PAR}^2+b\times\text{PAR}+c} \quad (2)$$

where the coefficients a, b and c are fitted in a least square manner. The model of Eilers and Peeters can be easily interpreted algebraically. At low light intensity, $b \times$ PAR and $a \times \text{PAR}^2$ can be neglected and y (ETR) increases approximately linearly with light intensity. At high light intensity, $a \times \text{PAR}^2$ dominates and thus y (ETR) is inversely proportional to the light intensity. The initial slope of the light limited part of the P-I curve constitutes a measure of the quantum yield of electron transport, indicated as alpha, which was calculated as:

$$\text{alpha}=\frac{1}{c} \quad (3)$$

The maximum value (Y_{max}) of rETR was calculated as:

$$Y_{max}=\frac{1}{b+2\sqrt{ac}} \quad (4)$$

Here, Y_{max} shows the saturation level of rETR (rETR_{max}). Saturation light intensity I_k corresponds to the PAR value at the crossing point of the lines defined by the initial slope and rETR_{max}. I_k is calculated from the expression rETR_{max}/alpha and is characteristic for the onset of light saturation.

Growth rate measurements

At the end of incubations, about 25 mL samples were taken from the culture bottles at the same time, ~ 7 h after the onset of the light phase. Cell numbers were determined using a Z2 Coulter Particle Counter and Size Analyzer (Beckman). Growth rate (μ) was calculated for each replicate according to the equation:

$$\mu=(\ln N_1-\ln N_0)/d \quad (5)$$

where N_0 and N_1 are cell numbers at the beginning and the end of a growth interval, and d is the duration of the growth period in days.

Particulate organic (POC) and inorganic carbon (PIC) measurements

Samples for total particulate carbon (TPC) and particulate organic carbon (POC) were gently filtered (200 mbar) onto pre-combusted (500°C, 8 h) GF/F filters and stored in the dark at −20°C. Prior to the measurement, POC filters were fumed with 37.1% HCl (w/w) for 2 h to remove all inorganic carbon. After 8 h of drying at 60°C, TPC and POC were measured using an isotope ratio mass spectrometer (Thermo Finnigan MAT 253 GmbH). Particulate inorganic carbon (PIC) was calculated as the difference between TPC and POC. POC and PIC production rates were calculated as:

$$\text{POC production rate}=\mu\left(\text{d}^{-1}\right)\times\text{POC content}\left(\text{pg C cell}^{-1}\right) \quad (6)$$

$$\text{PIC production rate }=\mu\left(\text{d}^{-1}\right)\ \times\text{PIC content }\left(\text{pg C cell}^{-1}\right) \quad (7)$$

Data analysis

Growth, POC and PIC production rates as a function of light intensity (PAR) were fitted at each P_{CO_2} level (51 Pa, 105 Pa, and 152 Pa) with the model of Eilers and Peeters (1988) (Eq. 2). The theoretical maximum rates for growth, POC and PIC production are calculated according to Eq. 4. Conversely, we fitted growth, POC and PIC production rates at each light intensity as a function of P_{CO_2} using the modified Michaelis–Menten equation:

$$y=\frac{X\times P_{CO_2}}{Y+P_{CO_2}}-s\times P_{CO_2} \quad (8)$$

derived by Bach et al. (2011). Here, s is the constant which describes the negative effect of increasing $[H^+]$ (which is quasi proportional to P_{CO_2} at constant TA). y is growth, POC or PIC production rate at a certain P_{CO_2} level. X and Y are random fit parameters which can be converted to the Michaelis–Menten parameters V_{max} and $K_{1/2}$ with a mathematical procedure described in Bach et al. (2011). The underlying assumption implicit in this equation is that growth, POC and PIC production rates follow an optimum curve over a broad range of P_{CO_2} values at constant TA, which has been shown for a variety of coccolithophore species (Langer et al. 2006; Bach et al. 2011; Sett et al. 2014; Bach et al. 2015).

The effect of the P_{CO_2} treatment on V_{max} was determined by means of a one-way analysis of variance (ANOVA). A two-way ANOVA was used to determine the main effect of P_{CO_2} and light treatments and their interactions for these

Table 1. Carbonate system parameters of the artificial seawater. DIC and TA samples were collected and measured before and at the end of incubations. The carbonate system parameters were calculated from TA, DIC, phosphate concentration (4 μmol kg^{-1}), temperature (20°C), and salinity (35) using the CO_2 System Calculations in MS Excel software (Pierrot et al. 2006).

P_{CO_2} Pa	TA μmol kg^{-1}	DIC μmol kg^{-1}	pH total scale	HCO_3^- μmol kg^{-1}	CO_3^{2-} μmol kg^{-1}	CO_2 μmol kg^{-1}	Ω calcite
51 ± 4^a	2294 ± 34^a	2066 ± 19^a	7.96 ± 0.04^a	1882 ± 17^a	167 ± 15^a	16.7 ± 1.6^a	4.0 ± 0.3^a
105 ± 9^b	2325 ± 14^b	2213 ± 19^a	7.69 ± 0.04^b	2080 ± 22^b	100 ± 8^b	34.1 ± 3.3^b	2.4 ± 0.2^b
152 ± 12^c	2331 ± 9.6^b	2196 ± 17^a	7.54 ± 0.03^c	2149 ± 17^c	74 ± 5^c	49.4 ± 4.4^c	1.8 ± 0.1^c

Characters a, b, c represent statistically different means between different P_{CO_2} treatments (Tukey Post hoc, $p < 0.001$). The values are expressed as mean values with standard deviation calculated from measurements before and at the end of incubations.

variables. A Tukey Post hoc test was performed to identify the source of the main effect determined by ANOVA. Normality of residuals was tested with a Shapiro–Wilk's test. Levene's test was conducted graphically to test for homogeneity of variances in case of significant data. A generalized least squares (GLS) model was used to stabilize heterogeneity if variances were inhomogeneous. All statistical calculations were performed using *R* version 2.15.2.

Results

Carbonate chemistry

All parameters (measured and calculated) of the carbonate system are presented in Table 1. Air pressure in the headspace of the 10 L bubbling bottles was about 25–35% higher than one standard atmosphere, leading to higher P_{CO_2} levels in air-saturated ASW than targeted P_{CO_2}. After aerating for 48 h at about 40, 84, and 112 Pa P_{CO_2}, the P_{CO_2} levels of the

Table 2. Results of two-way ANOVAs of the effects of P_{CO_2}, light intensity (PAR) and their interaction on μ, $rETR_{max}$, alpha, I_k, POC and PIC production rates, PIC : POC ratio, POC : PON ratio.

Parameter	Treatment	df	F value	*p* value
μ	P_{CO_2}	2	3928.30	<0.001
	PAR	5	18551.90	<0.001
	P_{CO_2}×PAR	10	1651.00	<0.001
$rETR_{max}$	P_{CO_2}	2	1544.10	=0.003
	PAR	5	1025.51	<0.001
	P_{CO_2}×PAR	10	25.89	<0.001
alpha	P_{CO_2}	2	21.80	<0.001
	PAR	5	644.00	<0.001
	P_{CO_2}×PAR	10	46.80	<0.001
I_k	P_{CO_2}	2	883.28	<0.001
	PAR	5	3312.69	<0.001
	P_{CO_2}×PAR	10	122.17	<0.001
POC production rate	P_{CO_2}	2	9174.71	<0.001
	PAR	5	3738.19	<0.001
	P_{CO_2}×PAR	10	55.36	<0.001
PIC production rate	P_{CO_2}	2	346.08	<0.001
	PAR	5	857.79	<0.001
	P_{CO_2}×PAR	10	107.97	<0.001
PIC : POC ratio	P_{CO_2}	2	627.001	<0.001
	PAR	5	28.994	<0.001
	P_{CO_2}×PAR	10	16.675	<0.001
POC : PON ratio	P_{CO_2}	2	20.46	<0.001
	PAR	5	19.85	<0.001
	P_{CO_2}×PAR	10	2.71	=0.009

PAR, photosynthetically active radiation (μmol photons m^{-2} s^{-1}); μ, growth rate (d^{-1}); $rETR_{max}$, maximum relative electron transport rate (μmol electrons m^{-2} s^{-1}); alpha, slope of the light-limited part of the photosynthesis versus irradiance curve; I_k, saturating photon flux density (μmol photons m^{-2} s^{-1}); POC production rate, particulate organic carbon production rate (pg C cell^{-1} d^{-1}); PIC production rate, particulate inorganic carbon production rate (pg C cell^{-1} d^{-1}).

ASW were about 51 Pa, 105 Pa, and 152 Pa, and resulting pH_T (reported on the total scale) were about 7.96, 7.69, and 7.54, respectively.

Growth rates

Light intensities and P_{CO_2} levels significantly affected growth rates in *G. oceanica*, both individually as well as interactively (Table 2). At a P_{CO_2} of 51 Pa, growth rates of *G. oceanica* increased with increasing light intensity until 800 μmol photons m^{-2} s^{-1}. At higher P_{CO_2} levels, however, growth rates only increased until 400 μmol photons m^{-2} s^{-1} and slightly declined thereafter (Fig. 1A).

At 50 μmol photons m^{-2} s^{-1}, growth rates of *G. oceanica* were similar at the three P_{CO_2} levels (Tukey Post hoc, $p > 0.1$). At 100 μmol photons m^{-2} s^{-1}, growth rate at 105 Pa P_{CO_2} was higher than at 51 and 152 Pa P_{CO_2} (Tukey Post hoc, $p < 0.001$) (Fig. 1; Table 3). At 200 μmol photons m^{-2} s^{-1} and above, growth rates decreased with elevated P_{CO_2} levels (Tukey Post hoc, all df = 2, all $p < 0.001$) (Fig. 1; Table 3). Fitted maximum growth rates declined significantly with rising P_{CO_2} levels (one-way ANOVA, $F = 3836$, df = 2, $p < 0.001$; Tukey Post hoc, df = 2, $p < 0.001$) (Fig. 1A; Table 4).

$rETR_{max}$, alpha and I_k

We identified statistically significant effects of light intensity, P_{CO_2} level and their interaction also on $rETR_{max}$, alpha and I_k (Table 2). $rETR_{max}$ followed the same pattern as described for growth rate in the previous section. At 51 Pa, $rETR_{max}$ of *G. oceanica* increased with increasing light radiation until 800 μmol photons m^{-2} s^{-1}. At higher P_{CO_2} levels, however, $rETR_{max}$ increased only until 400 μmol photons m^{-2} s^{-1} or 600 μmol photons m^{-2} s^{-1} and decreased significantly thereafter (Fig. 2A; Table 3). At 50 μmol photons m^{-2} s^{-1}, 100 μmol photons m^{-2} s^{-1}, and 200 μmol photons m^{-2} s^{-1}, $rETR_{max}$ did not show any significant differences among the three P_{CO_2} treatments (Tukey Post hoc, all df = 2, all $p > 0.05$).

Increasing light intensity resulted in a relatively constant decrease in alpha (Fig. 2B). The decline of alpha from lowest to highest light intensities was 23%, 32%, and 57% for 51 Pa, 105 Pa, and 152 Pa, respectively (Tukey Post hoc, all df = 1, all $p < 0.001$) (Fig. 2B). At 50 μmol photons m^{-2} s^{-1} or 100 μmol photons m^{-2} s^{-1}, alpha was not significantly different among the three P_{CO_2} treatments (Tukey Post hoc, both df = 2, both $p > 0.05$). At 200 μmol photons m^{-2} s^{-1} or 400 μmol photons m^{-2} s^{-1}, alpha at 105 Pa P_{CO_2} was lower than at 51 and 152 Pa P_{CO_2} (Tukey Post hoc, both $p < 0.01$). At 800 μmol photons m^{-2} s^{-1}, alpha decreased significantly with elevated P_{CO_2} treatments (Tukey Post hoc, both $p < 0.01$). It seems that effects of P_{CO_2} levels on alpha were amplified by increasing light intensity (Fig. 2B).

Saturation light intensity, I_k, more than doubled from lowest to highest light intensities. With light intensity increasing from 50 μmol photons m^{-2} s^{-1} to 800 μmol photons m^{-2} s^{-1}, I_k increased about 2.2, 2.4, and 3.5 times for 51 Pa, 105 Pa, and 152 Pa, respectively (Tukey Post hoc, df = 1, $p < 0.001$) (Fig. 2C; Table 3). At 50 μmol photons m^{-2} s^{-1}, 100 μmol photons m^{-2} s^{-1}, or 200 μmol photons m^{-2} s^{-1}, I_k did not show significant difference among the three P_{CO_2} treatments (Tukey Post hoc, all df = 2, all $p > 0.1$). At 400 μmol photons m^{-2} s^{-1} or 600 μmol photons m^{-2} s^{-1}, I_k at 51 Pa P_{CO_2} was lower than at 105 and 152 Pa P_{CO_2} treatments (Tukey Post hoc, both df = 1, both $p < 0.05$). At 800 μmol photons m^{-2} s^{-1}, I_k increased significantly with elevated P_{CO_2} (Tukey Post hoc, df = 2, $p < 0.01$). It seems that the positive effect of P_{CO_2} treatment on I_k was also amplified by increasing light intensity (Fig. 2C).

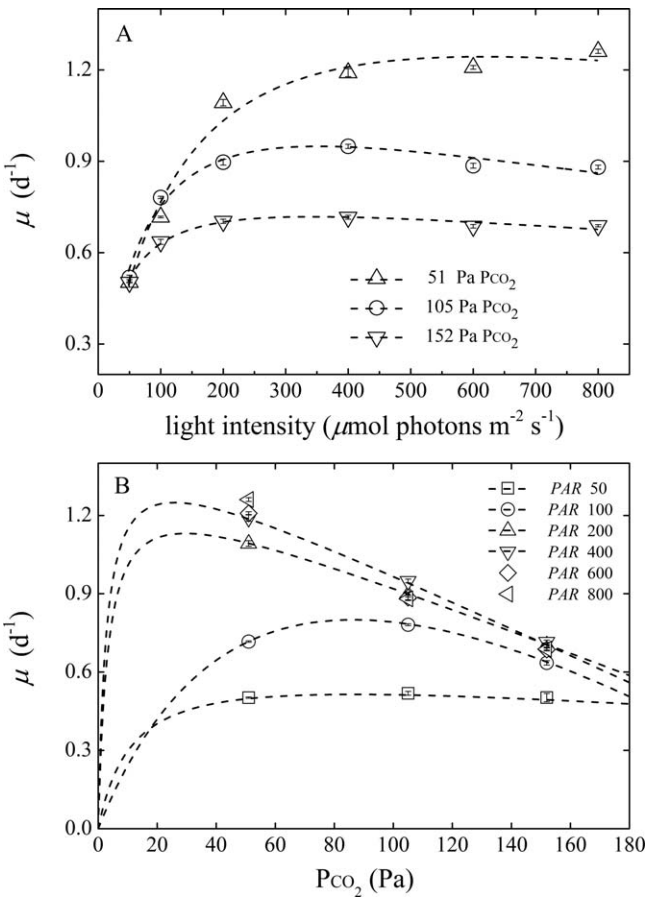

Fig. 1. Effects of light intensity and P_{CO_2} level on growth rate of *Gephyrocapsa oceanica*. (**A**) Growth rate as a function of light intensities at 51 (△), 105 (○) and 152 (▽) Pa P_{CO_2}. (**B**) Growth rate as a function of P_{CO_2} levels at light intensities of 50 μmol photons m^{-2} s^{-1}, 100 μmol photons m^{-2} s^{-1}, 200 μmol photons m^{-2} s^{-1}, 400 μmol photons m^{-2} s^{-1}, 600 μmol photons m^{-2} s^{-1} and 800 μmol photons m^{-2} s^{-1}. Dashed lines in panel (**A**) were fitted using Eq. 2. Dashed lines in panel (**B**) were fitted using Eq. 8. The values represent the mean of four replicates, with error bars showing ± one standard deviation. Please note that based on only three points, growth rate response curves at 600 μmol photons m^{-2} s^{-1} and 800 μmol photons m^{-2} s^{-1} in panel (**B**) cannot be fitted using Eq. 8.

Table 3. Experimental condition, growth rate, photosynthesis parameter and carbon production in dilute batch culture incubation.

P_{CO_2}	PAR	μ	$rETR_{max}$	alpha	I_k	POC/cell/d	PIC/cell/d	PIC/POC	POC/PON
51	50	0.50 (0.002)	95 (2)	0.29 (0.003)	321 (5)	8.18 (0.229)	10.79 (0.437)	1.30 (0.053)	7.55 (0.209)
	100	0.72 (0.003)	111 (3)	0.29 (0.001)	381 (11)	17.04 (0.670)	23.80 (2.492)	1.40 (0.146)	8.04 (0.316)
	200	1.09 (0.011)	117 (2)	0.27 (0.002)	434 (6)	19.51 (0.343)	33.80 (1.672)	1.73 (0.086)	6.74 (0.118)
	400	1.19 (0.013)	143 (2)	0.26 (0.004)	539 (4)	33.85 (2.514)	46.58 (12.711)	1.38 (0.097)	7.22 (0.536)
	600	1.21 (0.006)	154 (3)	0.23 (0.006)	678 (14)	32.59 (1.028)	52.69 (4.065)	1.62 (0.125)	7.32 (0.231)
	800	1.26 (0.007)	157 (2)	0.23 (0.006)	692 (10)	29.47 (0.233)	48.78 (1.374)	1.66 (0.047)	6.90 (0.055)
105	50	0.52 (0.007)	92 (1)	0.29 (0.002)	316 (5)	7.07 (0.098)	6.96 (0.311)	0.98 (0.439)	6.75 (0.094)
	100	0.78 (0.004)	101 (2)	0.29 (0.002)	352 (6)	17.84 (0.722)	17.27 (1.472)	0.97 (0.825)	6.73 (0.273)
	200	0.90 (0.010)	126 (2)	0.26 (0.004)	487 (8)	25.82 (3.484)	19.19 (3.577)	0.74 (0.139)	6.91 (0.933)
	400	0.95 (0.007)	157 (3)	0.24 (0.003)	643 (9)	28.66 (4.087)	18.71 (4.367)	0.65 (0.152)	6.05 (0.863)
	600	0.89 (0.008)	180 (10)	0.24 (0.005)	748 (38)	21.16 (1.988)	23.35 (2.075)	1.10 (0.098)	5.99 (0.563)
	800	0.88 (0.007)	155 (17)	0.20 (0.010)	773 (71)	19.89 (1.391)	21.64 (0.777)	1.12 (0.040)	6.27 (0.451)
152	50	0.50 (0.016)	84 (4)	0.28 (0.003)	295 (11)	8.19 (0.077)	5.55 (2.157)	0.81 (0.013)	6.76 (0.052)
	100	0.64 (0.008)	112 (2)	0.29 (0.004)	381 (4)	12.53 (1.106)	7.03 (1.457)	0.56 (0.116)	6.81 (0.601)
	200	0.70 (0.007)	130 (3)	0.27 (0.002)	471 (13)	15.52 (2.054)	8.13 (2.252)	0.52 (0.145)	7.62 (1.008)
	400	0.72 (0.006)	171 (10)	0.26 (0.006)	654 (35)	12.96 (0.938)	14.01 (1.585)	1.08 (0.122)	6.83 (0.494)
	600	0.69 (0.006)	153 (7)	0.20 (0.006)	773 (39)	13.88 (1.468)	10.33 (1.083)	0.74 (0.078)	6.50 (0.687)
	800	0.69 (0.004)	130 (11)	0.12 (0.011)	1028 (20)	14.92 (2.454)	13.26 (0.748)	0.89 (0.050)	6.20 (1.020)

POC/cell/d, particulate organic carbon production rate (pg C $cell^{-1}$ d^{-1}); PIC/cell/d, particulate inorganic carbon production rate (pg C $cell^{-1}$ d^{-1}); PIC/POC, PIC : POC ratio; POC/PON, POC : PON ratio. More detailed information is given as in Table 2. The values are expressed as the mean of four replicates. Data in the brackets are the standard deviations for four replicates.

POC production rate

Both, changing carbonate chemistry conditions and light intensity independently and interactively affected POC production rates (Table 2). POC production rates increased significantly at 51 Pa and 105 Pa with increasing light intensity until 400 μmol photons m^{-2} s^{-1}. At 51 Pa, POC production rates did not show a significant difference at 400–800 μmol photons m^{-2} s^{-1} (Tukey Post hoc, df = 1, $p > 0.1$) (Fig. 3A). At 105 Pa, POC production rates decreased significantly when light intensity increased from 400 μmol photons m^{-2} s^{-1} to 800 μmol photons m^{-2} s^{-1} (Tukey Post hoc, df = 1, $p < 0.001$) (Fig. 3A; Table 3). In comparison to 51 Pa, measured POC production rates at 105 Pa P_{CO_2} were higher at 200 μmol photons m^{-2} s^{-1} (Tukey Post hoc, df = 1, $p < 0.01$), but significantly lower at 400 μmol photons m^{-2} s^{-1}, 600 μmol photons m^{-2} s^{-1}, and 800 μmol photons m^{-2} s^{-1} (Fig. 3A,B).

Table 4. Calculated maximum values for growth, POC and PIC production rates. At each P_{CO_2} level, growth, POC and PIC production rates were fitted using equation 2, and the maximum values were calculated according to equation 4.

P_{CO_2} (Pa)	Maximum growth rate (d^{-1})	Maximum POC production rate (pg C $cell^{-1}$ d^{-1})	Maximum PIC production rate (pg C $cell^{-1}$ d^{-1})
51	1.24 ± 0.01^a	34.42 ± 2.65^a	49.90 ± 2.59^a
105	0.95 ± 0.01^b	29.33 ± 4.30^a	22.44 ± 1.44^b
152	0.72 ± 0.01^c	14.72 ± 0.94^b	12.78 ± 0.64^c

Different letters represent statistical different means (Tukey Post hoc, $p < 0.001$). The values are expressed as the mean of four replicates ± one standard deviation.

At 152 Pa, POC production rates increased with enhanced light radiation until 200 μmol photons m^{-2} s^{-1} (Tukey Post hoc, df = 1, $p < 0.05$) and levelled off with further increases in light intensity (Tukey Post hoc, df = 3, $p > 0.05$) (Fig. 3A). At 50 μmol photons m^{-2} s^{-1}, POC production rates did not show any difference at the three P_{CO_2} treatments (Tukey Post hoc, all df = 2, $p > 0.1$) (Fig. 3A,B). At 100–800 μmol photons m^{-2} s^{-1}, POC production rates at high P_{CO_2} were lower than at intermediate P_{CO_2} (Tukey Post hoc, all df = 1, $p < 0.05$ at 100, 200, 400, and 600 treatments; $p > 0.05$ at 800 treatment). At 400 μmol photons m^{-2} s^{-1}, 600 μmol photons m^{-2} s^{-1}, and 800 μmol photons m^{-2} s^{-1}, POC production rates at intermediate P_{CO_2} were significantly lower than at low P_{CO_2} (Tukey Post hoc, all df = 1, $p < 0.05$). Maximum POC production rates at 51 and 105 Pa P_{CO_2} were not significantly different (Tukey Post hoc, df = 1, both $p > 0.05$), and were higher than that at 152 Pa P_{CO_2} (Tukey Post hoc, df = 1, both $p < 0.001$) (Table 4).

PIC production rate

Both, changing carbonate chemistry conditions and light intensity independently and interactively affected PIC production rates (Table 2). At 50 μmol photons m^{-2} s^{-1}, PIC production rates decreased by about 35% and 48% from low to intermediate and high P_{CO_2} (Tukey Post hoc, both df = 1,

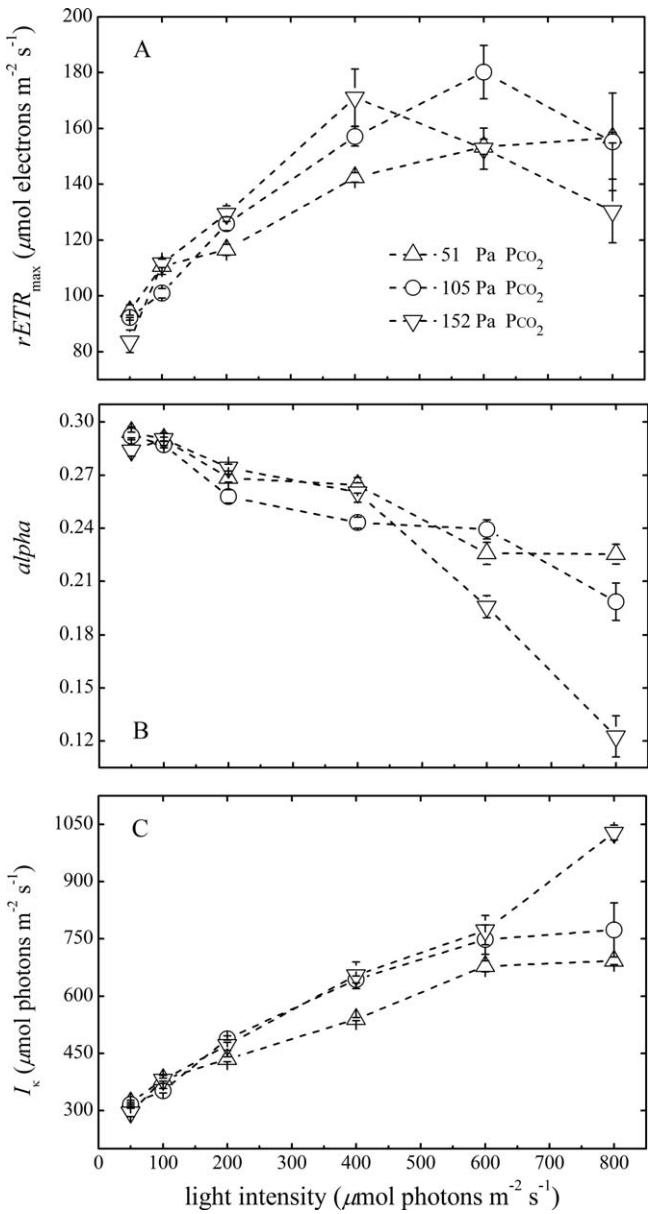

Fig. 2. rETR$_{max}$, alpha and I_k of *G. oceanica* as a function of light intensities at 51 (△), 105 (○) and 152 (▽) Pa P_{CO_2}. (**A**) The maximum of rETR (rETR$_{max}$) as a function of light intensity. (**B**) The initial slope of the light limited part of the P-I curve (alpha) as a function of light intensity. (**C**) Saturation light intensity (I_k) as a function of light intensity. rETR$_{max}$ was calculated according to Eq. 4, alpha was calculated with Eq. 3, and I_k was calculated from the expression rETR$_{max}$/alpha. The values represent the mean of four replicates, with error bars representing ± one standard deviation.

both $p > 0.05$) (Fig. 3C,D; Table 3). At 100–800 μmol photons m^{-2} s^{-1}, PIC production rates decreased by 27–56% at 105 Pa, and by 65–80% at 152 Pa in comparison to 51 Pa (Tukey Post hoc, all df = 1, all $p < 0.001$).

Light intensity had a positive effect on calcification rates at 51 and 105 Pa P_{CO_2} levels (Fig. 3C; Table 3). At 51 Pa P_{CO_2}, calcification rates were enhanced by about 4.5 times with enhanced light radiation until 800 μmol photons m^{-2} s^{-1}. At 105 Pa P_{CO_2}, PIC production rates only increased until 100 μmol photons m^{-2} s^{-1} but stayed constant with a further increase in light intensity (Tukey Post hoc, df = 4, all $p > 0.05$). At 152 Pa P_{CO_2}, PIC production rates did not show significant differences among six light treatments (Tukey Post hoc, df = 5, all $p > 0.05$). Maximum PIC production rates declined significantly with rising P_{CO_2} levels (one-way ANOVA, $F = 484$, df = 2, $p < 0.001$; Tukey Post hoc, df = 2, $p < 0.001$) (Table 4).

PIC : POC ratio and POC : PON ratio

Both, changing carbonate chemistry conditions and light intensity independently and interactively affected PIC : POC ratio and POC : PON ratio (Table 2). At each light treatment, PIC : POC ratios at 51 Pa P_{CO_2} were significantly higher than at 105 and 152 Pa P_{CO_2} (Tukey Post hoc, df = 1, $p < 0.05$) (Fig. 3E). Significant differences in PIC : POC ratios between 105 Pa and 152 Pa P_{CO_2} were found at 100 μmol photons m^{-2} s^{-1}, 400 μmol photons m^{-2} s^{-1}, and 600 μmol photons m^{-2} s^{-1} (Tukey Post hoc, all df = 1, all $p < 0.01$). There was no obvious trend between PIC : POC ratio and light intensity.

Both, elevated P_{CO_2} and higher light intensity reduced POC : PON ratios (Tukey Post hoc, df = 1, $p > 0.05$) (Fig. 3F). At 51 Pa P_{CO_2}, POC : PON ratios at 50 μmol photons m^{-2} s^{-1} and 100 μmol photons m^{-2} s^{-1} were slightly higher than at other treatment conditions (Tukey Post hoc, all $p > 0.05$) (Table 3).

Discussion

Changing carbonate chemistry modulates the light responses of photosynthetic carbon fixation, calcification and growth rates

POC production and growth rates of marine phytoplankton usually increase with increasing light intensity, level off at saturating light intensities and then decline again at inhibiting light levels (e.g., Geider et al. 1997; Gao et al. 2012; Fig. 4A). By fitting the light response curve given in Eq. 2 to our data, we found that rising P_{CO_2} reduced the maximum rates of growth and photosynthetic carbon fixation (Figs. 1A, 3A; Table 4). Presumably, rising P_{CO_2} could reduce the need for CCM activity thereby saving energy (Raven 1991; Hopkinson et al. 2011; McCarthy et al. 2012). In our case, the lower potential for energy dissipation toward higher P_{CO_2} (lower CCM activity) may exacerbate photo inhibition thereby explaining the reduced growth and POC production rates (Figs. 1, 3).

Another reason for higher growth and POC production rates at lower P_{CO_2} and increasing light intensities (Figs. 1B, 3B) may be that increasing light intensities facilitate the operation of CCMs (Rokitta and Rost 2012) thereby enabling cells to satisfy their inorganic carbon requirements for POC

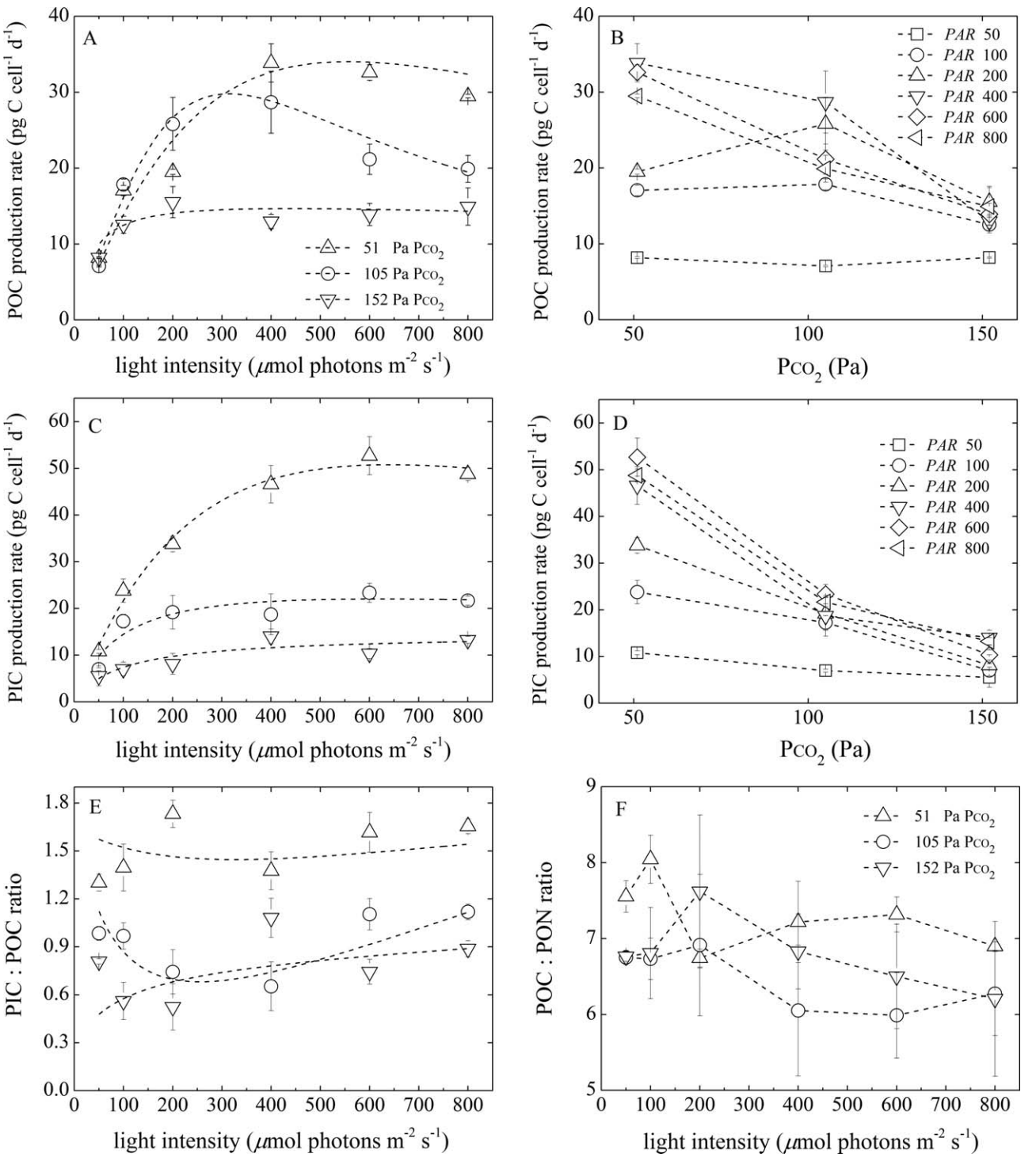

Fig. 3. Effects of light intensity and P_{CO_2} level on POC and PIC production rates, PIC : POC ratio and POC : PON ratio of *G. oceanica*. Panels (**A**), (**C**), (**E**), (**F**) depict POC production rate, PIC production rate, PIC : POC ratio and POC : PON ratio as a function of light intensities at 51 (△), 105 (○) and 152 (▽) Pa P_{CO_2}. Panels (**B**), (**D**) show POC production rate and PIC production rate as a function of P_{CO_2} at 50 μmol photons m^{-2} s^{-1}, 100 μmol photons m^{-2} s^{-1}, 200 μmol photons m^{-2} s^{-1}, 400 μmol photons m^{-2} s^{-1}, 600 μmol photons m^{-2} s^{-1}, and 800 μmol photons m^{-2} s^{-1}. The values represent the mean of four replicates, with error bars representing ± one standard deviation.

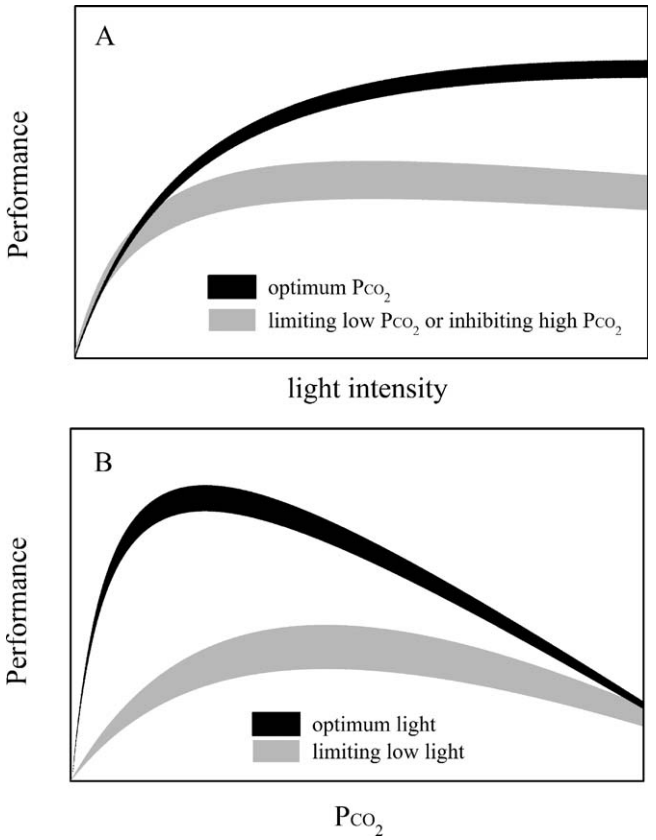

Fig. 4. Conceptual drawing for the interactive effects of light intensity and P_{CO_2} level on the performance (representing growth, photosynthetic carbon fixation, and calcification) of *G. oceanica*. (**A**) The modulating effect of P_{CO_2} on the light response curve. Maximum rates at limiting low P_{CO_2} and inhibiting high P_{CO_2} are lower than at optimum P_{CO_2}. (**B**) The modulating effect of light intensity on the P_{CO_2} sensitivity. Limiting low light intensity shifts the P_{CO_2} optimum toward higher level and reduces the maximum rate.

production and growth rates already at lower P_{CO_2} levels. In fact, at high light intensity, high P_{CO_2} grown cells were found to possess less photosystem I (PS1) per cell and keep a smaller proportion of PSII complexes open compared with low P_{CO_2} grown cells (Burns et al. 2006). Lower PSI and PSII absorbance capacities for light in high P_{CO_2} grown cells could also be expected to lead to lower POC production and growth rates. Furthermore, the proton concentration ($[H^+]$) in the cytosol of the coccolithophore *Emiliania huxleyi* was found to increase with increasing $[H^+]$ in seawater (Suffrian et al. 2011). Cells growing at high P_{CO_2} could suffer from the negative effect of high $[H^+]$ on POC production (Bach et al. 2011) even more so as this effect may be exacerbated by high light intensities (Ihnken et al. 2011).

Calcification is an energy-dependent process and often reduced in coccolithophores at P_{CO_2} levels projected for the end of this century (Riebesell and Tortell 2011; Meyer and Riebesell 2015). However, only some studies focussed on the interactive effects of CO_2 concentration and light intensity on coccolithophore calcification (Zondervan et al. 2002; Feng et al. 2008; Gao et al. 2009; Rokitta and Rost 2012). In this study, a increasing light intensity accelerated calcification rates strongly at lower P_{CO_2} whereas this positive effect was absent at higher P_{CO_2} (Fig. 3C), similar to growth and photosynthetic carbon fixation rates. This supports earlier findings that the sensitivity of calcification rates to light intensity can be modulated by carbonate chemistry (Zondervan et al. 2002; Feng et al. 2008; Gao et al. 2009; Rokitta and Rost 2012). The underlying physiological explanation could be that at limiting light intensity, light is the dominant factor determining the calcification rate and differences in carbonate chemistry conditions are presumably less important. This can be seen at the lowest light intensity in this study (50 μmol photons m^{-2} s^{-1}), where PIC production rates did not show a significant difference among the three P_{CO_2} treatments (Fig. 3D). At saturating light intensity, however, differences in CO_2 or H^+ apparently induce a significant effect on calcification rates (Feng et al. 2008).

For P_{CO_2} levels lower than 29 Pa, Sett et al. (2014) concluded that POC and PIC production and growth rates in the same *G. oceanica* strain were limited by inorganic carbon availability. Although such low P_{CO_2} levels were not included in our study, by fitting the light response curves (Figs. 1A, 3A,C) we conclude that both limiting low P_{CO_2} and inhibiting high P_{CO_2} levels reduce the maximum values for photosynthetic carbon fixation, calcification and growth rates of coccolithophores (Fig. 4A; Table 4).

Rising P_{CO_2} and increasing light intensity synergistically alter the electron transport rate in the light reaction

rETR is a measure for photosynthetic efficiency (Schreiber et al. 1995). To acclimate to high irradiances, phytoplankton cells regulate the photosystem stoichiometry (PSI : PSII) by lowering the amount of photosystem I (PSI) reaction centers relative to PSII complexes (Sonoike et al. 2001). Here we found that the $rETR_{max}$ response of *G. oceanica* (Fig. 2A) to high light intensities was depending on the incubation P_{CO_2} which implies that different P_{CO_2} levels induced changes in PSI : PSII. A study by Burns et al. (2006) revealed that at high light intensity, low P_{CO_2} grown cells contained significantly more PsaC protein (core subunit of photosystem I) in the PSI complex than high P_{CO_2} grown cells. Furthermore, Burns et al. (2006) found that across the range of growth irradiances, PsaC : PSII absorbance capacity (an indicator of PSI content relative to the capacity of PSII to capture light energy) increased in low P_{CO_2} grown cells, whereas they slightly decreased in high P_{CO_2} grown cells. Thus, the observed reduction in $rETR_{max}$ with increasing P_{CO_2} at high light intensities may be due to lower PSI : PSII.

Phytoplankton can alter light absorption for photosynthesis to enable acclimation over a wide range of irradiances (Henriksen et al. 2002). Algae tend to reduce the

pigment contents such as chlorophyll *a*, carotenoids or fucoxanthin in antenna systems to prevent excessive energy to be transferred to PSII reaction centres (Henriksen et al. 2002; Barcelos e Ramos et al. 2012). At 50 μmol photons m^{-2} s^{-1} in this study, the quantum yield of PSII (F_v/F_m, the ratio of photons transferred in the ETR to photons absorbed by PSII) at 152 Pa was only 6% lower than at 51 Pa. However, at 800 μmol photons m^{-2} s^{-1} the quantum yield of PSII at 152 Pa was 30% lower than at 51 Pa (data not shown). This indicates that high light intensity and high P_{CO_2} may synergistically reduce the quantum yield of PSII (the maximum efficiency of PSII), which leads to large diminution in alpha at high P_{CO_2} and high light conditions (Fig. 2B).

Light intensity modulates the P_{CO_2} sensitivity of photosynthetic carbon fixation, calcification and growth rates

Physiological responses to a broad range of P_{CO_2} levels of coccolithophores investigated in this respect so far displayed optimum curve patterns (Langer et al. 2006; Bach et al. 2011, 2015; Sett et al. 2014; Müller et al. 2015). Growth and production rates of POC and PIC increase with increasing P_{CO_2} levels, reach a maximum, and then decline linearly with further P_{CO_2} (proton concentration ($[H^+]$)) increase (Bach et al. 2011; Sett et al. 2014; Bach et al. 2015; Fig. 4B). The CO_2 and HCO_3^- availability was identified as the factor responsible for the observed decline of growth and production rates toward the left side of the optimum, the proton concentration ($[H^+]$) was the driving factor toward the right side of the optimum (Bach et al. 2011, 2015). The sensitivities of these rates to inorganic carbon availability and H^+ were clearly modulated by light intensity (Figs. 1B, 3B,D). Light availability is likely to affect the supply of inorganic carbon to photosynthesis, calcification and growth in general (Zondervan et al. 2002; Barcelos e Ramos et al. 2012; Rokitta and Rost 2012).

We did not directly determine the P_{CO_2} optimum for PIC production rates in this study as our treatment levels were limited. Sett et al. (2014), however, found that the P_{CO_2} optimum for calcification in the same *G. oceanica* strain was at about 29 Pa at 20°C and 150 μmol photons m^{-2} s^{-1}. According to this, the lowest P_{CO_2} level applied in our study (51 Pa) was too high to detect the optimum of the *G. oceanica* P_{CO_2} response curve. Nevertheless, assuming an optimum curve response and using the model described in Bach et al. (2011) as given in Eq. 8, the optimum P_{CO_2} for photosynthetic carbon fixation, calcification and growth rates shift toward lower levels with increasing light intensities (Figs. 1B, 3B). This is in line with findings by Rokitta and Rost (2012) who showed that the half-saturation DIC concentrations for carbon fixation of the calcifying algae *E. huxleyi* were 111 μmol kg^{-1} at 50 μmol photons m^{-2} s^{-1} and 20 μmol kg^{-1} at 300 μmol photons m^{-2} s^{-1}. The reasons for the shift could be

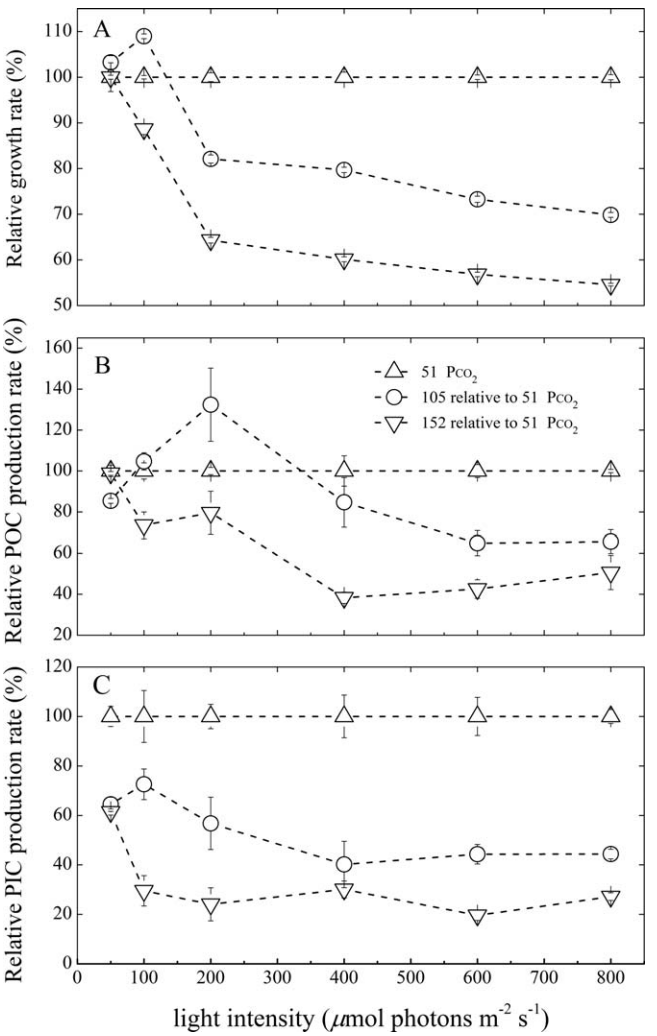

Fig. 5. Comparison of growth, POC and PIC production rates at 105 (○) and 152 (▽) Pa P_{CO_2} relative to those at 51 (△) Pa P_{CO_2}. The values represent the mean of four replicates, with error bars representing ± one standard deviation.

that higher light intensities provide more energy to allow for higher CCM activity which would help to overcome carbon limitation at lower P_{CO_2} levels (McGinn et al. 2003; Rokitta and Rost 2012). Following the growth rate response to light intensity shown in Fig. 1A, growth rate is expected to decrease toward increasingly inhibiting high light intensities beyond the measurement range of 800 μmol photons m^{-2} s^{-1}. If growth rates would drop more pronounced at low than at high P_{CO_2} levels, the P_{CO_2} optimum for growth shown in Fig. 1B is expected to be higher at inhibiting high light than at optimum light intensity.

Based on the results of this and other studies (Zondervan et al. 2002; Rost et al. 2003), we conclude that the optimum P_{CO_2} levels for growth, POC and PIC production rates at limiting low light are higher than at optimum light intensities (Figs. 1B, 3B,D, 4B). Furthermore, the maximum values for

these rates are lower at limiting low light than at optimum light intensities (Fig. 4B).

In an earlier study with *E. huxleyi*, Rokitta and Rost (2012) put forward a light dependent model suggesting that the rate of a physiological process is governed primarily by light intensity, and changes in P_{CO_2} levels will exacerbate or weaken the effects of light intensity on this rate. Our data supported the light dependent model (Figs. 1, 3). However, Rokitta and Rost (2012) found that the sensitivities of POC and PIC production rates of *E. huxleyi* to high P_{CO_2} are stronger at 50 μmol photons m^{-2} s^{-1} than at 300 μmol photons m^{-2} s^{-1}, whereas we observed a stronger effect of high P_{CO_2} on POC and PIC production rates at 600–800 μmol photons m^{-2} s^{-1} compared with 50 μmol photons m^{-2} s^{-1} (Fig. 5). This discrepancy is possibly due to the variable sensitivities of *E. huxleyi* and *G. oceanica* to light and P_{CO_2}.

The results of our study show that increasing light intensity decreases the P_{CO_2} optima for carbon fixation, calcification and growth rates of *G. oceanica*. In contrast, rising temperature had the opposite effect, increasing the P_{CO_2} optima for these rates (Sett et al. 2014). These opposing trends are likely due to the fact that temperature primarily modulates carbon demand by accelerating metabolic activity, whereas light also affects carbon supply through energy provision to carbon uptake mechanisms. In the future ocean, both light intensity and temperature in the upper mixed layer will generally increase (Sarmiento et al. 2004; IPCC 2013). How these combined effects will affect the competitive fitness of this and other coccolithophore species under future ocean scenarios is difficult to predict with the information presently available (Riebesell and Gattuso 2015). It emphasizes the need for further investigation on the interacting effect of simultaneous modification of life-sustaining properties such as temperature, CO_2, light, and nutrients in the marine environment.

References

Bach, L. T., U. Riebesell, and K. G. Schulz. 2011. Distinguishing between the effects of ocean acidification and ocean carbonation in the coccolithophore *Emiliania huxleyi*. Limnol. Oceanogr. **56**: 2040–2050. doi:10.4319/lo.2011.56.6.2040

Bach, L. T., U. Riebesell, M. A. Gutowska, L. Federwisch, and K. G. Schulz. 2015. A unifying concept of coccolithophore sensitivity to changing carbonate chemistry embedded in an ecological framework. Prog. Oceanogr. **135**: 125–138. doi:10.1016/j.pocean.2015.04.012

Barcelos e Ramos, J., K. G. Schulz, S. Febiri, and U. Riebesell. 2012. Photoacclimation to abrupt changes in light intensity by *Phaeodactylum tricornutum* and *Emiliania huxleyi*: The role of calcification. Mar. Ecol. Prog. Ser. **452**: 11–26. doi:10.3354/meps09606

Björkman, O., and B. Demmig. 1987. Photon yield of O_2 evolution and chlorophyll fluorescence characteristics at 77 K among vascular plants of diverse origins. Planta **170**: 489–504. doi:10.1007/BF00402983

Bopp, L., and others. 2001. Potential impact of climate change on marine export production. Global Biogeochem. Cycles **15**: 81–99. doi:10.1029/1999GB001256

Braarud, T., K. R. Gaarder, J. Marklaki, and E. Nordli. 1952. Coccolithophorids studied in the electron microscope. Observations on *Coccolithus huxleyi* and *Syracosphaera carterae*. Nytt Mag. Bot. **1**: 129–134.

Burns, R. A., T. D. B. MacKenzie, and D. A. Campbell. 2006. Inorganic carbon repletion constrains steady-states light acclimation in the cyanobacterium *Synechococcus elongatus*. J. Phycol. **42**: 610–621. doi:10.1111/j.1529-8817.2006.00220.x

Danbara, A., and Y. Shiraiwa. 1999. The requirement for selenium for the growth of marine coccolithophorids, *Emiliania huxleyi*, *Gephyrocapsa oceanica* and *Helladosphaera* sp. (Prymnewsiophyceae). Plant Cell Physiol. **40**: 762–766. doi:10.1093/oxfordjournals.pcp.a029603

Dickson, A. G., J. D. Afghan, and G. C. Anderson. 2003. Reference materials for oceanic CO_2 analysis: A method for the certification of total alkalinity. Mar. Chem. **80**: 185–197. doi:10.1016/S0304-4203(02)00133-0

Eilers, P., and J. Peeters. 1988. A model for the relationship between light intensity and the rate of photosynthesis in phytoplankton. Ecol. Model. **42**: 199–215. doi:10.1016/0304-3800(88)90057-9

Feng, Y., M. E. Warner, Y. Zhang, J. Sun, F. X. Fu, J. M. Rose, and D. A. Hutchins. 2008. Interactive effects of increased P_{CO_2}, temperature and irradiance on the marine coccolithophore *Emiliania huxleyi* (Prymnesiophyceae). Eur. J. Phycol. **43**: 87–98. doi:10.1080/09670260701664674

Gao, K., Z. Ruan, V. E. Villafañe, J. P. Gattuso, and E. W. Helbling. 2009. Ocean acidification exacerbates the effect of UV radiation on the calcifying phytoplankton *Emiliania huxleyi*. Limnol. Oceanogr. **54**: 1855–1862. doi:10.4319/lo.2009.54.6.1855

Gao, K., and others. 2012. Rising CO_2 and increased light exposure synergistically reduce marine primary productivity. Nat. Clim. Change **2**: 519–523. doi:10.1038/nclimate1507

Geider, R. J., H. L. MacIntyre, and T. M. Kana. 1997. Dynamic model of phytoplankton growth and acclimation: Responses of the balanced growth rate and the chlorophyll a: carbon ratio to light, nutrient-limitation and temperature. Mar. Ecol. Prog. Ser. **148**: 187–200. doi:10.3354/meps148187

Giordano, M., J. Beardall, and J. A. Raven. 2005. CO_2 concentrating mechanisms in algae: Mechanisms, environmental modulation and evolution. Annu. Rev. Plant Biol. **56**: 99–131. doi:10.1146/annurev.arplant.56.032604.144052

Guillard, R. R., and J. H. Ryther. 1962. Studies of marine planktonic diatoms. I. *Cyclotella nana* Hustedt, and *Detonula confervacea* (cleve) Gran. Can. J. Microbiol. **8**: 229–239. doi:10.1139/m62-029

Henriksen, P., B. Riemann, H. Kaas, H. M. Sørensen, and H. L. Sørensen. 2002. Effects of nutrient-limitation and

irradiance on marine phytoplankton pigments. J. Plankton Res. **24**: 835–858. doi:10.1093/plankt/24.9.835

Hopkinson, B. M., C. L. Dupont, A. E. Allen, and F. M. M. Morel. 2011. Efficiency of the CO_2-concentrating mechanism of diatoms. Proc. Natl. Acad. Sci. USA **8**: 3830–3837. doi:10.1073/pnas.1018062108

Houghton, J. T., and others. 2001. Climate change 2001: The scientific basis, p. 36–40. Cambridge Univ. Press.

Ihnken, S., S. Roberts, and J. Beardall. 2011. Differential responses of growth and photosynthesis in the marine diatom *Chaetoceros muelleri* to CO_2 and light availability. Phycologia **50**: 182–193. doi:10.2216/10-11.1

Intergovernmental Panel on Climate Change (IPCC). 2013. Summary for Policymakers, p: 3–33. *In* T. F. Stocker, and others [eds.], Climate change 2013: The physical science basis. Contribution of Working Group I to the Fifth Assessment Report of the Intergovernmental Panel on Climate Change. Cambridge Univ. Press.

Kaeriyama, H., F. Katsuki, M. Otsubo, M. Yamada, K. Ichimi, K. Tada, and P. J. Harrison. 2011. Effects of temperature and irradiance on growth of strains belonging to seven *Skeletonema* species isolated from Dokai Bay, southern Japan. Eur. J. Phycol. **46**: 113–124. doi:10.1080/09670262.2011.565128

Kester, D., I. W. Duedall, D. N. Connors, and R. M. Pytkowicz. 1967. Preparation of artificial seawater. Limnol. Oceanogr. **1**: 176–179. doi:10.4319/lo.1967.12.1.0176

Langer, G., M. Geisen, K. H. Baumann, J. Kläs, U. Riebesell, S. Thoms, and J. R. Young. 2006. Species-specific responses of calcifying algae to changing seawater carbonate chemistry. Geochem. Geophys. Geosyst. **7**: 1–12. doi:10.1029/2005GC001227

McCarthy, A., S. P. Rogers, S. J. Duffy, and D. A. Campbell. 2012. Elevated carbon dioxide differentially alters the photophysiology of *Thalassiosira pseudonana* (Bacillariophyceae) and *Emiliania huxleyi* (Haptophyta). J. Phycol. **48**: 635–646. doi:10.1111/j.1529-8817.2012.01171.x

McGinn, P. J., G. D. Price, R. Maleszka, and M. R. Badger. 2003. Inorganic carbon limitation and light control the expression of transcripts related to the CO_2-concentrating mechanism in the cyanobacterium *Synechocystis* sp. strain PCC 6803. Plant Physiol. **132**: 218–229. doi:10.1104/pp.102.019349

Merico, A., T. Tyrrell, E. J. Lessard, T. Oguz, P. J. Stabeno, S. I. Zeeman, and T. E. Whitledge. 2004. Modelling phytoplankton succession on the Bering Sea shelf: Role of climate influences and trophic interactions in generating *Emiliania huxleyi* blooms 1997–2000. Deep-Sea Res. Part I **51**: 1803–1826. doi:10.1016/j.dsr.2004.07.003

Meyer, J., and U. Riebesell. 2015. Reviews and syntheses: Responses of coccolithophores to ocean acidification: A meta-analysis. Biogeosciences **12**: 1671–1682. doi:10.5194/bg-12-1671-2015

Müller, M. N., T. W. Trull, and G. M. Hallegraeff. 2015. Different responses of three Southern Ocean *Emiliania huxleyi* ecotypes to changing seawater carbonate chemistry. Mar. Ecol. Prog. Ser. **531**: 81–90. doi:10.3354/meps11309

Pierrot, D., E. Lewis, and D. W. R. Wallace. 2006. MS Excel program developed for CO_2 system calculations. ORNL/CDIAC-105. Carbon Dioxide Information Analysis Centre, Oak Ridge National Laboratory, U.S. Department of Energy. doi:10.3334/CDIAC/otg.CO2SYS_XLS_CDIAC105a

Raven, J. A. 1991. Physiology of inorganic C acquisition and implications for resource use efficiency by marine phytoplankton: Relation to increased CO_2 and temperature. Plant Cell Environ. **14**: 779–794. doi:10.1111/j.1365-3040.1991.tb01442.x

Riebesell, U. 2004. Effects of CO_2 enrichment on marine phytoplankton. J. Oceanogr. **60**: 719–729. doi:10.1007/s10872-004-5764-z

Riebesell, U., and P. D. Tortell. 2011. Effects of ocean acidification on pelagic organisms and ecosystems, p. 99–121. *In* J. P. Gattuso and L. Hansson [eds.], Ocean acidification. Oxford Univ. Press.

Riebesell, U., and J. P. Gattuso. 2015. Lessons learned from ocean acidification research. Nat. Clim. Chang. **5**: 12–14. doi:10.1038/nclimate2456

Rokitta, S. D., and B. Rost. 2012. Effects of CO_2 and their modulation by light in the life-cycle stages of the coccolithophore *Emiliania huxleyi*. Limnol. Oceanogr. **57**: 607–618. doi:10.4319/lo.2012.57.2.0607

Rost, B., U. Riebesell, and S. Burkhardt. 2003. Carbon acquisition of bloom-forming marine phytoplankton. Limnol. Oceanogr. **48**: 56–67. doi:10.4319/lo.2003.48.1.0055

Rost, B., and U. Riebesell. 2004. Coccolithophores and the biological pump: Responses to environmental changes, p. 99–125. *In* H. R. Thierstein and J. R. Young [eds.], Coccolithophores: From molecular biology to global impact. Springer.

Roy, R. N., and others. 1993. Thermodynamics of the dissociation of boric acid in seawater at S 5 35 from 0 degrees C to 55 degrees C. Mar. Chem. **44**: 243–248. doi:10.1016/0304-4203(93)90206-4

Sabine, C. L., and others. 2004. The oceanic sink for anthropogenic CO_2. Science **305**: 367–371. doi:10.1126/science.1097403

Sarmiento, J. L., and others. 2004. Response of ocean ecosystems to climate warming. Global Biogeochem. Cycle **18**: GB3003. doi:10.1029/2003GB002134

Schippers, P., M. Lürling, and M. Scheffer. 2004. Increase of atmospheric CO_2 promotes phytoplankton productivity. Ecol. Lett. **7**: 446–451. doi:10.1111/j.1461-0248.2004.00597.x

Schreiber, U., W. Bilger, and C. Neubauer. 1995. Chlorophyll fluorescence as a nonintrusive indicator for rapid assessment of in vivo photosynthesis, p. 49–70. *In* E. D. Schulze and M. M. Caldwell [eds.], Ecophysiology of photosynthesis. Springer.

Sett, S., L. T. Bach, K. G. Schulz, S. Koch-Klavsen, M. Lebrato, and U. Riebesell. 2014. Temperature modulates coccolithophorid sensitivity of growth, photosynthesis and calcification to increasing seawater P_{CO_2}. PLoS ONE **9**: e88308. doi:10.1371/journal.pone.0088308

Sonoike, K., Y. Hihara, and M. Ikeuchi. 2001. Physiological significance of the regulation of photosystem stoichiometry upon high light acclimation of *Synechocystis* sp. PCC 6803. Plant Cell Physiol. **42**: 379–384. doi:10.1093/pcp/pce046

Suffrian, K., K. G. Schulz, M. A. Gutowska, U. Riebesell, and M. Bleich. 2011. Cellular pH measurements in *Emiliania huxleyi* reveal pronounced membrane proton permeability. New Phytol. **190**: 595–608. doi:10.1111/j.1469-8137.2010.03633.x

Xu, K., and K. S. Gao. 2012. Reduced calcification decreases photoprotective capability in the coccolithophorid *Emiliania huxleyi*. Plant Cell Physiol. **53**: 1267–1274. doi:10.1093/pcp/pcs066

Zondervan, I., B. Rost, and U. Riebesell. 2002. Effect of CO_2 concentration on the PIC/POC ratio in the coccolithophore *Emiliania huxleyi* grown under light-limiting conditions and different day lengths. J. Exp. Mar. Biol. Ecol. **272**: 55–70. doi:10.1016/S0022-0981(02)00037-0

Acknowledgments

The authors are grateful to Silke Lischka for reading and revising the manuscript, to Andrea Ludwig and Jana Meyer for dissolved inorganic carbon measurements, and to Kerstin Nachtigall for particulate organic and inorganic carbon measurements. We also thank the China Scholarship Council (CSC) for its support of Yong Zhang. This work was supported by the German Federal Ministry of Education and Research (Bundesministerium für Bildung und Forschung) in the framework of the collaborative project Biological Impacts of Ocean Acidification (BIOACID). Kai G. Schulz is the recipient of an Australian Research Council Future Fellowship (FT120100384).

Submitted 25 February 2015
Revised 29 July 2015
Accepted 3 August 2015

Associate editor: Heidi Sosik

Chapter 4. Population- and genotype-specific responses of *Emiliania huxleyi* to a broad CO_2 range

Yong Zhang[1], Lennart T. Bach[1], Kai T. Lohbeck[1,2], Kai G. Schulz[3], and Ulf Riebesell[1]

[1]Biological Oceanography, GEOMAR Helmholtz-Centre for Ocean Research Kiel, Kiel, Germany

[2]Evolutionary Ecology of Marine Fishes, GEOMAR Helmholtz-Centre for Ocean Research Kiel, Kiel, Germany

[3]Centre for Coastal Biogeochemistry, School of Environmental Science and Management, Southern Cross University, Lismore, NSW, Australia

Running head: *Emiliania huxleyi* pCO_2 response

Corresponding author: yzhang@geomar.de

To be submitted

Abstract

The ongoing oceanic uptake of anthropogenic CO_2 is steadily shifting the seawater carbonate chemistry and reducing the surface ocean pH. A large number of studies have paid special attention to the effect of rising pCO_2 on physiological processes of the coccolithophore *Emiliania huxleyi*. However, inconsistent results still remain. In the present study, we investigated the responses of growth, particulate organic (POC) and inorganic (PIC) carbon production rates of 17 *E. huxleyi* genotypes from the coastal North Atlantic (Bergen, Norway), the central Atlantic (Azores, Portugal) and the pelagic North Atlantic (Gran Canaria, Spain) to a broad pCO_2 gradient ranging from about 116 to 3073 µatm. Growth, POC and PIC production rates of three populations and of individual genotypes within populations displayed optimum response patterns along the pCO_2 gradient. That we found distinct population specific responses indicates limited dispersal in *E. huxleyi*. Different carbonate chemistry sensitivity in physiological rates may be related to local pCO_2 variability. Within each population, we found genotype-by-environment interactions, phenotypic plasticity and trade-offs, which may contribute to maintain high genetic diversity in *E. huxleyi*. Our data indicate that different pCO_2 response patterns found in previous studies may be caused by both different genotypes and a narrow pCO_2 gradient mostly ranging from 200 to 1200 µatm. The existence of distinct populations and different genotypes within populations may be the mechanisms allowing *E. huxleyi* species to distribute in and acclimate to the changing environmental conditions.

Introduction

Rising partial pressures of atmospheric carbon dioxide (pCO_2), primarily from human fossil fuel combustion, has caused shifts in seawater carbonate chemistry speciation and a reduction of surface ocean pH (IPCC, 2013). Elevated carbon dioxide concentration due to rising pCO_2 is thought to fertilize the photosynthetic carbon fixation, calcification and growth rates of the coccolithophores (Riebesell and Tortell, 2011). However, when pCO_2 increased to be higher than the optima pCO_2, increasing proton concentration ($[H^+]$) was suggested to reduce these rates (Bach et al., 2011; 2015).

Coccolithophores form a layer of calcium carbonate ($CaCO_3$) plates around the cells, which drives the carbonate counter pump and releases CO_2 to the environment by reducing the ocean's alkalinity. Moreover they contribute to the carbon pump via carbon-fixation by photosynthesis, which takes up CO_2 from the surface ocean (Rost and Riebesell, 2004). Contradictory CO_2 response patterns in growth, photosynthetic carbon fixation and calcification rates of different coccolithophore *Emiliania huxleyi* strains have been reported at a narrow pCO_2 range by several studies (Table 1). Intra-specific variability between *E. huxleyi* genotypes were suggested to cause differences in the response patterns of physiological rates by Langer et al. (2009), who investigated different pCO_2 response patterns of four *E. huxleyi* strains isolated at four different locations at about 200 to 1200 µatm. Until now, there are inconsistent results on how *E. huxleyi* genotypes respond to a range of pCO_2 in terms of growth, photosynthetic carbon fixation and calcification rates (Meyer and Riebesell, 2015).

Both oceanographic boundaries formed by ocean currents, and biological factors can limit dispersal of marine phytoplankton and reduce gene flow between geographic populations, which

results in differentiated populations (Palumbi, 1994). Some marine coccolithophores such as *E. huxleyi* and *Gephyrocapsa oceanica*, are characterized by significant genetic differentiation and distinct growth rates among different populations or genotypes (Brand, 1982; Cook et al., 2013). This indicates that separated populations apparently are able to acclimate to highly dynamic environments. Within a population, a genotype-by-environment (G x E) interaction is evident when distinct genotypes perform differently across environmental conditions (De Jong, 1990). Such variation is particularly important for a population to cope with global change (Lohbeck et al., 2012; Gsell et al., 2012). A trade-off occurs when a trait that is advantageous at one environment confers a disadvantage at others (Litchman and Klausmeier, 2008). Standard deviation in growth rate within-population was found to be larger than between-population (Zhang et al., 2014). Thus, single genotype of a population was not suggested to represent the response of a phytoplankton functional group to changing environmental conditions (Schaum et al., 2012; Zhang et al., 2014).

In this study, we used six *E. huxleyi* genotypes each from the Azores, Portugal, and the Norwegian coast off Bergen, and five genotypes from Gran Canaria, Spain. We investigated the responses of growth, photosynthetic carbon fixation and calcification rates of three populations and of six (or five) genotypes within each population to a broad pCO_2 gradient ranging from about 116 to 3073 µatm. Based on our results, we discuss a possible role of inter- and intra-population variations of natural *E. huxleyi* communities to cope with ocean change.

Material and method

Cell isolation sites

Emiliania huxleyi (Lohm.) Hay and Mohler (morphotype A) genotypes B95, B63, B62, B51, B41 and B17 were isolated by K. T. Lohbeck from the Raunefjord, southwest of Bergen (60°18'N, 05°15'E) in May 2009 (Lohbeck et al., 2012) with about 8 °C. *E. huxleyi* genotypes A23, A22, A21, A19, A13 and A10 were isolated by S. L. Eggers near Faial, at the Azores (38°34'N, 28°42'W) in May or June 2010 with about 18 °C. *E. huxleyi* genotypes C98, C91, C90, C41 and C35 were isolated by K. T. Lohbeck from Gran Canaria (27°58'N, 15°36'W) in February 2014 with about 19 °C (Table S1). Surface seawater pCO_2 range from about 320 to 400 µatm at the Azores and Gran Canaria, and from about 220 to 400 µatm off Bergen (Table S2). Seasonal variability is evident in pCO_2, with amplitude of 80 µatm at the Azores, 200 to 250 µatm at Bergen and 60 to 80 µatm at Gran Canaria.

Experimental setup

Stock cultures of *E. huxleyi* were kept at 15 °C in 50 ml tissue culture flasks (Sarstedt) with ventilation caps since they were isolated. The cultures were grown in monoclonal, non-axenic populations since isolation. Microscopic inspections verified that no significant bacterial fraction and no other algae were present. Based on the local temperature ranges at the Azores, Bergen and Gran Canaria, 17 *E. huxleyi* genotypes were cultured at 16 °C in this study. Six experiments were conducted. Three genotypes (one comes from the Azores, one comes from Bergen and one comes from Gran Canaria) were chosen in every experiment. Cells were grown in artificial seawater (ASW) medium in dilute batch culture conditions at 200 µmol photons m^{-2} s^{-1} of photosynthetically active radiation (*PAR*) in two RUMED Light Thermostats (Rubarth Apparate GmbH) at a 16:8 h light:dark cycle.

In every experiment, about 36 liters ASW were pumped out off a 1000 liter stock tank, in which ASW was prepared according to Kester et al. (1967) with a salinity of 35 without the initial addition of dissolved inorganic carbon and total alkalinity in form of $NaHCO_3$. The ASW was enriched with 64 μmol kg^{-1} nitrate (NO_3^-), 4 μmol kg^{-1} phosphate (PO_4^{3-}), f/8 concentrations for trace metals and vitamins (Guillard and Ryther, 1962), 10 nmol kg^{-1} SeO_2 (Danbara and Shiraiwa, 1999), and 2 mL kg^{-1} of sterile filtered (0.2 μm pore size, Sartobran® P 300, Sartorius) North Sea water to prevent possible trace metal limitation during culturing. Enriched the ASW medium was transferred to eleven autoclaved 2.5 L polycarbonate bottles (Nalgene® Bottles). According to eleven expected pCO_2 levels of about 120 to 3000 μatm, calculated Na_2CO_3 (2 mol L^{-1}, Merck, Suprapur quality and dried for 2 hours at 200 °C before dissolution) and hydrochloric acid (certified HCl with a concentration of 3.571 mol L^{-1}, Merck) were added to each bottle. After being rotated carefully, ASW in each 2.5 L polycarbonate bottles was respectively filtered (0.2 μm pore size, Sartobran® P 300, Sartorius) with gentle pressure and carefully pumped into three 0.25 L glass bottles for acclimation culture and into three 0.5 L glass bottles for experimental culture. Bottles for both acclimation and the main experiment were filled with ASW medium leaving a minimum headspace of about 1% to keep gas exchange at a minimum. All glass bottles were stored at the experimental temperature of 16 °C for at least 12 hours prior to inoculation. During the acclimation period, cells were acclimated to experimental conditions for at least 7 generations, which corresponded to 4 to 7 days depending on cell division rate. Initial cell density was 200 cells ml^{-1}, and in order to avoid significant changes in carbonate chemistry speciation, final cell density did not exceed 100,000 cells mL^{-1}. Culture bottles were manually rotated twice a day at 5 and 12 hours after the onset of the light phase to reduce sedimentation of the cells.

Carbonate chemistry measurements

Samplings started 6 hours after the onset of the light period and lasted no longer than 2 hours. Samples for total alkalinity (TA) measurements were filtered (0.2 µm pore size, Filtropur S 0.2, Sarstedt) by gentle pressure, stored at 4 ^{o}C and processed within 14 days. TA was measured in duplicate by open-cell potentiometric titration using an 862 Compact Titrosample (Metrohm) according to Dickson et al. (2003). pH samples were filtered (0.2 µm pore size, Filtropur S 0.2, Sarstedt) by gentle pressure into 100 mL Duran flasks (Schott). The bottles were filled with samples from bottom to top and with overflow, tightly closed without headspace, stored at 4 ^{o}C and processed within 7 days. With adding a small amount of a pH indicator dye (*m*-cresol purple, Sigma-Aldrich), pH was measured using a spectrophotometer (Cary 100 UV-Visible Spectrophotometer, Agilent) according to Dickson et al. (2007). The carbonate system was calculated from TA, pH, phosphate, temperature, and salinity using the software CO2SYS (Lewis and Wallace, 1998) with temperature and salinity dependent stoichiometric equilibrium constants K_1 and K_2 for carbonic acid taken from Roy et al. (1993).

Growth rate measurements

At the end of incubations, about 25 mL samples were taken from the culture bottles, always at the same time of the day (about 8 hours after the onset of the light phase). Cell number was determined using a Z2 Coulter Particle Counter and Size Analyzer (Beckman). Growth rate (μ) was calculated according to the equation: $\mu = (\ln N_1 - \ln N_0)/d$, where N_0 and N_1 are cell numbers at the beginning and the end of a growth interval, and d is the duration of the growth period in days.

Particulate organic (POC) and inorganic (PIC) carbon measurements

Samples for total particulate carbon (TPC) and total organic carbon (TOC) were taken 10 hours after the onset of the light period. Sampling procedures lasted on longer than 2 hours. TPC and TOC samples were gently filtered onto pre-combusted (500 ^{o}C, 8 hours) GF/F filters and stored in the dark at –20 ^{o}C. At high pCO_2 levels, cell concentrations were lower and then effect of background carbon on TPC and TOC would be relatively high. In order to avoid the influence of background carbon (BC) on TOC, ASW without algae samples were filtered at eleven pCO_2 levels.

Prior to the measurement, TOC and BC filters were fumed with 37.1% HCl (w/w) for 2 hours to remove all inorganic carbon. After 8 hours of drying at 60 ^{o}C, TPC, TOC and BC were measured using an Elemental Analyzer coupled to an isotope ratio mass spectrometer (EuroEA, Hekatech GmbH). Particulate organic carbon (POC) was calculated as the difference between TOC and BC. Particulate inorganic carbon (PIC) was calculated as the difference between TPC and TOC. POC and PIC production rate were calculated as:

$$\text{POC production rate} = \mu\ (d^{-1}) \times (\text{TOC - BC}) \text{ content (pg C cell}^{-1}) \quad [1]$$

$$\text{PIC production rate} = \mu\ (d^{-1}) \times (\text{TPC -TOC}) \text{ content (pg C cell}^{-1}) \quad [2]$$

Please note that influence of background carbon on PIC was avoided by using equation [2].

Data analysis

A broad range of pCO_2 treatments were set up with no replication on the genotype level. A nonlinear regression model was used to analyze the data. This approach provides more information for ecological modelling than the analysis of variance (ANOVA), nevertheless

without loss of statistical power (Cottingham et al., 2005).

Growth, POC and PIC production rates are expected to increase with increasing pCO_2, reach a maximum, and then decline linearly with further pCO_2 increase (Bach et al., 2011; Sett et al., 2014). Thus, the Michaelis-Menten kinetic was modified by subtracting a linear term and then the modified Michaelis-Menten equation [3] was used to fit these rates at a broad pCO_2 gradient.

$$y = \frac{X \times pCO_2}{Y + pCO_2} - s \times pCO_2 \quad [3]$$

where X and Y are random fit parameters, and s is the sensitivity constant which describes the negative effect of increasing H^+ (which is quasi proportional to pCO_2 at constant TA). Based on the fitted X, Y and s, we calculated the pCO_2 optima (K_m) for growth, POC and PIC production rates according to equation [4]. Then X, Y, s and K_m were used to calculate the maximum values (V_{max}) for analyzed parameters according to function [3].

$$K_m = \sqrt{\frac{X \times Y}{s}} - Y \quad [4]$$

For further details, *see* Bach et al. (2011). The difference in temperature range between Bergen and the Azores or Gran Canaria is relatively large (Table S1). And temperature was found to affect the sensitivity of physiological responses of coccolithophores to pCO_2 (Schlüter et al., 2014; Sett et al., 2014). The relative values for growth, POC and PIC production rates were calculated as ratios of growth, POC and PIC production rates at each pCO_2 level to the maximum (highest) rates. We obtained the relative sensitivity constant by fitting function [3] based on relative growth, POC and PIC production rates. It is more useful to compare the relative sensitivity constant among populations, because relative sensitivity constant directly describes the sensitivity of each parameter to increasing H^+ at the population level. However, sensitivity constant (SC) of each parameter for individual genotypes can be used to compare within each population. This is due to

the fact that all genotypes within population experience the same environmental conditions.

Statistical differences in K_m, V_{max} and relative sensitivity constant were determined by means of a one-way analysis of variance (ANOVA). A Tukey Post hoc test was performed to identify the source of the main effect determined by ANOVA. Normality of residuals was tested with a Shapiro-Wilk's test. Levene's test was conducted graphically to test for homogeneity of variances in case of significant data. A generalized least squares (*GLS*) model was used to stabilize heterogeneity if variances were inhomogeneous. All statistical calculations were performed using R version 2.15.2.

Results

Population-specific responses in growth, POC and PIC production rates.

Growth, POC and PIC production rates of three *E. huxleyi* populations displayed optimum-curve response patterns along the pCO_2 gradient ranging from about 120 to 2640 µatm. Three parameters of each population increased with increasing pCO_2, reached a maximum, and then declined with further pCO_2 increase (Figure 1).

Optimum pCO_2 of growth rates were between 244 and 436 µatm for the Azores population, between 436 and 542 µatm for the Bergen population, and between 384 and 400 µatm for the Gran Canaria population (Table 2). The growth optimum pCO_2 level of the Bergen population was significantly higher than that of the Azores or Gran Canaria populations (Tukey Post hoc, $p < 0.01$) (Figure 2A). Maximum growth rates of the Azores population with about 1.23 d^{-1} and of the Bergen population with about 1.28 d^{-1} were significantly higher than that of the Gran Canaria population with about 1.00 d^{-1} (Tukey Post hoc, $p < 0.001$) (Figure 2B). Relative sensitivity

constant of growth rate was significantly lower in the Bergen population with about 0.11 x 10^{-3}, in comparison to the Azores population with about 0.20 x 10^{-3} and the Gran Canaria population with about 1.60 x 10^{-3} (Figure 2C).

Optimum pCO_2 for POC production rate were between 512 and 756 µatm for the Azores population, between 633 and 984 µatm for the Bergen population, and between 413 and 644 µatm for the Gran Canaria population (Table 2). Optimum pCO_2 for POC production rate of the Bergen population was significantly higher than the Gran Canaria population (Tukey Post hoc, $p < 0.01$) (Figure 2D). pCO_2 optimum for POC production rate of the Azores population did not show marked difference with the Bergen or Gran Canaria populations (Tukey Post hoc, $p > 0.05$). Maximum POC production rates of the Azores population with about 14.28 pg C $cell^{-1}$ d^{-1} and of the Bergen population with about 16.28 pg C $cell^{-1}$ d^{-1} were significantly higher than that of the Gran Canaria population with about 7.61 pg C $cell^{-1}$ d^{-1} (Tukey Post hoc, $p < 0.001$) (Figure 2E). Relative sensitivity constant for POC production rate of the Bergen population with about 0.28 x 10^{-3} was lower than that of the Azores population with about 0.50 x 10^{-3} and the Gran Canaria population with about 0.47 x 10^{-3} (Tukey Post hoc, $p < 0.01$) (Figure 2F).

Optimum pCO_2 for PIC production rate were between 323 and 635 µatm for the Azores population, between 488 and 625 µatm for the Bergen population, and between 195 and 545 µatm for the Gran Canaria population (Table 2). Optimum pCO_2 for PIC production rate of the Bergen population was significantly higher than the Gran Canaria population (Tukey Post hoc, $p < 0.05$) (Figure 2G). There were no marked differences in pCO_2 optimum for PIC production rate between the Azores and Bergen populations, or between the Azores and Gran Canaria populations (Tukey Post hoc, both $p > 0.1$). Maximum PIC production rate of the Azores population with about 14.13

pg C $cell^{-1}$ d^{-1} was higher than the Gran Canaria population with about 9.93 pg C $cell^{-1}$ d^{-1} (Tukey Post hoc, $p < 0.05$) (Figure 2H). Maximum PIC production rate of the Bergen population with about 11.69 pg C $cell^{-1}$ d^{-1} did not show significant difference with that of the Azores or Gran Canaria populations (Tukey Post hoc, $p > 0.1$). There were no statistically significant differences in relative sensitivity constants for PIC production rates among the Azores, Bergen and Gran Canaria populations (ANOVA, $F = 2.30$, $p = 0.13$) (Figure 2I).

Genotype-specific responses in growth, POC and PIC production rates.

Growth, POC and PIC production rates of 17 *E. huxleyi* genotypes displayed optimum response patterns to a broad pCO_2 gradient ranging from 116 to 3073 µatm (Figure 3). At each pCO_2 level, six or five genotypes within each population showed similar growth, POC and PIC production rates. There was no genotype that displayed high growth, POC and PIC production rates across all pCO_2 levels.

Within the Azores or Bergen populations, the maximum growth rates were positively correlated with the sensitivity constants of growth rates ($p< 0.05$) (Figure 4A,B). Maximum POC production rates were not significantly positively correlated with the sensitivity constants of POC production rates within the Azores or Bergen populations (Figure 4D,E). The maximum PIC production rates were significantly positively correlated with the sensitivity constants of PIC production rates within these two populations ($p< 0.05$) (Figure 4G,H). Within the Gran Canaria population, positive correlations between maximum values and sensitivity constants for growth, POC and PIC production rates failed significance (Figure 4C,F,I). This may be due to a lack of sufficient statistical power to detect differences with the small sample size used in this study.

Based on 17 *E. huxleyi* genotypes, we found significant positive correlations between the maximum values and the sensitivity constants for POC and PIC production rates (p = 0.05 for POC correlation; p< 0.01 for PIC correlation) (Figure S1). Positive correlation between the maximum growth rates and the relative sensitivity constants of growth rates of 17 genotypes was not significant.

Inter-population variations in growth rate were larger than within-population variations across all pCO_2 levels (Figure 5). Normalized standard deviations of growth rates inter- and within-population increased with increasing pCO_2. Normalized standard deviations of POC production rates inter- and within-population were larger at above 1500 µatm pCO_2 than at lower pCO_2 levels. Whereas, normalized standard deviations of POC and PIC production rates inter- and within-population did not show clear response patterns to rising pCO_2.

Discussion

Optimum responses of *E. huxleyi* to a broad pCO_2 range

Recently, a number of studies investigated the effect of rising pCO_2 on physiological processes of *E. huxleyi* and much of the work on CO_2 or pH sensitivity focuses on a few genotypes or a narrow pCO_2 gradient normally ranging from about 200 to 1200 µatm (Table 1). Measuring at a narrow pCO_2 range, previous studies showed different pCO_2 response patterns in terms of growth, POC and PIC production rates of *E. huxleyi* (*see* reviews of Meyer and Riebesell, 2015; Table 1). Extending the pCO_2 range towards lower (120 µatm) and higher (3073 µatm) values in this study, we identified optimum response curves for growth, photosynthetic carbon fixation and calcification rates of 17 *E. huxelyi* genotypes from three geographically distinct populations. The

reasons for the optimum pCO_2 response pattern may be that limiting carbon concentrations at low pCO_2 levels can directly limit the growth, carbon fixation, and calcification rates of *E. huxelyi*. With rising pCO_2 levels, increasing DIC is thought to stimulate growth, carbon fixation and calcification rates by supplying increasing amounts of substrate. However, low pH at high pCO_2 levels is suggested to reduce physiological rates (Bach et al., 2011; 2015). This might be linked to the fact that activities of enzymes involved in carbon fixation are inhibited by low pH (Portis et al., 1986). Thus, over a broad pCO_2 range, there should be thresholds for pCO_2 levels (optimum pCO_2). Below optimum pCO_2 growth, photosynthetic carbon fixation and calcification rates of *E. huxleyi* could be enhanced by the increasing CO_2 and HCO_3^- concentrations, while above optimum pCO_2 these rates are likely to be reduced by the low pH (Krug et al., 2011). The carbon availability was identified as the factor responsible for the observed rates on the left side of the optimum, the low pH was the most likely driving factor on the right side of the optimum.

Based on the results found in this study, we concluded that different pCO_2 response patterns in growth, POC and PIC production rates of *E. huxleyi* can be caused by both different genotypes and a narrow pCO_2 range (Table 1). The reasons are following. Large differences in pCO_2 optima for growth, POC or PIC production rates were investigated among individual genotypes in this study. When selected narrow pCO_2 range were lower (or higher) than the pCO_2 optima for physiological rates of one genotype, these rates of this genotype can show increasing (or decreasing) trend to selected narrow pCO_2 range. When the selected narrow pCO_2 range includes the pCO_2 optima for physiological rates of another genotype, these rates of this genotype can show optimum responses to the selected narrow pCO_2 range. Thus, depending on the pCO_2 optima and the selected narrow pCO_2 range, different genotypes in *E. huxleyi* species can display increasing,

decreasing or optimum responses to a narrow pCO_2 range in terms of their physiological rates. However, a broad pCO_2 range can include all pCO_2 optima for physiological rates, and these rates of all genotypes will display optimum response patterns to the broad pCO_2 range.

Population-specific responses of *E. huxleyi* to a broad pCO_2 range

Based on 17 genotypes isolated from three different geographic locations, we were able to identify physiologically distinct populations of *E. huxelyi*. Each population was characterized by significant difference in growth, POC and PIC production rates response to a broad pCO_2 gradient. These results indicate dispersal limitation in the cosmopolitan coccolithophore *E. huxelyi*. Recently, several studies reported genetically distinct *E. huxleyi* populations from different ocean regions (Cook et al., 2013; Read et al., 2013; Zhang et al., 2014). These findings are in line with population specific physiological properties reported in the present study.

In comparison to the Azores and Gran Canaria populations, significant lower relative sensitivity constants for growth and POC production rates of the Bergen population indicate that the Bergen population was tolerant to changing carbonate chemistry in terms of its growth and POC production rates. Genotypes within the Bergen population were isolated from the coastal seawater, while those in the Azores and Gran Canaria populations were isolated from the open oceans. The carbonate chemistry system in coastal zone is more dynamic and complex than in the open ocean (Cai, 2011). In fact, seasonal surface seawater pCO_2 variability in Bergen is larger than in the Azores and Gran Canaria (Table S2). Thus, pCO_2 tolerance of the Bergen population with respect to its growth and POC production rates may be related to the high surface seawater pCO_2 variability in its sampling location.

E. huxleyi populations were found to adapt to local temperature regimes (Zhang et al., 2014). 16 ^{o}C, the culture temperature in this study, is lower than the surface seawater temperature (SST) in Gran Canaria (Table S1). Thus, in comparison to the Azores or Bergen populations, lower maximum rates for growth, POC and PIC productions of the Gran Canaria population are likely to be caused by low culture temperature (Figure 2B,E,H).

Optimum pCO_2 and relative sensitivity constants for growth, POC and PIC production rates between the Azores and Gran Canaria populations did not show significant differences (Figure 2). These results indicate that physiological responses of the Azores population to pCO_2 were close to the Gran Canaria population. This can be explained by the geographic distance: the geographic origins of the Azores and Gran Canaria populations may be correlated with the seawater, partly because the Azores Current feeds the Canary Current (Tomczak and Godfrey, 1994). Several studies also found that population genetic differentiation among near locations was smaller than among long-distance locations in coccolithophores *E. huxleyi* and *Gephyrocapsa oceanica* or in diatom *Pseudo-nitzschia pungens* (Brand, 1982; Casteleyn et al., 2010). These findings are agreement with our physiological dataset.

Genotype-specific responses of *E. huxleyi* to a broad pCO_2 range

Genotype-specific reaction norm examples are a typical way to analyze the occurrence of genotype by environment (G x E) interactions and the phenotypic plasticity within a population (Gsell et al., 2012). Across the pCO_2 treatments, reaction norm slopes for growth, POC and PIC production rates of different genotypes were different (Figure 3), which indicated the G x E interactions within each population. G x E interactions show that physiological processes of *E.*

huxleyi genotypes were CO_2-depent and no genotype grows or fixes carbon well across all pCO_2 levels (Rynearson and Armbrust, 2004; Gsell et al., 2012). At every pCO_2 level, all genotypes within each population displayed distinct growth, POC and PIC production rates, which showed phenotypic variability. The presence of phenotypic variability within a population may be relevant for the adaptive potential of a population to dramatically different environments (Lohbeck et al., 2012).

Genotype-specific responses also revealed trade-offs in the co-occurring genotypes. For 17 *E. huxleyi* genotypes, significant positive correlations between the maximum rates and the sensitivity constants for POC and PIC production rates indicate that the higher the genotype-specific carbon fixation and calcification rates, the more sensitive they are to $[H^+]$ after the pCO_2 optima in *E. huxleyi* species. These results showed that fitness relevant traits of *E. huxleyi* species changed with rising pCO_2. Within each population, the maximum values of four analyzed parameters were positively correlated with their sensitivity constants, which indicates that genotypes that have lower fitness relevant traits in one treatment may perform well in the other treatment. This suggests that with rising pCO_2 levels, the pCO_2 sensitive genotypes are probably replaced by the pCO_2 tolerant genotypes, while at least a proportion of genotypes within a population may be suited to changing environmental conditions (Rynearson and Armbrust, 2004).

Ecological and biogeochemical implications

Although this control laboratory experiment cannot extrapolate to the natural conditions, large differences in pCO_2 optima suggest that when predicting responses of phytoplankton functional groups to ocean acidification, a large number of the organisms should be used. As has been

investigated in other phytoplankton species (Hutchins et al., 2013; Schaum et al., 2013), our data show different biogeochemical niches for the globally distributed *E. huxleyi*. Due to their different pCO_2 sensitivities, both the distributions and the dominances of the *E. huxleyi* populations can be affected by rising pCO_2 in the future oceans. G x E interactions and phenotypic plasticity found in this and previous studies may help to maintain the genotypic diversity of natural phytoplankton populations (Gsell et al., 2012; Lohbeck et al., 2012). In addition, G x E interactions also indicate that it is not possible to predict the advantageous genotypes from one environment to the next (Gsell et al., 2012). Trade-offs in key genotypes cause differentiation of adaptive strategies and may consequently allow coexistence of multiple genotypes. In order to reduce the negative effect of high $[H^+]$ on fitness relevant traits, these genotypes showing less sensitive to $[H^+]$ may have the potential to increase their percentages in *E. huxleyi* species. Our results suggest that the community or population compositions may shift at changing ocean environments such as ocean acidification, which may have important influence on the marine biogeochemical cycling.

Acknowledgements

The authors are grateful to Jana Meyer for particulate organic and inorganic carbon measurements. This work was supported by the German Federal Ministry of Education and Research (Bundesministerium für Bildung und Forschung) in the framework of the collaborative project Biological Impacts of Ocean Acidification (BIOACID). Kai G. Schulz is the recipient of an Australian Research Council Future Fellowship (FT120100384). We also thank the China Scholarship Council (CSC) for its support of Yong Zhang.

References

Bach L.T., Riebesell U., Schulz K.G. (2011) Distinguishing between the effects of ocean acidification and ocean carbonation in the coccolithophore *Emiliania huxleyi*. *Limnology and Oceanography* 56: 2040–2050.

Bach L.T., Riebesell U., Gutowska M.A., Federwisch L., Schulz K.G. (2015) A unifying concept of coccolithophore sensitivity to changing carbonate chemistry embedded in an ecological framework. *Progress in Oceanography* 135: 125–138.

Brand L.E. (1982) Genetic variability and spatial patterns of genetic differentiation in the reproductive rates of the marine coccolithophores *Emiliania huxleyi* and *Gephyrocapsa oceanica*. *Limnology and Oceanography* 27: 236–245.

Cai W.J. (2011) Estuarine and coastal ocean carbon paradox: CO_2 sinks or sites of terrestrial carbon incineration? *Annural Review of Marine Science* 3: 123–145.

Casteleyn G., Leliaert F., Backeljau T., Debeer A., Kotaki Y., Rhodes L., Lundholm N., Sabbe K., Vyverman W. (2010) Limits to gene flow in a cosmopolitan marine planktonic diatom. *Proceedings of the National Academy of Sciences of the United States of America* 107: 12952–12957.

Cook S.S., Jones R.C., Vaillancourt R.E., Hallegraeff G.M. (2013) Genetic differentiation among Australian and Southern Ocean populations of the ubiquitous coccolithophore *Emiliania huxleyi* (Haptophyta). *Phycologia* 52: 368–374.

Cottingham K.L., Lennon J.T., Brown B.L. (2005) Knowing when to draw the line: designing more informative ecological experiments. *Frontiers in Ecology and the Environment* 3: 145–152

Danbara A., Shiraiwa Y. (1999) The requirement for selenium for the growth of marine coccolithophorids, *Emiliana huxleyi*, *Gephyrocapsa oceanica* and *Helladosphaera*sp. (Prymnewsiophyceae). *Plant and Cell Physiology* 40: 762–766.

De Jong G. (1990) Quantitative genetics of reaction norms. *Journal of Evolutionary Biology* 3: 447–468.

Dickson A.G., Afghan J.D., Anderson G.C. (2003) Reference materials for oceanic CO_2 analysis: a method for the certification of total alkalinity. *Marine Chemistry* 80: 185–197.

Dickson A.G., Sabine C.L., Christian J.R. (2007) Guide to best practices for ocean CO_2 measurements. *PICES Special Publication* 3: 1–191.

Fiorini S., Middelburg J.J., Gattuso J.P. (2011) Testing the effects of elevated pCO_2 on coccolithophores (prymnesiophyceae): comparison between haploid and diploid life stages. *Journal of Pycology* 47: 1281–1291.

González-Dávila M., Santana-Casiano M. (2003) Seasonal and interannual variability of sea-surface carbon dioxide species at the European Station for Time Series in the Ocean at the Canary Islands (ESTOC) between 1996 and 2000. *Global Biogeochemical Cycles* 17: 1076. doi: 10.1029/2002GB001993.

Gsell A.S., de Senerpont-Domis L.N., Przytulska-Bartosiewicz A., Mooij W.M., van Donk E., Ibelings B.W. (2012) Genotype-by-temperature interactions may help to maintain clonal diversity in *Asterionella formosa* (Bacillariophyceae). *Journal of Phycology* 48: 1197–1208.

Guillard R.R., Ryther J.H. (1962) Studies of marine planktonic diatoms: I. Cyclotella nana Hustedt, and Detonulaconfervacea (cleve) Gran. *Canadian Journal of Microbiology* 8: 229–239.

Hoppe C.J.M., Langer G., Rost B. (2011) *Emiliania huxleyi* shows identical responses to elevated pCO_2 in TA and DIC manipulations. *Journal of Experimental Marine Biology and Ecology* 406: 54–62.

Hutchins D.A., Fu F.X., Webb E.A., Walworth N., Tagliabue A. (2013) Taxon-specific response of marine nitrogen fixers to elevated carbon dioxide concentrations. *Nature Geoscience* 6: 790–795.

Iglesias-Rodriguez M.D., Halloran P.R., Rickaby R.E.M., Hall I.R., Colmenero-Hidalgo E., Gittins J.R., Green D.R.H., Tyrrell T., Gibbs S.J., von Dassow P., Rehm E., Armbrust E.V., Boessenkool K.P. (2008) Phytoplankton calcification in a high-CO_2 world. *Science* 320: 336–340.

Intergovernmental Panel on Climate Change (2013) Climate Change 2013: The Physical Science Basis. Contribution of Working Group I to the Fifth assessment report of the Intergovernmental Panel on Climate Change. pp. 5–12. Cambridge University Press, Cambridge, United Kingdom.

Jones B.M., Iglesias-Rodriguez M.D., Skipp P.J., Edwards R.J., Greaves M.J., Young J.R., Elderfield H., O'Connor C.D. (2013) Responses of the *Emiliania huxleyi* proteome to ocean acidification. *PLoS One* 8(4): e61868. doi: 10.1371/journal.pone.0061868

Kester D., Duedall I.W., Connors D.N., Pytkowicz R.M. (1967) Preparation of artificial seawater. *Limnology and Oceanography* 1: 176–179.

Krug S.A., Schulz K.G., Riebesell U. (2011) Effects of changes in carbonate chemistry speciation on *Coccolithus braarudii*: a discussion of coccolithophorid sensitivities. *Biogeosciences* 8: 771–777.

Langer G., Nehrke G., Probert I., Ly J., Ziveri P. (2009) Strain-specific responses of *Emiliania huxleyi* to changing seawater carbonate chemistry. *Biogeosciences*, 6: 2637–2646.

Lewis E., Wallace D.W.R. (1998) Program developed for CO_2 system calculations. Carbon Dioxide Information Analysis Centre, Oak Ridge National Laboratory, U.S. Department of Energy.http://cdiac.ornl.gov/oceans/co2rprt.html.

Litchman E., Klausmeier C.A. 2008. Trait-based community ecology of phytoplankton. *Annual Review of Ecology, Evolution, and Systematics* 39: 615– 639

Locarnini R.A., Mishonov A.V., Antonov J.I., Boyer T.P. and Garcia H.E. (2006). In: Levitus S. [Eds.], World ocean atlas 2005. Volume 1: Temperature. pp. 123–134. U.S. Government Printing Office.

Lohbeck K.T., Riebesell U., Reusch T.B.H. 2012. Adaptive evolution of a key phytoplankton species to ocean acidification. *Nature Geoscience* 5: 346–351.

Meyer J., Riebesell U. (2015) Reviews and syntheses: responses of coccolithophores to ocean acidification: a meta-analysis. *Biogeosciences* 12: 1671–1682.

Omar A.M., Olsen A., Johannessen T., Hoppema M., Thomas H., Borges A.V. (2010) Spatiotemporal variations of fCO_2 in the North Sea. *Ocean Science* 6: 77–89.

Palumbi S.R. (1994) Genetic divergence, reproductive isolation, and marine speciation. *Annual Review of Ecology, Evolution, and Systematics* 25: 547–572.

Portis A.R., Salvucci M.E., Ogren W.L. (1986) Activation of Ribulosebisphosphate Carboxylase/Oxygenase at physiological CO_2 and Ribulosebisphosphate concentrations by Rubisco activase. *Plant Physiology* 82: 967–971.

Read B.A., Kegel J., Klute M.J., Kuo A., Lefebvre S.C., Maumus F., Mayer C., Miller J., Monier

A., Salamov A., Young J., Aguilar M., Claverie J.M., Frickenhaus S., Gonzalez K., Herman E.K., Lin Y.C., Napier J., Ogata H., Sarno A.F., Shmutz J., Schroeder D., de Vargas C., Verret F., von Dassow P., Valentin K., de Peer Y.V., Wheeler G., Emiliania Huxleyi Annotation Consortium, Dacks J.B, Delwiche C.F., Dyhrman S.T., Gloeckner G., John U., Richards T., Worden A.Z., Zhang X., Grigoriev I.V. 2013. Pan genome of the phytoplankton *Emiliania* underpins its global distribution. *Nature* 499: 209–213.

Riebesell U., Tortell P.D. (2011) Effects of ocean acidification on pelagic organisms and ecosystems. In: Gattuso J.P. and Hansson L. [Eds.], Ocean acidification.pp. 99–116. Oxford University Press, Oxford, United Kingdom.

Riebesell U., Zondervan I., Rost B., Tortell P.D., Zeebe R.E., Morel F.M.M. (2000) Reduced calcification of marine plankton in response to increased atmospheric CO_2. *Nature* 407: 364–367.

Ríos A.F., Pérez F.F., Álvarez M., Mintrop L., González-Dávila M., Santana-Casiano M., Lefévre N., Watson A.J. (2005) Seasonal sea-surface carbon dioxide in the Azores area. *Marine Chemistry* 96: 35–51.

Rost B., Riebesell U. (2004) Coccolithophores and the biological pump: responses to environmental changes. In: Thierstein H.R. and Young J.R. [Eds.], Coccolithophores: from molecular biology to global impact. pp. 99–125. Springer, Berlin, Germany.

Roy R.N., Roy L.N., Vogel K.M., Porter-Moore C., Pearson T., Good C.E, Millero F.J., Campbell D.C. (1993) Thermodynamics of the dissociation of boric acid in seawater at S 5 35 from 0 degrees C to 55 degrees C. *Marine Chemistry* 44: 243–248.

Rynearson T.A., Armbrust E.V. (2004) Genetic differentiation among populations of the planktonic marine diatom *Ditylum brightwellii* (Bacillariophyceae). *Journal of Phycology* 40: 34–43.

Samuelsen T.J. (1970) The biology of six species of Anomura (Crustacea, Decapoda) from Raunefjorden, western Norway. *Sarsia* 45: 25–52.

Santana-Casiano M., González-Dávila M., Rueda M., Llinás O., González-Dávila E. (2007) The interannual variability of oceanic CO_2 parameters in the northeast Atlantic subtropical gyre at the ESTOC site. *Global Biogeochemical Cycles* 21: GB1015. doi: 10.1029/2006GB002788.

Schaum, E., Rost B., Millar A.J., Collins S. (2013) Variation in plastic responses of a globally distributed picoplankton species to ocean acidification. *Nature Climate Change* 3: 298–302.

Schlüter L., Lohbeck K.T., Gutowska M.A., Gröger J.P., Riebesell U., Reusch T.B.H. (2014) Adaptation of a globally important coccolithophore to ocean warming and acidification. *Nature Climate Change* 4: 1024–1030.

Sett S., Bach L.T., Schulz K.G., Koch-Klavsen S., Lebrato M., Riebesell U. (2014) Temperature modulates coccolithophorid sensitivity of growth, photosynthesis and calcification to increasing seawater pCO_2. *PLoS ONE 9*: e88308. doi:10.1371/journal.pone.0088308

Shi D., Xu Y., Morel F.M.M. (2009) Effects of the pH/pCO_2 control method on medium chemistry and phytoplankton growth. *Biogeosciences* 6: 1199–1207.

Tomczak M., Godfrey J.S. (1994) Regional oceanography: an introduction. pp. 229–252. Butler & Tanner Ltd. Frome and London, Great Britain.

Wisshak M., Form A., Jakobsen J., Freiwald A. (2010) Temperate carbonate cycling and water mass properties from intertidal to bathyal depths (Azores). *Biogeosciences* 7: 2379–2396.

Zhang Y., Klapper R., Lohbeck K.T., Bach L.T., Schulz K.G., Reusch T.B.H., Riebesell U. (2014)

Between- and within-population variations in thermal reaction norms of the coccolithophore *Emiliania huxleyi*. *Limnology and Oceanography* 59: 1570–1580.

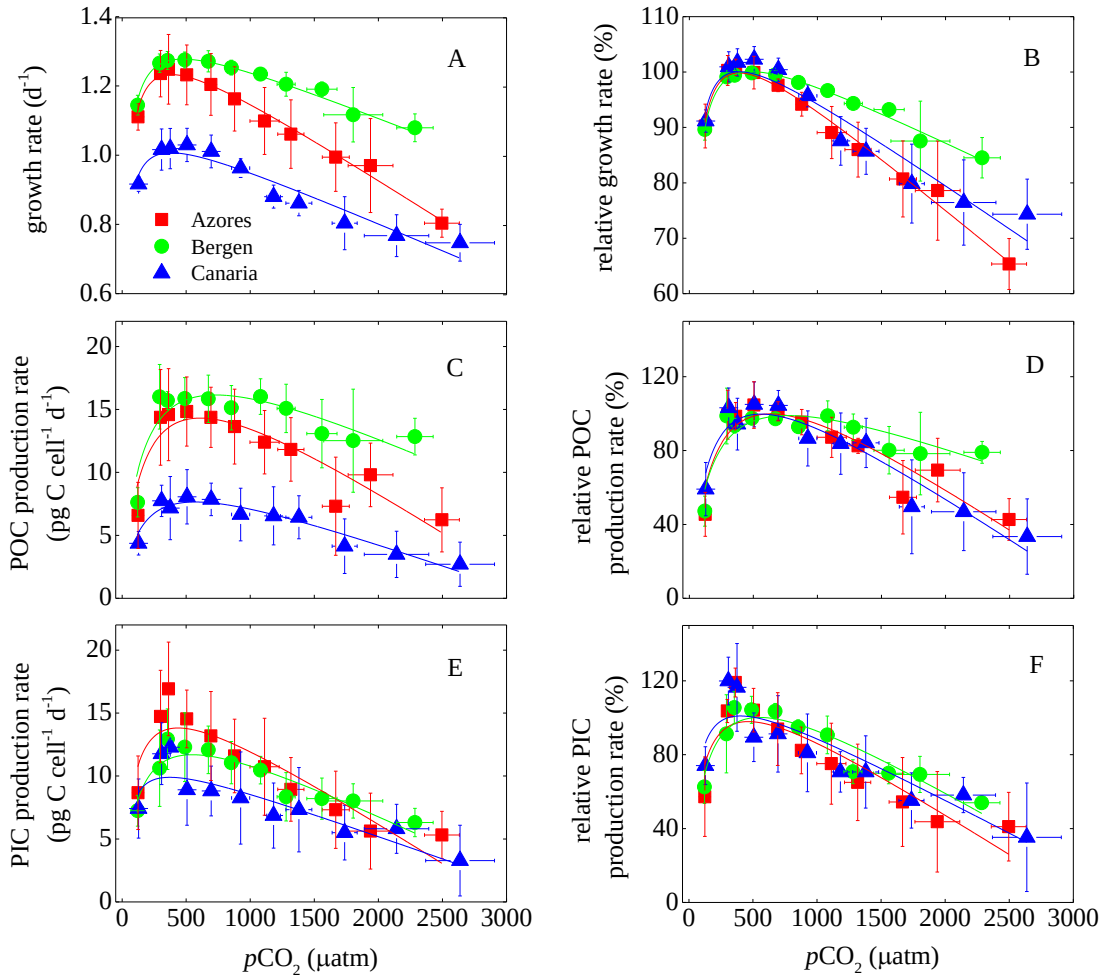

Figure 1. Physiological response patterns of three *Emiliania huxleyi* populations at a broad pCO_2 gradient ranging from about 120 to 2640 µatm. (A) Growth rate. (B) Relative growth rate. (C) POC production rate. (D) Relative POC production rate. (E) PIC production rate. (F) Relative PIC production rate. Relative growth, POC and PIC production rates are the percentages of their maximum rates. Growth, POC and PIC production rates of each population were the average rates of six genotypes in the Azores and Bergen populations, and of five genotypes in the Gran Canaria population, respectively. Optimum response curves are obtained by fitting equation [3].

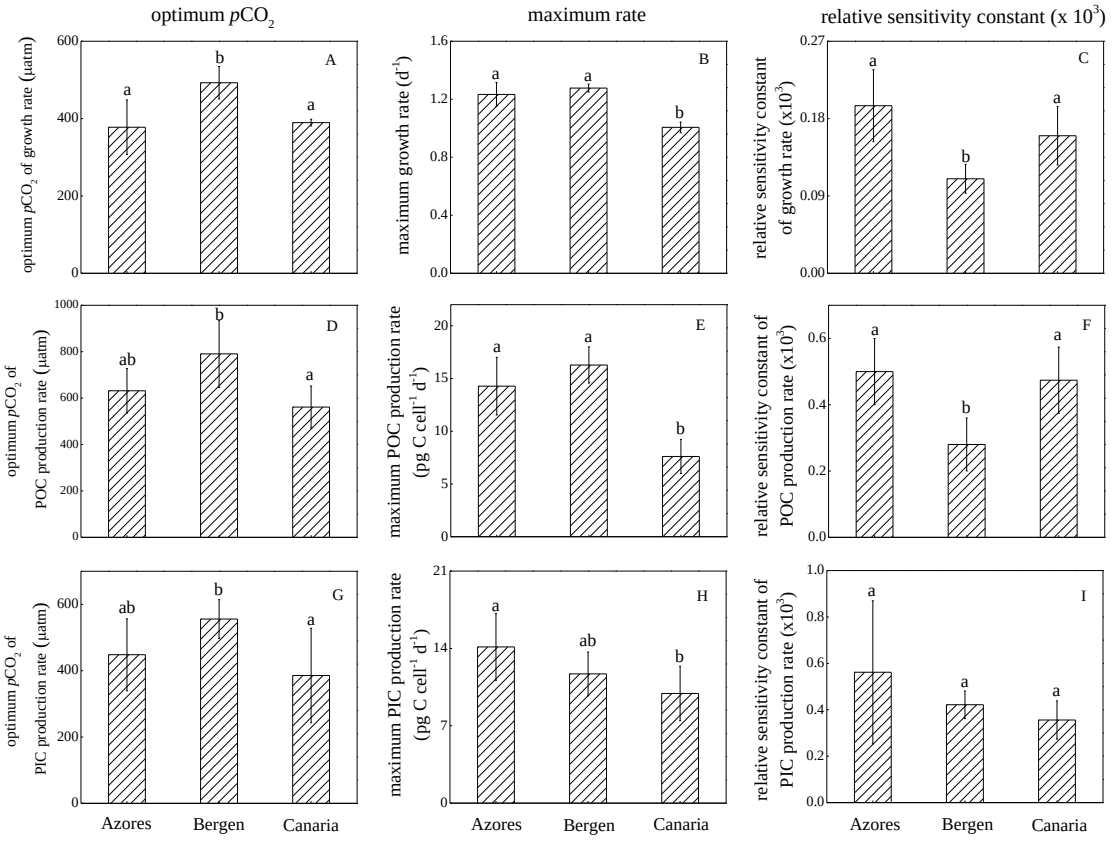

Figure 2. Optima pCO_2, maximum values and relative sensitivity constant for growth, POC and PIC production rates of three *E. huxleyi* populations. Different letters in each panel represent statistically different means (Tukey Post hoc, $p < 0.05$).

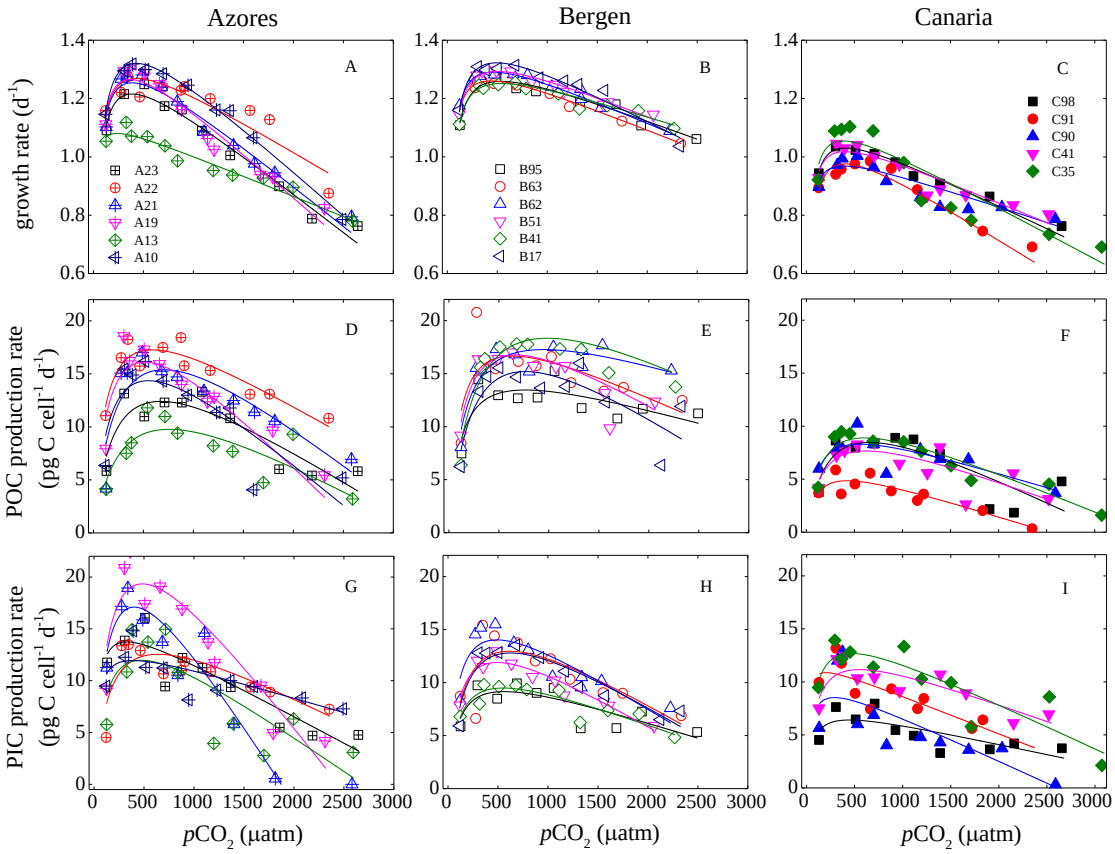

Figure 3. Physiological response pattern of each *E. huxleyi* genotype within the Azores, Bergen and Gran Canaria populations at a broad pCO_2 gradient ranging from about 116 to 3073 µatm. Panels (A), (B), (C) depict growth rate of each genotype within the Azores, Bergen and Gran Canaria populations. Panels (D), (E), (F) depict POC production rate of each genotype within the Azores, Bergen and Gran Canaria populations. Panels (G), (H), (I) depict PIC production rate of each genotype within the Azores, Bergen and Gran Canaria populations. Optimum response curves are obtained by fitting equation [3].

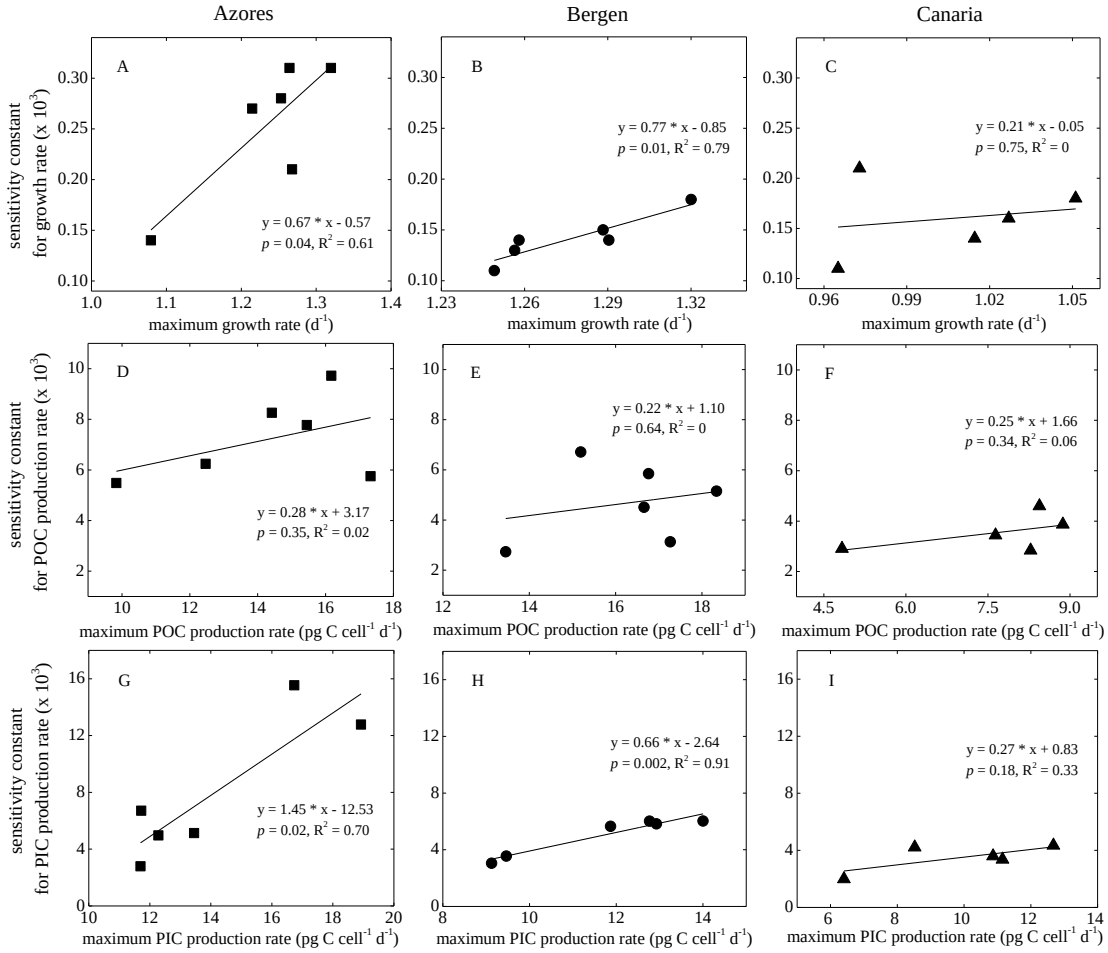

Figure 4. Correlations between maximum values and sensitivity constants for growth, POC and PIC production rates within the Azores, Bergen and Gran Canaria populations. Solid lines were fitted linearly based on maximum values and sensitivity constants of six genotypes within the Azores and Bergen populations, and of five genotypes within the Gran Canaria population.

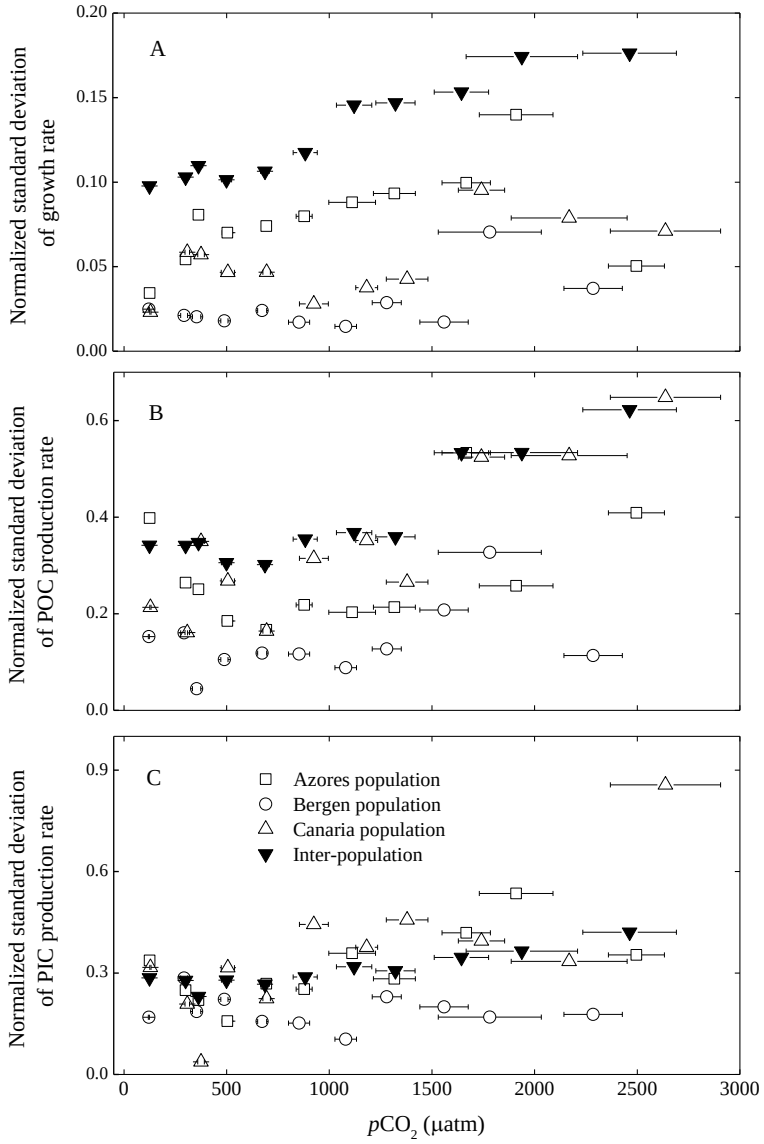

Figure 5. Comparison of intra-population variations and inter-population variations in growth, POC and PIC production rates. Intra-population variations in growth, POC and PIC production rates are calculated based on six genotypes within the Azores and Bergen populations and on five genotypes within the Gran Canaria population. Inter-population variations are calculated based on seventeen genotypes in all three populations. Normalized standard deviation of each parameter is calculated as the ratio of the standard deviation to absolute values.

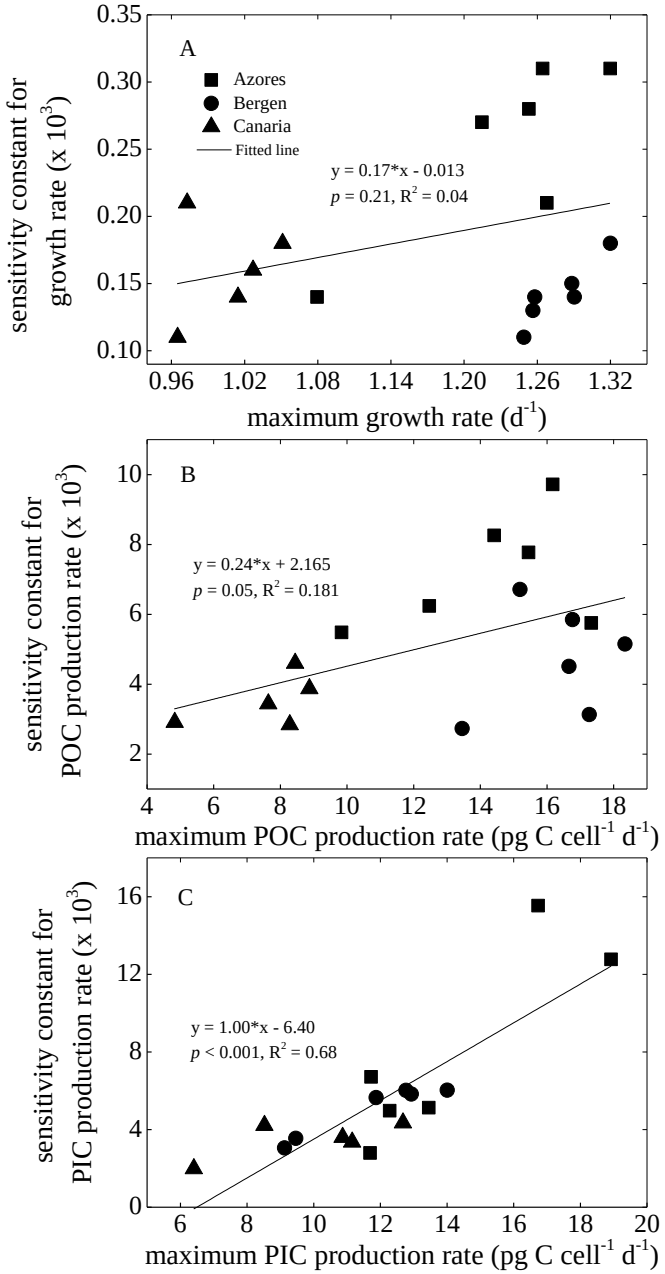

Figure S1. Correlations between maximum values and sensitivity constants for growth, POC and PIC production rates of 17 *E. huxleyi* genotypes. Solid lines were fitted linearly based on maximum values and sensitivity constants of 17 genotypes from the Azores, Bergen and Gran Canaria.

Table 1. Summary of the physiological responses of different *Emiliania huxleyi* genotypes to different pCO_2 ranges at constant alkalinity condition. Constant total alkalinity (TA) indicates that either carbonate chemistry was adjusted by adding calculated Na_2CO_3 and HCl at the same TA between treatments, or seawater was bubbled with CO_2 gas mixtures. Symbols indicate: ↑ increased response, — no response, ↓ decreased response, ∩ optimum response.

E. huxleyi genotype	Isolated site	pCO_2 range (µatm)	Growth rate	POC production rate	PIC production rate	Reference
AC472	South Pacific, Western New Zealand	400 to 760	↑	—	↑	Fiorini et al. (2011)
PLY M219 (NZEH)	New Zealand	380 to 750	↓	↓	↓	Shi et al. (2009)
PLY M219 (NZEH)	New Zealand	404 to 1066	↓	↑	↓	Hoppe et al. (2011)
PML B92/11A	Bergen, Norway	152 to 885	—	↑	↓	Riebesell et al. (2000)
PML B92/11A	Bergen, Norway	20 to 6000	∩	∩	∩	Bach et al. (2011)
PML B92/11A	Bergen, Norway	20 to 6000	∩	∩	∩	Sett et al. (2014)
RCC1212	South Atlantic, off South Africa	194 to 1096	↓	∩	↓	Langer et al. (2009)
RCC1216	Tasman Sea, off New Zealand	218 to 1201	↓	↑	↓	Langer et al. (2009)
RCC1238	North Atlantic, off Japan	206 to 929	↑	∩	—	Langer et al. (2009)
RCC1256	North Atlantic, off Iceland	193 to 915	↓	∩	∩	Langer et al. (2009)
RCC1256	Iceland	191 to 846	↓	↓	↓	Hoppe et al. (2011)
NZEH	New Zealand	280 to 750	↓	↑	↑	Iglesias-Rodriguez et al. (2008)
NZEH	New Zealand	395 to 1340	↓	↑	↑	Jones et al. (2013)

Table 2. pCO_2 optima (K_m), maximum values (V_{max}), sensitivity constant (*SC*) and relative sensitivity constant (*RSC*) for growth, POC and PIC production rates of each *E. huxleyi* genotype. K_m is calculated by using equation [4], V_{max}, *SC* and *RSC* equation [3]. *See* text for details about calculations of all parameters.

	Growth rate				POC production rate				PIC production rate			
Geno-type	K_m (µatm)	V_{max} (d^{-1})	*SC* ($x10^3$)	*RSC* ($x10^3$)	K_m (µatm)	V_{max} (pg C $cell^{-1}$ d^{-1})	*SC* ($x10^3$)	*RSC* ($x10^3$)	K_m (µatm)	V_{max} (pg C $cell^{-1}$ d^{-1})	*SC* ($x10^3$)	*RSC* ($x10^3$)
A 23	392	1.21	0.27	0.22	673	12.47	6.24	0.50	323	13.45	5.13	0.38
A 22	436	1.27	0.21	0.16	591	17.33	5.75	0.33	635	12.28	4.97	0.40
A 21	392	1.25	0.28	0.22	707	15.45	7.77	0.50	396	16.73	15.54	1.11
A 19	371	1.26	0.31	0.24	512	16.17	9.72	0.56	480	18.92	12.77	0.67
A 13	244	1.08	0.14	0.13	756	9.84	5.48	0.63	471	11.72	6.71	0.57
A 10	432	1.32	0.31	0.20	549	14.42	8.26	0.48	385	11.69	2.79	0.24
B 95	534	1.26	0.13	0.10	762	13.46	2.73	0.20	562	9.13	3.05	0.33
B 63	436	1.26	0.14	0.11	633	16.66	4.51	0.27	615	12.93	5.83	0.45
B 62	456	1.29	0.15	0.11	945	17.27	3.13	0.18	488	14.00	6.03	0.43
B 51	499	1.29	0.14	0.11	660	16.77	5.85	0.35	492	11.87	5.65	0.48
B 41	542	1.25	0.11	0.09	984	18.34	5.15	0.38	553	9.46	3.55	0.37
B 17	490	1.32	0.18	0.14	761	15.19	6.71	0.30	625	12.77	6.02	0.47
C 98	400	1.03	0.16	0.16	644	8.44	4.60	0.54	440	6.40	1.99	0.31
C 91	393	0.97	0.21	0.21	413	4.83	2.91	0.60	195	10.87	3.60	0.33
C 90	384	0.97	0.11	0.12	546	8.28	2.84	0.34	284	8.52	4.22	0.50
C 41	393	1.01	0.14	0.14	609	7.64	3.44	0.45	545	11.15	3.36	0.30
C 35	378	1.05	0.18	0.17	596	8.87	3.87	0.44	464	12.68	4.35	0.34

Table S1. Sea surface temperatures (SST) at the Azores, Bergen and Gran Canaria.

	Location	Mean mothly SST range (°C)	Minimum monthly SST (°C)	Maximum monthly SST (°C)	References
Azores	38°34′ N, 28°42′ W	15.6 – 22.3	12.6	32.9	Wisshak et al. 2010
Bergen	60°18′N, 05°15′E	6.0 – 16.0	– 2	16.6	Samuelsen1970 Locarnini et al. 2006
Canaria	27°58’N, 15°36’W	18.0 – 24.0	15.0	28.0	Santana-Casiano et al. 2007

Table S2. Seasonal surface seawater pCO_2 and pH at the Azores, Bergen and Gran Canaria.

	Location	Mean seasonal pCO_2 (µatm)	Mean seasonal pH (total scale)	Seasonal pCO_2 variability (µatm)	References
Azores	38°34'N, 28°42'W	320 – 400	8.005 – 8.05	80	Ríos et al. 2005 Wisshak et al. 2010
Bergen	60°18'N, 05°15'E	220 – 400	7.95 – 8.15	200 – 250	Omar et al. 2010
Canaria	27°58'N, 15°36'W	320 – 400	8.005 – 8.05	60 – 80	González-Dávila et al. 2003

Chapter 5. Synthesis and future perspectives

This thesis investigated the effects of temperature, carbonate chemistry and light intensity on calcifying marine phytoplankton (coccolithophores) in terms of their growth, photosynthetic carbon fixation and calcification rates. This section will bring together the data from chapters 2-4. Results in chapters 2 and 4 showed the population- and genotype-responses of the coccolithophore *Emiliania huxleyi* to a broad range of temperatures and pCO_2, respectively. Based on these results, I discuss the possible role of inter- and intra-population variation to cope with climate change. Interacting effects of pCO_2 and light on the coccolithophore *Gephyrocapsa oceanica* were determined in Chapter 3. Results obtained in this study are discussed with regard to its role in possible implications for biogeochemical cycling. Finally, perspectives for future research are given.

5.1 Population- and genotype-specific responses of *Emiliania huxleyi* to a broad range of temperatures

Surface seawater temperature will continue to increase in the future (Hansen et al. 2006). A large number of studies have investigated the effect of temperature on growth rates of marine phytoplankton (e. g. Suzuki and Takahashi, 1995; Buitenhuis et al., 2008; Kaeriyama et al., 2011; Boyd et al., 2013; Hyun et al., 2014). Most of these studies focus on different phytoplankton species. Few research pays attention to different genotypes from the same species (Kremp et al., 2012). In chapter 2, we choose 11 *Emiliania huxleyi* genotypes from two sites, and present population- and genotype-specific growth responses of *E. huxleyi* to a broad range of

temperatures.

Marine phytoplankton species are distributed throughout the world's oceans and can show specific responses to a variety of abiotic stresses (Collins et al., 2014). Due to their adaptation to the local environments, phytoplankton can show difference in physiology, growth, metabolism and other indeterminate characteristics (Des Marais et al., 2013). Local adaptation is defined as a process whereby the frequency of fitness-related traits was increased by specific environment, which increase the survival or reproductive success of individuals or populations (Taylor, 1991). Growth rate can be considered a proxy of fitness (Wood et al., 2005). High latitude phytoplankton species are exposed to relatively low temperatures in their natural environments and low latitude phytoplankton species experience relatively high temperatures (Thomas et al., 2012). In chapter 2, the *E. huxleyi* population from Bergen grew well at lower temperatures, and the population from the Azores performed better at higher temperatures. These findings are indicative for local temperature adaptations of these two *E. huxleyi* populations. Other studies also found local temperature adaption of marine phytoplankton (e. g. Brand, 1982; Suzuki and Takahashi, 1995; Thomas et al., 2012). In addition, coastal *E. huxleyi* genotypes were found to be more tolerant to low salinities (Paasche, 2002) and to high pCO_2 levels (in chapter 4) than open ocean genotypes. These findings show that local adaptation in *E. huxleyi* can be important to cope with changing environmental conditions.

If changes in ambient conditions reduce growth and genotypes within population do not mutate, phytoplankton can secure their populations by two different mechanisms. One way is by expression of a common phenotypic plasticity for all individuals of each population, and the other way is by expression of phenotypic variation within each population (Whitman and Agrawal,

2009). The former allows all individuals to acclimate to new environments, and the latter enables growth of a portion of individuals that show the relatively better adapted phenotypes for the respective environmental conditions (Alpermann et al., 2010). In chapters 2 and 4, phenotypic plasticity within each population was identified: growth rates of individual *E. huxleyi* genotypes were different at different temperatures or pCO_2 levels. Phenotypic plasticity indicates that single environmental factor such as temperature or pCO_2 may alter the phenotypes within an entire population, which may provide thousands of phenotypes for natural selection (Agrawal et al., 2001). In addition, new environmentally induced phenotypes are correlated with the specific environment, which allows new environments to immediately select (Badyaev, 2005). Thus, phenotypic plasticity may be an adaptive strategy as it allows genotypes to cope with a range of environments.

It has been suggested that genetic variability within a population reflects its potential to adapt to changing environments (Barrett and Schluter, 2008). Genetic variability within the Azores and Bergen populations of *E. huxleyi* were identified in chapter 2, which indicates that *E. huxleyi* is well prepared to confront frequent environmental changes. As expected from the genetic variation we found within population, different genotype-by-environment (G x E) interactions were identified: slopes of thermal or pCO_2 reaction norms of different *E. huxleyi* genotypes were different (chapters 2 and 4). G x E interactions show that the growth response of individual genotype is environment dependent, and it is not possible to predict the advantageous genotypesfrom one environment to another (Gsell et al., 2012). G x E interactions were also investigated in the diatom *Asterionella formosa*, where it was suggested that G x E interactions contribute to maintain genetic diversity of marine phytoplankton (Gsell et al., 2012). In summary,

G x E interactions indicate the presence and importance of high standing genetic variation, and such high standing genetic variation is likely to be important for populations to adapt to changing environments.

5.2 Interacting effects of light intensity and pCO_2 level on *Gephyrocapsa oceanica*.

CO_2 and light are two essential factors for metabolic processes of marine phytoplankton. Increases in surface seawater pCO_2 level and mean light intensity in the upper mixed layer in the future oceans may principally affect phytoplankton productivity, community structure and marine carbon cycling (Charalampopoulou et al., 2011). Coccolithophores are an important functional group of phytoplankton (Rost and Riebesell, 2004). They form a layer of calcium carbonate ($CaCO_3$) plates around the cells, which drives the carbonate counter pump and releases CO_2 to the environment by reducing the ocean's alkalinity. Moreover they contribute to the organic carbon pump via carbon-fixation by photosynthesis, which takes up CO_2 from the surface ocean (Rost and Riebesell, 2004).

In the natural environment, the vertical motion of water masses causes phytoplankton to experience a broad range of light intensities (Denman and Gargett, 1983). At low light intensity, photosynthetic carbon fixation and growth rates of *G. oceanica* did not change or were slightly facilitated by ocean acidification (chapter 3). Several studies also investigated the CO_2 fertilization at low light intensity (about 30 to 150 µmol photons m^{-2} s^{-1}): carbon fixation and growth rates of *E. huxleyi* and of several diatom species were enhanced by elevated pCO_2 (Burkhardt et al., 1999; Rost et al., 2002; Hoppe et al., 2011). Rising pCO_2 reduced the maximum rates for growth, photosynthetic carbon fixation and calcification of *G. oceanica* (chapter 3). Recently, other studies

also showed that rising pCO_2 and high light act synergistically to reduce growth rates and primary productions of diatoms (Gao et al., 2012; Li and Campbell, 2013). Thus, it is not possible to assess whether or not ocean acidification will increase or reduce the contribution of the coccolithophores to the organic carbon pump. Because this is depending on the magnitude of the combined effects of rising pCO_2 and increasing light on different marine phytoplankton groups. In fact, extrapolating these laboratory studies to the global ocean may be too simple. This is due to the fact that besides CO_2 and light, other factors in natural environments such as temperature and nutrients may also have different influences on the marine phytoplankton groups. In addition, single strains does not represent the complex structure of phytoplankton populations or communities in the oceans. And these controlled laboratory experiments may provide an inaccurate assessment for phytoplankton groups experiencing complex natural environmental conditions. Thus, large-scale field experiments such as MESOCOSM experiment need to be used, and these field experiments need to be performed at different sites or oceans at different time.

E. huxleyi and *G. oceanica* are tolerant to high light intensity (Chapter 3; Nanninga and Tyrrell, 1996). Photosynthesis-inhibiting light intensities for these two species are normally higher than for other marine phytoplankton (Chapter 3; Tyrrell and Merico, 2004; Trimborn et al., 2007). Blooms of *E. huxleyi* and *G. oceanica* tend to develop during the summer months under highly stratified conditions (Tyrrell and Merico, 2004). In chapter 3 and other studies, a lack of photo-inhibition in *E. huxleyi* and *G. oceanica* up to at least 800 µmol photons m^{-2} s^{-1} was found and may protect these two species from high-light damage in their natural environment (Nanninga and Tyrrell, 1996; Trimborn et al., 2007).

Physiological rates of coccolithophores are expected to show an optimum response patterns

to a broad pCO_2 range (Bach et al., 2011; Sett et al., 2014; Bach et al., 2015). Owing to their low efficiency CCMs, present day pCO_2 levels are normally lower than the pCO_2 saturation of carbon fixation rates of coccolithophores (Rost et al., 2003). With increasing light intensity, the pCO_2 optima of growth, photosynthetic carbon fixation and calcification rates were shifted towards lower levels (chapter 3). Increasing light intensity not only directly enhances the carbon fixation rates of coccolithophores but also may shift the pCO_2 optima of carbon fixation rate towards lower levels, which are close to present day pCO_2 levels. The latter further increases the carbon fixation rates of coccolithophores and may increase their competitive fitness. In comparison to photosynthetic carbon fixation, elevated pCO_2 levels normally have larger effects on calcification rates. Or the pCO_2 response of calcification rates is normally more sensitive than that of carbon fixation rates (chapters 3 and 4). Different coccolithophore species show different pCO_2 sensitivities in their calcification rates (Riebesell et al., 2008). In the natural environment, if pCO_2 optima of calcification rates of phytoplankton species are higher than the present day pCO_2 levels, increasing light intensity may have a positive effect on calcification rates. The reasons may be that increasing light intensity both increase the calcification rate and shift the pCO_2 optima towards present day pCO_2 levels. If pCO_2 optima of calcification rates are lower than the present day pCO_2 levels, it is not possible to assess the combined effects of increasing light intensity and pCO_2 on calcification rate. Because in this case, calcification rate is directly enhanced by increasing light intensity, but at the same time it may be reduced by lowering pH after the pCO_2 optimum. This case is also available to growth rate. Temperature was found to affect the pCO_2 optima of growth, photosynthetic carbon fixation and calcification rates of coccolithophores (Sett et al., 2014). Thus, when predicting future primary productivity and ecosystem functioning in the marine environment,

individual and interacting effects of key environmental factors such as CO_2, light, temperature and nutrients need to be considered.

5.3 Population- and genotype-specific responses of *Emiliania huxleyi* to a broad pCO_2 range.

Owing to their sensitivity to ocean acidification, coccolithophores are one of the best-studied groups of marine organisms with regard to their responses to ocean acidification (Meyer and Riebesell, 2015). *E. huxleyi* is the most abundant coccolithophore in contemporary oceans and can form blooms in temperate and subpolar regions (Tyrrell and Merico, 2004). A large number of studies have investigated the effect of ocean acidification on physiological processes of *E. huxleyi* (for a summary see Meyer and Riebesell, 2015). While inconsistent results still remain due to a narrow range of pCO_2 and different *E. huxleyi* genotypes. In chapter 4, we identified optimum response curves for growth, carbon fixation and calcification rates to a broad pCO_2 range in 17 *E. huxleyi* genotypes from three geographically distinct populations. Below pCO_2 optima, photosynthetic carbon fixation, calcification and growth rates were directly enhanced by increasing dissolved inorganic carbon concentrations, while above pCO_2 optima, these rates were reduced by lowering pH (Bach et al., 2011; Bach et al., 2015). Thus, the pCO_2 optima seem to be important for these rates in changing environments.

With lower sensitivity and higher optimum pCO_2 for growth and carbon fixation rates, the Bergen population (coastal population) was more tolerant to changing carbonate chemistry in terms of its growth and carbon fixation (chapter 4) in comparison to the Azores and Gran Canaria populations (open ocean populations). In chapter 2, we found that the temperature optimum for

growth rate of the Bergen population was about 22 ^{o}C, which is higher than the maximum local temperature in Bergen. Based on the results found in chapters 2 and 4, it is expected that with increasing temperature and pCO_2 level in the surface ocean, the Bergen population may benefit from the changing environments in the future oceans.

Within each population, some genotypes are more sensitive to rising pCO_2 with regard to their growth rate than others. These sensitive genotypes within a population are probably replaced by the more tolerant genotypes and then the population composition may change. Due to trade-offs, however, one genotype within a population will not be tolerant to all environmental conditions and cannot dominate anywhere. A trade-off occurs when a trait that is advantageous at one environment confers a disadvantage at others (Litchman and Klausmeier, 2008). Trade-offs within each population were found in chapter 4: genotypes with high maximum growth rates are sensitive to high pCO_2 levels. In natural environments, trade-offs cause differentiation of ecological strategies and may consequently allow coexistence of multiple genotypes (species) (Litchman et al., 2007). The results found in chapters 2 and 4 show that local adaption, phenotypic plasticity, G x E interactions and trade-offs may be important mechanisms, which allow phytoplankton to cope with changing environmental conditions.

5.4 Perspectives for future research

In chapter 2, we measured the growth rate responses of *E. huxleyi* genotypes from the Azores and Bergen to seven temperatures. We showed that these two *E. huxleyi* populations appear to be adapted to the local temperature range. In order to support and supplement above results, it would be beneficial to determine the thermal reaction norms of the *E. huxleyi* genotypes from Gran

Canaria. Furthermore, genetic variation within the Gran Canaria population should be identified in future work. In order to explain why the Bergen population showed a narrower temperature niche for its growth rate in comparison to the Azores population, I suggest that the Bergen population would grow well at lower extreme temperatures. However, I was not able to test this hypothesis in chapter 2. Thus, it would be interesting to repeat the experiment but include the Gran Canaria population and broaden the temperature range to lower levels.

In chapter 3, interactive modulating effects of light intensity and pCO_2 levels on *G. oceanica* were investigated. In the natural environment, light intensity changes frequently. It would therefore be interesting to investigate the combined effects of dynamic light and pCO_2 levels on *G. oceanica* or on other marine phytoplankton. Then, we could observe how dynamic light modulates pCO_2 response patterns for physiological rates. As discussed in chapter 3, we suggest that light intensity shifts the pCO_2 optima for physiological rates of coccolithophores. In order to confirm this suggestion, physiological rates of coccolithophores should be measured at a broad pCO_2 range at limiting low light, middle light and inhibiting high light intensities.

In chapter 4, results indicate that pCO_2 response patterns in physiological rates of the Azores population are similar to the Gran Canaria population. In order to support this result, it may be useful to test the genetic differences among the Azores, Bergen and Gran Canaria populations.

Population- and genotype-specific responses of *E. huxleyi* to a broad range of temperatures and pCO_2 were investigated in chapters 2 and 4. The following step would be to investigate the combined effects of temperature and pCO_2 on three *E. huxleyi* populations. Increases in pCO_2 and temperature, decrease in nutrient availability in the surface oceans and increase in light intensity in the upper mixed layer may affect the phytoplankton community composition. Thus, combined

effects of important/key environmental factors such as pCO_2, temperature, nutrients and light on different marine phytoplankton groups should be investigated in future work. In order to test whether or not simple laboratory (bottle) experimental results will be available to the global oceans, we should pay more attentions to MESOCOSM experiment. This is because each MESOCOSM experiment can show the responses of natural communities to climate changes in physiology, ecology and evolution.

References

Agrawal A.A. (2001) Phenotypic plasticity in the interactions and evolution of species. *Science* 294: 321–325.

Alpermann T.J., Tillmann U., Beszteri B., Cembella A.D., John U. (2010) Phenotypic variation and genotypic diversity in a planktonic population of the toxigenic marine dinoflagellate *Alexandrium tamarense* (Dinophyceae). *Journal of Phycology* 46: 18–32.

Bach L.T., Riebesell U., Gutowska M.A., Federwisch L., Schulz K.G. (2015) A unifying concept of coccolithophore sensitivity to changing carbonate chemistry embedded in an ecological framework. *Progress in Oceanography* 135: 125–138.

Bach L.T., Riebesell U., Schulz K.G. (2011) Distinguishing between the effects of ocean acidification and ocean carbonation in the coccolithophore *Emiliania huxleyi*. *Limnology and Oceanography* 56: 2040–2050.

Badyaev A.V. (2005) Stress-induced variation in evolution: from behavioural plasticity to genetic assimilation. *Proceedings of the Royal Society B* 272: 877–886.

Barrett R.D., Schluter D. (2008) Adaptation from standing genetic variation. *Trends in Ecology and Evolution* 23: 38–44.

Boyd P.W., Rynearson T.A., Armstrong E.A., Fu F.X., Hayashi K., Hu Z.X., Hutchins D.A., Kudela R.M., Litchman E., Mulholland M.R., Passow U., Strzepek R.F., Whittaker K.A., Yu E., Thomas M.K. (2013) Marine phytoplankton temperature versus growth responses from polar to tropical waters – outcome of a scientific community-wide study. *PLoS ONE* 8: e63091. doi: 10.1371/journal.pone.0063091

Brand L.E. (1982) Genetic variability and spatial patterns of genetic differentiation in the reproductive rates of the marine coccolithophores *Emiliania huxleyi* and *Gephyrocapsa oceanica*. *Limnology and Oceanography* 27: 236–245.

Buitenhuis E.T., Pangerc T., Franklin D.J., Quéré C.L., Malin G. (2008) Growth rates of six coccolithophorid strains as a function of temperature. *Limnology and Oceanography* 53: 1181–1185.

Burkhardt S., Riebesell U., Zondervan I. (1999) Effects of growth rate, CO_2 concentration, and cell size on the stable carbon isotope fractionation in marine phytoplankton. *Geochimica et Cosmochimica Acta* 63: 3729–3741.

Charalampopoulou A., Poulton A.J., Tyrrell T., Lucas M.I. (2011) Irradiance and pH affect coccolithophore community composition on a transect between the North Sea and the Arctic Ocean. *Marine Ecology Progress Series* 431: 25–43.

Collins S., Rost B., Rynearson T.A. (2014) Evolutionary potential of marine phytoplankton under ocean acidification. *Evolutionary Applications* 7: 140–155.

Denman K.L., Gargett A.E. (1983) Time and space scales of vertical mixing and advection of phytoplankton in the upper ocean. *Limnology and Oceanography* 28: 801–815.

Des Marais D.L., Hernandez K.M., Juenger T.E. (2013) Genotype-by-environment interaction and plasticity: exploring genomic responses of plants to the abiotic environment. *Annual Review of Ecology, Evolution and Systematics* 44: 5–29

Gao K., Xu J., Gao G., Li Y., Hutchins D.A., Huang B.Q., Wang L., Zheng Y., Jin P., Cai X., Häder D.P., Li W., Xu K., Liu N., Riebesell U. (2012) Rising CO_2 and increased light exposure synergistically reduce marine primary productivity. *Nature Climate Change* 2:

519–523.

Gsell A.S., De Senerpont-Domis L.N., Przytulska-Bartosiewicz A., Mooij W.M., Van Donk E., Ibelings B.W. (2012) Genotype-by-temperature interactions may help to maintain clonal diversity in *Asterionella Formosa* (Bacillariophyceae). *Journal of Phycology* 48: 1197–1208.

Hansen J., Sato M., Ruedy R., Lo K., Lea D.W., Medina-Elizade M. (2006) Global temperature change. *Proceedings of the National Academy of Sciences of the United States of America* 103: 1428–14293.

Hoppe C.J.M., Langer G., Rost B. (2011) *Emiliania huxleyi* shows identical responses to elevated pCO_2 in TA and DIC manipulations. *Journal of Experimental Marine Biology and Ecology* 406: 54–62.

Hyun B., Choi K.H., Jang P.G., Jang M.C., Lee W.J., Moon C.H., Shin K. (2014) Effects of increased CO_2 and temperature on the growth of four diatom species (*Chaetoceros debilis*, *Chaetoceros didymus*, *Skeletonema costatum* and *Thalassiosira nordenskioeldii*) in laboratory experiments. *Journal of Environmental Science International* 23: 1003–1012.

Kaeriyama H., Katsuki E., Otsubo M., Yamada M., Ichimi K., Tada K., Harrison P.J. (2011) Effects of temperature and irradiance on growth of strains belonging to seven *Skeletonema* species isolated from Dokai Bay, southern Japan. *European Journal of Phycology* 46: 113–124.

Kremp A., Godhe A., Egardt J., Dupont S., Suikkanen S., Casabianca S., Penna A. (2012) Intraspecific variability in the response of bloom-forming marine microalgae to changed climate conditions. *Ecology and Evolution* 2: 1195–1207.

Li G., Campbell D.A. (2013) Rising CO_2 interacts with growth light and growth rate to alter photosystem II photoinactivation of the coastal diatom *Thalassiosira pseudonana*. *PLoS ONE* 8: e55562. doi:10.1371/journal.pone.0055562

Litchman E., Klausmeier C.A. (2008) Trait-based community ecology of phytoplankton. *Annual Review of Ecology, Evolution, and Systematics* 39:615–639.

Litchman E., Klausmeier C.A., Schofield O.M., Falkowski P.G. (2007) The role of functional traits and trade-offs in structuring phytoplankton communities: scaling from cellular to ecosystem level. *Ecology Letters* 10: 1170–1181.

Meyer J., Riebesell U. (2015) Reviews and syntheses: Responses of coccolithophores to ocean acidification: a meta-analysis. *Biogeosciences* 12: 1671–1682.

Nanninga H.J., Tyrrell T. (1996) Importance of light for the formation of algal blooms by *Emiliania huxleyi*. *Marine Ecology Progress Series* 136: 195–203.

Paasche E. (2002) A review of the coccolithophorid *Emiliania huxleyi* (Prymnesiophyceae), with particular reference to growth, coccolith formation, and calcification-photosynthesis interactions. *Phycologia* 40: 503–529.

Riebesell U., Bellerby R.G.J., Engel A., Fabry V.J., Hutchins D.V., Reusch T.B.H., Schulz K.G., Morel F.M.M. (2008) Comment on 'phytoplankton calcification in a high-CO_2 world'. *Science* 322: 1466b.

Rost B., Riebesell U. (2004) Coccolithophores and the biological pump: responses to environmental changes. In: Thierstein H.R. and Young J.R. [Eds.], Coccolithophores: from molecular biology to global impact. pp. 99–125. Springer, Berlin, Germany.

Rost B., Riebesell U., Burkhardt S. (2003) Carbon acquisition of bloom-forming marine phytoplankton. *Limnology and Oceanography* 48: 56–67.

Rost B., Zondervan I., Riebesell U. (2002) Light-dependent carbon isotope fractionation in the coccolithophorid *Emiliania huxleyi*. *Limnology and Oceanography* 47: 120–128.

Sett S., Bach L.T., Schulz K.G., Koch-Klavsen S., Lebrato M., Riebesell U. (2014) Temperature modulates coccolithophorid sensitivity of growth, photosynthesis and calcification to increasing seawater pCO_2. *PLoS ONE* 9: e88308. doi:10.1371/journal.pone.0088308

Suzuki Y., Takahashi M. (1995) Growth responses of several diatom species isolated from various environments to temperature. *Journal of Phycology* 31: 880–888.

Taylor E.B. (1991) A review of local adaptation in Salmonidae, with particular reference to Pacific and Atlantic salmon. *Aquaculture* 98: 185–207.

Thomas M.K., Kremer C.T., Klausmeier C.A., Litchman E. (2012) A global pattern of thermal adaptation in marine phytoplankton. *Science* 338: 6110, 1085–1088.

Trimborn S., Langer G., Rost B. (2007) Effect of varying calcium concentrations and light intensities on calcification and photosynthesis in *Emiliania huxleyi*. *Limnology and Oceanography* 52: 2285–2293.

Tyrrell T., Merico A. (2004) *Emiliania huxleyi*: bloom observations and the conditions that induce them. In: Thierstein H.R. and Young J.R. [Eds.], Coccolithophores: from molecular biology to global impact. pp. 75–97. Springer, Berlin, Germany.

Whitman D.W., Agrawal A.A. (2009) What is phenotypic plasticity and why is it important? In: Whitman D.W and Ananthakrishnan T.N. [Eds.], Phenotypic plasticity of insects: mechanisms and consequences. pp 1–63. Science Publishers.

Wood A.M., Everroad R.C., Wingard L.M. (2005) Measuring growth rates in microalgal cultures. In: Andersen R.A. [Ed.], Algal culturing technique. pp. 269–285. Elsevier Academic Press, Burlington, Vermont.

Acknowledgements

I would like to thank Prof. Ulf Riebesell for his patience and guidance and giving me the opportunity to study at GEOMAR in Germany. Four years have passed and I have learned a lot since I started to work in his group: experimental design, techniques, writing, cooperating, English language and German culture. Thanks to Prof. Ulf Riebesell for giving me important suggestions to improve the experimental designs and the manuscripts.

I would like to thank Dr. Lennart Bach for introducing me the new techniques, for discussing about the physiological processes of coccolithophores, the experimental data set and the manuscript structures. Many thanks as well to Dr. Kai Lohbeck for giving me the opportunity to learn about evolutionary biology. Thanks to Dr. Kai Lohbeck for always answering my questions on evolutionary biology and teaching me to organize the manuscript structure. Thanks as well to Dr. Kai Schulz for giving me some suggestions and new ideas to improve the manuscripts.

I also appreciate the help of Kerstin Nachtigall, Jana Meyer, Andrea Ludwig and Tania Klüver and for teaching me new techniques. I would like to thank Silke Lischka, Scarlett Sett, Allanah Paul, Tim Boxhammer for fruitful discussions, help and advice. Thanks as well to Silvana Gagliardi for help. Special thanks to Prof. Baosheng Qiu, who suggested and supported me to do science.

I would like to thank my wife, Emei Xie, my baby, Shu Zhang, and my parents for supporting me whatever I have done and giving me energy during my working. Thanks as well to all of my friends in Kiel.

Declaration of work

Apart from the guidance of my supervisor, the content and design of this thesis is the result of work completed by myself. I declare that this thesis as a whole has not been submitted to other higher education institutions. Chapter 2 has been published as it appears in this thesis. This thesis has been prepared subject to the Rules of Good Scientific Practice of the German Research Foundation.

Declarer: